

1 Title Page

Bimodal Inference in Mice and Men

Authors:

Veith Weilnhammer^{1,2}, Heiner Stuke^{1,2}, Kai Standvoss^{1,3,5}, Philipp Sterzer^{1,3,4,5}

Affiliations:

¹ Department of Psychiatry, Charité-Universitätsmedizin Berlin, corporate member of Freie Universität Berlin and Humboldt-Universität zu Berlin, 10117 Berlin, Germany

² Berlin Institute of Health, Charité-Universitätsmedizin Berlin and Max Delbrück Center, 10178 Berlin, Germany

³ Bernstein Center for Computational Neuroscience, Charité-Universitätsmedizin Berlin, 10117 Berlin, Germany

⁴ Berlin School of Mind and Brain, Humboldt-Universität zu Berlin, 10099 Berlin, Germany

⁵ Einstein Center for Neurosciences Berlin, 10117 Berlin, Germany

Corresponding Author:

Veith Weilnhammer, Department of Psychiatry, Charité Campus Mitte, Charitéplatz 1, 10117 Berlin, phone: 0049 (0)30 450 517 317, email: veith.weilnhammer@gmail.com

¹ 2 Abstract

² Perception is known to cycle through periods of enhanced and reduced sensitivity to external
³ information. Here, we asked whether such slow fluctuations arise as a noise-related epiphe-
⁴ nomenon of limited processing capacity or, alternatively, represent a structured mechanism
⁵ of perceptual inference. Using two large-scale datasets, we found that humans and mice
⁶ waver between alternating intervals of externally- and internally-oriented modes of sensory
⁷ analysis. During external mode, perception aligned more closely with the external sensory
⁸ information, whereas internal mode was characterized by enhanced biases toward perceptual
⁹ history. Computational modeling indicated that dynamic changes in mode are enabled by
¹⁰ two interlinked factors: (i), the integration of subsequent inputs over time and, (ii), slow anti-
¹¹ phase oscillations in the perceptual impact of external sensory information versus internal
¹² predictions that are provided by perceptual history. **We propose that between-mode**
¹³ **fluctuations may benefit perception by generating unambiguous error signals**
¹⁴ **that enable optimal inference and learning in volatile environments.**

¹⁵ 3 One sentence summary

¹⁶ Humans and mice fluctuate between external and internal modes of sensory processing.

¹⁷

¹⁸

¹⁹ **4 Introduction**

²⁰ The capacity to respond to changes in the environment is a defining feature of life^{1–3}. In-
²¹ triguingly, the ability of living things to process their surroundings fluctuates considerably
²² over time^{4,5}. In humans and mice, perception^{6–12}, cognition¹³ and memory¹⁴ cycle through
²³ prolonged periods of enhanced and reduced sensitivity to external information, suggesting
²⁴ that the brain detaches from the world in recurring intervals that last from milliseconds
²⁵ to seconds and even minutes^{4,5}. Yet breaking from external information is risky, as swift
²⁶ responses to the environment are often crucial to survival.

²⁷ What could be the reason for these fluctuations in perceptual performance¹¹? First, periodic
²⁸ fluctuations in the ability to parse external information^{11,15,16} may arise simply due to band-
²⁹ width limitations and noise. Second, it may be advantageous to actively reduce the costs
³⁰ of neural processing by seeking sensory information only in recurring intervals^{5,17}, otherwise
³¹ relying on random or stereotypical responses to the external world. Third, spending time
³² away from the ongoing stream of sensory inputs may also reflect a functional strategy that
³³ facilitates flexible behavior and learning¹⁸: Intermittently relying more strongly on informa-
³⁴ tion acquired from past experiences may enable agents to build up stable internal predictions
³⁵ about the environment despite an ongoing stream of external sensory signals¹⁹. By the same
³⁶ token, recurring intervals of enhanced sensitivity to external information may help to detect
³⁷ changes in both the state of the environment and the amount of noise that is inherent in
³⁸ sensory encoding¹⁹.

³⁹ In this work, we sought to elucidate whether periodicities in the sensitivity to external
⁴⁰ information represent an epiphenomenon of limited processing capacity or, alternatively, re-
⁴¹ sult from a structured and adaptive mechanism of perceptual inference. To this end, we
⁴² analyzed two large-scale datasets on perceptual decision-making in humans²⁰ and mice²¹.
⁴³ When less sensitive to external stimulus information, humans and mice showed stronger se-
⁴⁴ rial dependencies^{22–33}, which have been conceptualized as internal predictions that reflect

45 the auto-correlation of natural environments³⁴ and bias perceptual decisions toward preced-
46 ing choices^{30,31,35}. Computational modeling indicated that ongoing changes in perceptual
47 performance may be driven by systematic fluctuations between externally- and internally-
48 oriented modes of sensory analysis. **We propose that that such bimodal inference**
49 **may improve, (i), the ability to robustly determine the statistical properties of**
50 **volatile environments and, (ii), the ability to calibrate internal beliefs about the**
51 **precision of sensory information relative to prior (Bayesian) beliefs.**

52 5 Results

53 5.1 Human perception fluctuates between epochs of enhanced and 54 reduced sensitivity to external information

55 We began by selecting 66 studies from the Confidence Database²⁰ that investigated how
56 human participants ($N = 4317$) perform binary perceptual decisions (Figure 1A; see Methods
57 section for details on inclusion criteria). As a metric for perceptual performance (i.e., the
58 sensitivity to external sensory information), we asked whether the participant's response
59 and the presented stimulus matched (*stimulus-congruent* choices) or differed from each other
60 (*stimulus-incongruent* choices; Figure 1B and C) in a total of 21.05 million trials.

61 In a first step, we asked whether the ability to accurately perceive sensory stimuli is con-
62 stant over time or, alternatively, fluctuates in periods of enhanced and reduced sensitivity to
63 external information. We found perception to be stimulus-congruent in $73.46\% \pm 0.15\%$ of
64 trials (mean \pm standard error of the mean; Figure 2A), which was highly consistent across
65 the selected studies (Supplemental Figure S1A). In line with previous work⁸, we found that
66 the probability of stimulus-congruence was not independent across successive trials: At the
67 group level, stimulus-congruent perceptual choices were significantly autocorrelated for up to
68 15 trials. Autocorrelation coefficients decayed exponentially over time (rate $\gamma = -1.92 \times 10^{-3}$

69 $\pm 4.5 \times 10^{-4}$, $T(6.88 \times 10^4) = -4.27$, $p = 1.98 \times 10^{-5}$; Figure 2B). Importantly, the autocor-
70 relation of stimulus-congruent perception was not a trivial consequence of the experimental
71 design, but remained significant when controlling for the trial-wise autocorrelation of task
72 difficulty (Supplemental Figure S2A) or the sequence of presented stimuli (Supplemental
73 Figure S2B).

74 In addition, stimulus-congruence was significantly autocorrelated not only at the group-
75 level, but also in individual participants, where the autocorrelation of stimulus-congruent
76 perception exceeded the respective autocorrelation of randomly permuted data within an
77 interval of $3.24 \pm 2.39 \times 10^{-3}$ trials (Figure 2C). In other words, if a participant's experience
78 was congruent (or incongruent) with the external stimulus information at a given trial, her
79 perception was more likely to be stimulus-congruent (or incongruent) for approximately 3
80 trials into the future.

81 To further corroborate the autocorrelation of stimulus-congruence, we used logistic regression
82 models that predicted the stimulus-congruence of perception at the index trial $t = 0$ from the
83 stimulus-congruence at the preceding trials within a lag of 25 trials. We found that regression
84 weights were significantly greater than zero for up to 16 trials (Supplemental Figure S3).

85 These results confirm that the ability to process sensory signals is not constant over time, but
86 unfolds in multi-trial epochs of enhanced and reduced sensitivity to external information⁸.

87 As a consequence of this autocorrelation, the dynamic probability of stimulus-congruent
88 perception (i.e., computed in sliding windows of ± 5 trials; Figure 1C) fluctuated considerably
89 within participants (average minimum: $35.46\% \pm 0.22\%$, maximum: $98.27\% \pm 0.07\%$). In
90 line with previous findings⁹, such fluctuations in the sensitivity to external information had
91 a power density that was inversely proportional to the frequency in the slow spectrum¹¹
92 ($\text{power} \sim 1/f^\beta$, $\beta = -1.32 \pm 3.14 \times 10^{-3}$, $T(1.84 \times 10^5) = -419.48$, $p = 0$; Figure 2D).

93 This feature, which is also known as *1/f noise*^{36,37}, represents a characteristic of ongoing
94 fluctuations in complex dynamic systems such as the brain³⁸ and the cognitive processes it

95 entertains^{9,10,13,39,40}.

96 **5.2 Human perception fluctuates between external and internal
97 modes of sensory processing**

98 In a second step, we sought to explain why perception cycles through periods of enhanced and
99 reduced sensitivity to external information^{4,5}. We reasoned that observers may intermittently
100 rely more strongly on internal information, i.e., on predictions about the environment that
101 are constructed from previous experiences^{19,31}.

102 In perception, *serial dependencies* represent one of the most basic internal predictions that
103 cause perceptual decisions to be systematically biased toward preceding choices^{22–33}. Such
104 effects of perceptual history mirror the continuity of the external world, in which the recent
105 past often predicts the near future^{30,31,34,35,41}. Therefore, as a metric for the perceptual
106 impact of internal information, we computed whether the participant’s response at a given
107 trial matched or differed from her response at the preceding trial (*history-congruent* and
108 *history-incongruent perception*, respectively; Figure 1B and C).

109 First, we ensured that perceptual history played a significant role in perception despite the
110 ongoing stream of external information. With a global average of $52.7\% \pm 0.12\%$ history-
111 congruent trials, we found a small but highly significant perceptual bias towards preceding
112 experiences ($\beta = 16.18 \pm 1.07$, $T(1.09 \times 10^3) = 15.07$, $p = 10^{-46}$; Figure 2A) that was
113 largely consistent across studies (Supplemental Figure 1B) and more pronounced in partic-
114 ipants who were less sensitive to external sensory information (Supplemental Figure 1C).

115 Logistic regression confirmed the internal information provided by perceptual history made
116 a significant contribution to perception ($\beta = 0.11 \pm 5.79 \times 10^{-3}$, $z = 18.53$, $p = 1.1 \times 10^{-76}$)
117 over and above the ongoing stream of external sensory information ($\beta = 2.2 \pm 5.87 \times 10^{-3}$,
118 $z = 375.11$, $p = 0$) and general response biases toward one of the two potential outcomes
119 ($\beta = 15.19 \pm 0.08$, $z = 184.98$, $p = 0$; see Supplemental Figure S4A for model comparisons

¹²⁰ within individual participants).

¹²¹ In addition, we confirmed that history-congruence was not a corollary of the sequence of
¹²² presented stimuli: History-congruent perceptual choices were more frequent at trials when
¹²³ perception was stimulus-incongruent ($56.03\% \pm 0.2\%$) as opposed to stimulus-congruent
¹²⁴ ($51.77\% \pm 0.11\%$, $\beta = -4.26 \pm 0.21$, $T(8.57 \times 10^3) = -20.36$, $p = 5.28 \times 10^{-90}$; Figure 2A,
¹²⁵ lower panel). Despite being adaptive in auto-correlated real-world environments^{19,34,35,42},
¹²⁶ perceptual history thus represented a source of bias in the randomized experimental designs
¹²⁷ studied here^{24,28,30,31,43}.

¹²⁸ Second, we asked whether perception cycles through multi-trial epochs during which per-
¹²⁹ ception is characterized by stronger or weaker biases toward preceding experiences. Indeed,
¹³⁰ in close analogy to stimulus-congruence, history-congruence was significantly autocorrelated
¹³¹ for up to 21 trials (Figure 2B). Following a peak at the first trial, the respective autocorre-
¹³² lation coefficients decreased exponentially over time (rate $\gamma = -6.11 \times 10^{-3} \pm 5.69 \times 10^{-4}$,
¹³³ $T(6.75 \times 10^4) = -10.74$, $p = 7.18 \times 10^{-27}$). History-congruence remained significantly auto-
¹³⁴ correlated when controlling for task difficulty (Supplemental Figure S2A) and the sequence
¹³⁵ of presented stimuli (Supplemental Figure S2B). In individual participants, the autocorre-
¹³⁶ lation of history-congruence was elevated above randomly permuted data for a lag of 4.87
¹³⁷ $\pm 3.36 \times 10^{-3}$ trials (Figure 2C), confirming that the autocorrelation of history-congruence
¹³⁸ was not only a group-level phenomenon. The autocorrelation of history-congruence was con-
¹³⁹ firmed by logistic regression models that successfully predicted the history-congruence of
¹⁴⁰ perception at an index trial $t = 0$ from the history-congruence at the preceding trials within
¹⁴¹ a lag of 17 trials (Supplemental Figure S3).

¹⁴² Third, we asked whether the impact of internal information fluctuates as **a scale-invariant**
¹⁴³ **process with a 1/f power law (i.e., a feature typically associated with fluctua-**
¹⁴⁴ **tions in the sensitivity to external information**^{9,10,13,39,40}). The dynamic probability
¹⁴⁵ of history-congruent perception (i.e., computed in sliding windows of ± 5 trials; Figure 1C)

¹⁴⁶ varied considerably over time, ranging between a minimum of $12.77\% \pm 0.14\%$ and a maxi-
¹⁴⁷ mum $92.23\% \pm 0.14\%$. In analogy to stimulus-congruence, we found that history-congruence
¹⁴⁸ fluctuated as **a scale-invariant process with a 1/f power law**, with power densities that
¹⁴⁹ were inversely proportional to the frequency in the slow spectrum¹¹ ($\text{power} \sim 1/f^\beta$, $\beta =$
¹⁵⁰ $-1.34 \pm 3.16 \times 10^{-3}$, $T(1.84 \times 10^5) = -423.91$, $p = 0$; Figure 2D).

¹⁵¹ Finally, we ensured that fluctuations in stimulus- and history-congruence are linked to each
¹⁵² other. When perceptual choices were less biased toward external information, participants
¹⁵³ relied more strongly on internal information acquired from perceptual history (and vice
¹⁵⁴ versa, $\beta = -0.1 \pm 8.59 \times 10^{-4}$, $T(2.1 \times 10^6) = -110.96$, $p = 0$). Thus, while sharing
¹⁵⁵ the characteristic of **a scale-invariant process with a 1/f power law**, fluctuations in
¹⁵⁶ stimulus- and history-congruence were shifted against each other by approximately half a
¹⁵⁷ cycle and showed a squared coherence of $6.49 \pm 2.07 \times 10^{-3}\%$ (Figure 2E and F; we report
¹⁵⁸ the average phase and coherence for frequencies below $0.1/N_{trials}$; see Methods for details).

¹⁵⁹ In sum, our analyses indicate that perceptual decisions may result from a competition be-
¹⁶⁰ tween external sensory signals with internal predictions provided by perceptual history. Cru-
¹⁶¹ cially, we show that the impact of these external and internal sources of information is not
¹⁶² stable over time, but fluctuates systematically, emitting overlapping autocorrelation curves
¹⁶³ and antiphase 1/f profiles.

¹⁶⁴ These links between stimulus- and history-congruence suggest that the fluctuations in the
¹⁶⁵ impact of external and internal information may be generated by a unifying mechanism that
¹⁶⁶ causes perception to alternate between two opposing *modes*¹⁸ (Figure 1D): During *external*
¹⁶⁷ *mode*, perception is more strongly driven by the available external stimulus information.
¹⁶⁸ Conversely, during *internal mode*, participants rely more heavily on internal predictions that
¹⁶⁹ are implicitly provided by preceding perceptual experiences. Fluctuations in mode (i.e.,
¹⁷⁰ the degree of bias toward external versus internal information) may thus provide a novel
¹⁷¹ explanation for ongoing fluctuations in the sensitivity to external information^{4,5,18}.

172 **5.3 Internal and external modes of processing facilitate re-**
173 **response behavior and enhance confidence in human perceptual**
174 **decision-making**

175 Alternatively, however, fluctuating biases toward externally- and internally-oriented modes
176 may not represent a perceptual phenomenon, but result from cognitive processes that are
177 situated up- or downstream of perception. For instance, it may be argued that participants
178 may be prone to stereotypically repeat the preceding choice when not attending to the
179 experimental task. Thus, fluctuations in mode may arise due to systematic changes in the
180 level of tonic arousal⁴⁴ or on-task attention^{45,46}. Since arousal and attention typically link
181 closely with response times^{45,47} (RTs), this alternative explanation entails that RTs increase
182 monotonically as one moves away from externally-biased and toward internally-biases modes
183 of sensory processing.

184 As expected, stimulus-congruent (as opposed to stimulus-incongruent) choices were associ-
185 ated with faster responses ($\beta = -0.14 \pm 1.61 \times 10^{-3}$, $T(1.99 \times 10^6) = -85.91$, $p = 0$;
186 Figure 2G). Intriguingly, whilst controlling for the effect of stimulus-congruence, we found
187 that history-congruent (as opposed to history-incongruent) choices were also characterized
188 by shorter RTs ($\beta = -9.73 \times 10^{-3} \pm 1.38 \times 10^{-3}$, $T(1.99 \times 10^6) = -7.06$, $p = 1.66 \times 10^{-12}$;
189 Figure 2G).

190 When analyzing the speed of response against the mode of sensory processing (Figure 2H),
191 we found that RTs were shorter during externally-oriented perception ($\beta_1 = -11.07 \pm 0.55$,
192 $T(1.98 \times 10^6) = -20.14$, $p = 3.17 \times 10^{-90}$). Crucially, as indicated by a quadratic relationship
193 between the mode of sensory processing and RTs ($\beta_2 = -19.86 \pm 0.52$, $T(1.98 \times 10^6) =$
194 -38.43 , $p = 5 \times 10^{-323}$), participants became faster at indicating their perceptual decision
195 when biases toward both internal and external mode grew stronger. This argued against
196 the view that the dynamics of pre-perceptual variables such as arousal or attention provide
197 a plausible alternative explanation for the fluctuating perceptual impact of internal and

¹⁹⁸ external information.

¹⁹⁹ Second, it may be assumed that participants tend to repeat preceding choices when they are
²⁰⁰ not yet familiar with the experimental task, leading to history-congruent choices that are
²⁰¹ caused by insufficient training. In the Confidence database²⁰, training effects were visible
²⁰² from RTs that were shortened by increasing exposure to the task ($\beta = -7.53 \times 10^{-5} \pm 6.32 \times$
²⁰³ 10^{-7} , $T(1.81 \times 10^6) = -119.15$, $p = 0$). Intriguingly, however, history-congruent choices
²⁰⁴ became more frequent with increased exposure to the task ($\beta = 3.6 \times 10^{-5} \pm 2.54 \times 10^{-6}$,
²⁰⁵ $z = 14.19$, $p = 10^{-45}$), speaking against the proposition that insufficient training induces
²⁰⁶ seriality in response behavior.

²⁰⁷ As a third caveat, it could be argued that biases toward internal information reflect a post-
²⁰⁸ perceptual strategy that repeats preceding choices when the subjective confidence in the
²⁰⁹ perceptual decision is low. According to this view, subjective confidence should increase
²¹⁰ monotonically as biases toward external mode become stronger.

²¹¹ Stimulus-congruent (as opposed to stimulus-incongruent) choices were associated with en-
²¹² hanced confidence ($\beta = 0.04 \pm 1.18 \times 10^{-3}$, $T(2.06 \times 10^6) = 36.86$, $p = 2.93 \times 10^{-297}$;
²¹³ Figure 2I). Yet whilst controlling for the effect of stimulus-congruence, we found that history-
²¹⁴ congruence also increased confidence ($\beta = 0.48 \pm 1.38 \times 10^{-3}$, $T(2.06 \times 10^6) = 351.89$, $p =$
²¹⁵ 0; Figure 2I).

²¹⁶ When depicted against the mode of sensory processing (Figure 2J), subjective confidence was
²¹⁷ indeed enhanced when perception was more externally-oriented ($\beta_1 = 92.63 \pm 1$, $T(2.06 \times 10^6)$
²¹⁸ = 92.89, $p = 0$). Importantly, however, participants were more confident in their perceptual
²¹⁹ decision for stronger biases toward both internal and external mode ($\beta_2 = 39.3 \pm 0.94$,
²²⁰ $T(2.06 \times 10^6) = 41.95$, $p = 0$). In analogy to RTs, subjective confidence thus showed
²²¹ a quadratic relationship to the mode of sensory processing (Figure 2J), contradicting the
²²² notion that biases toward internal mode may reflect a post-perceptual strategy employed in
²²³ situations of low subjective confidence.

²²⁴ The above results indicate that reporting behavior and metacognition do not map linearly
²²⁵ onto the mode of sensory processing, suggesting that slow fluctuations in the respective
²²⁶ impact of external and internal information are most likely to affect perception at an early
²²⁷ level of sensory analysis^{48,49}. Such low-level processing may integrate perceptual history with
²²⁸ external inputs into a decision variable⁵⁰ that influences not only perceptual choices, but also
²²⁹ downstream functions such as speed of response and subjective confidence. Consequently,
²³⁰ our findings predict that human participants lack full metacognitive insight into how strongly
²³¹ external signals and internal predictions contribute to perceptual decision-making. Stronger
²³² biases toward perceptual history thus lead to two seemingly contradictory effects: more
²³³ frequent errors (Supplemental Figure 1C) and increasing subjective confidence (Figure 2I-J).

²³⁴ This observation generates an intriguing prediction regarding the association of between-
²³⁵ mode fluctuations and perceptual metacognition: Metacognitive efficiency should be lower
²³⁶ in individuals who spend more time in internal mode, since their confidence reports are less
²³⁷ predictive of whether the corresponding perceptual decision is correct. We computed each
²³⁸ participant's M-ratio⁵¹ ($\text{meta-}d'/d' = 0.85 \pm 0.02$) to probe this hypothesis independently of
²³⁹ inter-individual differences in perceptual performance. Indeed, we found that biases toward
²⁴⁰ internal information (i.e., as defined by the average probability of history-congruence) were
²⁴¹ stronger in participants with lower metacognitive efficiency ($\beta = -2.98 \times 10^{-3} \pm 9.82 \times 10^{-4}$,
²⁴² $T(4.14 \times 10^3) = -3.03$, $p = 2.43 \times 10^{-3}$).

²⁴³ **5.4 Fluctuations between internal and external mode modulate
244 perceptual performance beyond the effect of general response
245 biases**

²⁴⁶ The above sections provide correlative evidence that recurring intervals of stronger perceptual
²⁴⁷ history temporally reduce the participants' sensitivity to external information. Importantly,
²⁴⁸ the history-dependent biases that characterize internal mode processing must be differenti-

249 ated from general response biases. In binary perceptual decision-making, general response
250 biases are defined by a propensity to choose one of the two outcomes more often than the
251 alternative. Indeed, in the experiments considered here, participants selected the more fre-
252 quent of the two possible outcomes in $58.71\% \pm 0.22\%$ of trials.

253 Two caveats have to be considered to make sure that the effect of history-congruence is
254 distinct from the effect of general response biases. First, history-congruent states become
255 more likely for larger response biases that cause a increasing imbalance in the likelihood of
256 the two outcomes ($\beta = 0.24 \pm 6.93 \times 10^{-4}$, $T(2.09 \times 10^6) = 342.43$, $p = 0$). One may thus
257 ask whether the autocorrelation of history-congruence could be entirely driven by general
258 response biases. Yet the above analyses account for general response biases by computing
259 group-level autocorrelations (see Figure 2C) relative to randomly permuted data (i.e., by
260 subtracting the autocorrelation of randomly permuted data from the raw autocorrelation
261 curve). This precludes that general response biases contribute to the observed autocorrela-
262 tion of history-congruence (see Supplemental Figure S5 for a visualization of the correction
263 procedure for simulated data with general response biases ranging from 60 to 90%).

264 Second, it may be argued that fluctuations in perceptual performance may be solely driven
265 by ongoing changes in the strength of general response biases. To assess the links between
266 dynamic fluctuations in stimulus-congruence on the one hand and history-congruence as
267 well as general response bias on the other hand, we computed all variables as dynamic
268 probabilities in sliding windows of ± 5 trials (see Figure 1C). Linear mixed effects modeling
269 indicated that fluctuations in history-congruent biases were larger in amplitude than the
270 corresponding fluctuations in general response biases ($\beta_0 = 0.03 \pm 7.34 \times 10^{-3}$, $T(64.94) =$
271 4.46 , $p = 3.28 \times 10^{-5}$). Crucially, ongoing fluctuations in history-congruence had a significant
272 effect on stimulus-congruence ($\beta_1 = -0.05 \pm 5.63 \times 10^{-4}$, $T(2.1 \times 10^6) = -84.21$, $p = 0$)
273 beyond the effect of ongoing changes in general response biases ($\beta_2 = -0.06 \pm 5.82 \times 10^{-4}$,
274 $T(2.1 \times 10^6) = -103.51$, $p = 0$). In sum, the above control analyses confirm that the observed

275 influence of preceding choices on perceptual decision-making cannot not be reduced to general
276 response biases.

277 **5.5 Internal mode is characterized by lower thresholds as well as**
278 **by history-dependent changes in biases and lapses**

279 In a final control analysis, we asked whether history-independent changes in biases and
280 lapses may provide an alternative explanation of internal mode processing. To this end, we
281 estimated full and history-conditioned psychometric curves to investigate how internal and
282 external mode relate to biases (i.e., the horizontal position of the psychometric curve), lapses
283 (i.e., the asymptotes of the psychometric curve) and thresholds (i.e., 1/sensitivity, estimated
284 from the slope of the psychometric curve). We used a maximum likelihood procedure to
285 predict trial-wise choices y ($y = 0$ and $y = 1$ for outcomes A and B respectively) from the
286 choice probabilities y_p . y_p was computed from difficulty-weighted inputs s_w via a parametric
287 error function defined by the parameters γ (lower lapse), δ (upper lapse), μ (bias) and t
288 (threshold; see Methods for details):

$$y_p = \gamma + (1 - \gamma - \delta) * (\text{erf}(\frac{s_w + \mu}{t}) + 1)/2 \quad (1)$$

289 Across the full dataset (i.e., irrespective of the preceding perceptual choice y_{t-1}), biases μ
290 were distributed around zero (-0.05 ± 0.03 ; $\beta_0 = 7.37 \times 10^{-3} \pm 0.09$, $T(36.8) = 0.08$, $p =$
291 0.94; see Figure 3A and B, upper panel). When conditioned on perceptual history, biases
292 μ varied according to the preceding perceptual choice, with negative biases for $y_{t-1} = 0$
293 (-0.22 ± 0.04 ; $\beta_0 = 0.56 \pm 0.12$, $T(43.39) = 4.6$, $p = 3.64 \times 10^{-5}$) and positive biases for
294 $y_{t-1} = 1$ (0.29 ± 0.03 ; $\beta_0 = 0.56 \pm 0.12$, $T(43.39) = 4.6$, $p = 3.64 \times 10^{-5}$). Absolute biases
295 $|\mu|$ were larger in internal mode (1.84 ± 0.03) as compared to external mode (0.86 ± 0.02 ;
296 $\beta_0 = -0.62 \pm 0.07$, $T(45.62) = -8.38$, $p = 8.59 \times 10^{-11}$; controlling for differences in lapses
297 and thresholds).

298 Lower and upper lapses amounted to $\gamma = 0.13 \pm 2.83 \times 10^{-3}$ and $\delta = 0.1 \pm 2.45 \times 10^{-3}$ (see
299 Figure 3A, C and D). Lapses were larger in internal mode ($\gamma = 0.17 \pm 3.52 \times 10^{-3}$, $\delta = 0.14$
300 $\pm 3.18 \times 10^{-3}$) as compared to external mode ($\gamma = 0.1 \pm 2.2 \times 10^{-3}$, $\delta = 0.08 \pm 2 \times 10^{-3}$;
301 $\beta_0 = -0.05 \pm 5.73 \times 10^{-3}$, $T(47.03) = -9.11$, $p = 5.94 \times 10^{-12}$; controlling for differences
302 in biases and thresholds).

303 Conditioning on the previous perceptual choice revealed that the between-mode difference
304 in lapse was not general, but depended on perceptual history: For $y_{t-1} = 0$, only higher
305 lapses δ differed between internal and external mode ($\beta_0 = -0.1 \pm 9.58 \times 10^{-3}$, $T(36.87) =$
306 -10.16 , $p = 3.06 \times 10^{-12}$), whereas lower lapses γ did not ($\beta_0 = 0.01 \pm 7.77 \times 10^{-3}$, $T(33.1)$
307 $= 1.61$, $p = 0.12$). Vice versa, for $y_{t-1} = 1$, lower lapses γ differed between internal and
308 external mode ($\beta_0 = -0.11 \pm 0.01$, $T(40.11) = -9.59$, $p = 6.14 \times 10^{-12}$), whereas higher
309 lapses δ did not ($\beta_0 = 0.01 \pm 7.74 \times 10^{-3}$, $T(33.66) = 1.58$, $p = 0.12$).

310 Thresholds t were estimated at 3 ± 0.06 (see Figure 3A and E). Thresholds t were larger
311 in internal mode (3.66 ± 0.09) as compared to external mode (2.02 ± 0.03 ; $\beta_0 = -1.77 \pm$
312 0.25 , $T(50.45) = -7.14$, $p = 3.48 \times 10^{-9}$; controlling for differences in biases and lapses).

313 In contrast to the bias μ and the lapse rates γ and δ , thresholds t were not modulated by
314 perceptual history ($\beta_0 = 0.04 \pm 0.06$, $T(2.97 \times 10^3) = 0.73$, $p = 0.47$).

315 In sum, the above analyses showed that internal and external mode differ with respect
316 to biases, lapses and thresholds. Internally-biased processing was characterized by higher
317 thresholds, indicating a reduced sensitivity to sensory information, as well as by larger biases
318 and lapses. Importantly, between-mode differences in biases and lapses strongly depended
319 on perceptual history. This confirmed that internal mode processing cannot be explained
320 solely on the ground of a general (i.e., history-independent) increase in lapses or bias.

321 **5.6 Mice waver between external and internal modes of perceptual**
322 **decision-making**

323 In a prominent functional explanation for serial dependencies^{22–28,32,33,48}, perceptual his-
324 tory is cast as an internal prediction that leverages the temporal autocorrelation of natural
325 environments for efficient decision-making^{30,31,34,35,41}. We reasoned that, since this autocor-
326 relation is one of the most basic features of our sensory world, fluctuating biases toward
327 preceding perceptual choices should not be a uniquely human phenomenon.

328 To test whether externally and internally oriented modes of processing exist beyond the
329 human mind, we analyzed data on perceptual decision-making in mice that were extracted
330 from the International Brain Laboratory (IBL) dataset²¹. Here, we restricted our analyses
331 to the *basic* task²¹, in which mice responded to gratings of varying contrast that appeared
332 either in the left or right hemifield of with equal probability. We excluded sessions in which
333 mice did not respond correctly to stimuli presented at a contrast above 50% in more than
334 80% of trials (see Methods), which yielded a final sample of $N = 165$ adequately trained
335 mice that went through 1.46 million trials.

336 In line with humans, mice were biased toward perceptual history in $54.03\% \pm 0.17\%$ of trials
337 ($T(164) = 23.65$, $p = 9.98 \times 10^{-55}$; Figure 4A and Supplemental Figure S1D). Perceptual
338 history effects remained significant ($\beta = 0.51 \pm 4.49 \times 10^{-3}$, $z = 112.84$, $p = 0$) when
339 controlling for external sensory information ($\beta = 2.96 \pm 4.58 \times 10^{-3}$, $z = 646.1$, $p = 0$)
340 and general response biases toward one of the two potential outcomes ($\beta = -1.78 \pm 0.02$,
341 $z = -80.64$, $p = 0$; see Supplemental Figure S4C-D for model comparisons and β values
342 computed within individual mice).

343 In the *basic* task of the IBL dataset²¹, stimuli were presented at random in either the left
344 or right hemifield. Stronger biases toward perceptual history should therefore decrease per-
345 ceptual performance. Indeed, history-congruent choices were more frequent when perception
346 was stimulus-incongruent ($61.59\% \pm 0.07\%$) as opposed to stimulus-congruent ($51.81\% \pm$

³⁴⁷ 0.02%, $T(164) = 31.37$, $p = 3.36 \times 10^{-71}$; $T(164) = 31.37$, $p = 3.36 \times 10^{-71}$; Figure 4A,
³⁴⁸ lower panel), confirming that perceptual history was a source of error^{24,28,30,31,43} as opposed
³⁴⁹ to a feature of the experimental paradigm. Overall, perception was stimulus-congruent in
³⁵⁰ $81.37\% \pm 0.3\%$ of trials (Figure 4A).

³⁵¹ At the group level, we found significant autocorrelations in both stimulus-congruence (86
³⁵² consecutive trials) and history-congruence (8 consecutive trials), which remained significant
³⁵³ when taking into account the respective autocorrelation of task difficulty and external stim-
³⁵⁴ ulation (Supplemental Figure 2C-D). In contrast to humans, mice showed a negative auto-
³⁵⁵ correlation coefficient of stimulus-congruence at trial 2. This was due to a feature of the
³⁵⁶ experimental design: Errors at a contrast above 50% were followed by a high-contrast stimu-
³⁵⁷ lus at the same location. Thus, stimulus-incongruent choices on easy trials were more likely
³⁵⁸ to be followed by stimulus-congruent perceptual choices that were facilitated by high-contrast
³⁵⁹ visual stimuli²¹.

³⁶⁰ The autocorrelation of history-congruence closely overlapped with the human data and de-
³⁶¹ cayed exponentially after a peak at the first trial (rate $\gamma = -6.7 \times 10^{-3} \pm 5.94 \times 10^{-4}$,
³⁶² $T(3.69 \times 10^4) = -11.27$, $p = 2.07 \times 10^{-29}$; Figure 4B). On the level of individual mice, au-
³⁶³ tocorrelation coefficients were elevated above randomly permuted data within a lag of 4.59
³⁶⁴ ± 0.06 trials for stimulus-congruence and 2.58 ± 0.01 trials for history-congruence (Figure
³⁶⁵ 4C).

³⁶⁶ To further corroborate a significant autocorrelation of stimulus- and history-congruence in
³⁶⁷ mice, we used logistic regression models that predicted the stimulus-/history-congruence of
³⁶⁸ perception at the index trial $t = 0$ from the stimulus/history-congruence at the preceding
³⁶⁹ trials within a lag of 25 trials. We found that regression weights were significantly greater
³⁷⁰ than zero for more than 25 trials for stimulus-congruence. For history-congruence, regression
³⁷¹ weights significantly greater than zero for 8 trials prior to the index trial (Supplemental
³⁷² Figure S3). In analogy to humans, mice showed anti-phase 1/f fluctuations in the sensitivity

³⁷³ to internal and external information (Figure 4D-F).

³⁷⁴ Next, we asked how external and internal modes relate to the trial duration (TD, a coarse
³⁷⁵ measure of RT in mice that spans the interval from stimulus onset to feedback²¹). Stimulus-
³⁷⁶ congruent (as opposed to stimulus-incongruent) choices were associated with shorter TDs (δ
³⁷⁷ $= -262.48 \pm 17.1$, $T(164) = -15.35$, $p = 1.55 \times 10^{-33}$), while history-congruent choices were
³⁷⁸ characterized by longer TDs ($\delta = 30.47 \pm 5.57$, $T(164) = 5.47$, $p = 1.66 \times 10^{-7}$; Figure 4G).

³⁷⁹ Across the full spectrum of the available data, TDs showed a linear relationship with the
³⁸⁰ mode of sensory processing, with shorter TDs during external mode ($\beta_1 = -4.16 \times 10^4 \pm$
³⁸¹ 1.29×10^3 , $T(1.35 \times 10^6) = -32.31$, $p = 6.03 \times 10^{-229}$, Figure 4H). However, an explorative
³⁸² post-hoc analysis limited to TDs that differed from the median TD by no more than $1.5 \times$
³⁸³ MAD (median absolute distance⁵²) indicated that, when mice engaged with the task more
³⁸⁴ swiftly, TDs did indeed show a quadratic relationship with the mode of sensory processing
³⁸⁵ ($\beta_2 = -1.97 \times 10^3 \pm 843.74$, $T(1.19 \times 10^6) = -2.34$, $p = 0.02$, Figure 4I).

³⁸⁶ As in humans, it is an important caveat to consider whether the observed serial dependencies
³⁸⁷ in murine perception reflect a phenomenon of perceptual inference, or, alternatively, an
³⁸⁸ unspecific strategy that occurs at the level of reporting behavior. We reasoned that, if mice
³⁸⁹ indeed tended to repeat previous choices as a general response pattern, history effects should
³⁹⁰ decrease during training of the perceptual task. We therefore analyzed how stimulus- and
³⁹¹ history-congruent perceptual choices evolved across sessions in mice that, by the end of
³⁹² training, achieved proficiency (i.e., stimulus-congruence $\geq 80\%$) in the *basic* task of the IBL
³⁹³ dataset²¹.

³⁹⁴ As expected, we found that stimulus-congruent perceptual choices became more frequent (β
³⁹⁵ $= 0.34 \pm 7.13 \times 10^{-3}$, $T(8.51 \times 10^3) = 47.66$, $p = 0$; Supplemental Figure S6) and TDs were
³⁹⁶ progressively shortened ($\beta = -22.14 \pm 17.06$, $T(1.14 \times 10^3) = -1.3$, $p = 0$) across sessions.
³⁹⁷ Crucially, the frequency of history-congruent perceptual choices also increased during train-
³⁹⁸ ing ($\beta = 0.13 \pm 4.67 \times 10^{-3}$, $T(8.4 \times 10^3) = 27.04$, $p = 1.96 \times 10^{-154}$; Supplemental Figure

³⁹⁹ S6).

⁴⁰⁰ As in humans, longer within-session task exposure was associated with an increase in history-
⁴⁰¹ congruence ($\beta = 3.6 \times 10^{-5} \pm 2.54 \times 10^{-6}$, $z = 14.19$, $p = 10^{-45}$) and a decrease in TDs (β
⁴⁰² $= -0.1 \pm 3.96 \times 10^{-3}$, $T(1.34 \times 10^6) = -24.99$, $p = 9.45 \times 10^{-138}$). In sum, these findings
⁴⁰³ strongly argue against the proposition that mice show biases toward perceptual history due
⁴⁰⁴ to an unspecific response strategy.

⁴⁰⁵ As in humans, fluctuations in the strength of history-congruent biases were, (i), larger in
⁴⁰⁶ amplitude than the corresponding fluctuations in general response biases ($\beta_0 = -5.26 \times 10^{-3}$
⁴⁰⁷ $\pm 4.67 \times 10^{-4}$, $T(2.12 \times 10^3) = -11.28$, $p = 1.02 \times 10^{-28}$) and, (ii), had a significant effect on
⁴⁰⁸ stimulus-congruence ($\beta_1 = -0.12 \pm 7.17 \times 10^{-4}$, $T(1.34 \times 10^6) = -168.39$, $p = 0$) beyond the
⁴⁰⁹ effect of ongoing changes in general response biases ($\beta_2 = -0.03 \pm 6.94 \times 10^{-4}$, $T(1.34 \times 10^6)$
⁴¹⁰ $= -48.14$, $p = 0$). This confirmed that, in both humans and mice, perceptual performance
⁴¹¹ is modulated by systematic fluctuations between externally- and internally-oriented modes
⁴¹² of sensory processing.

⁴¹³ Finally, we fitted full and history-conditioned psychometric curves to the data from the
⁴¹⁴ IBL database. When estimated based on the full dataset (i.e., irrespective of the preceding
⁴¹⁵ perceptual choice y_{t-1}), biases μ were distributed around zero ($3.87 \times 10^{-3} \pm 9.81 \times 10^{-3}$;
⁴¹⁶ $T(164) = 0.39$, $p = 0.69$; Figure 5A and B, upper panel). When conditioned on the preceding
⁴¹⁷ perceptual choice, biases were negative for $y_{t-1} = 0$ ($-0.02 \pm 8.7 \times 10^{-3}$; $T(164) = -1.99$, $p =$
⁴¹⁸ 0.05 ; Figure 5A and B, middle panel) and positive for $y_{t-1} = 1$ ($0.02 \pm 9.63 \times 10^{-3}$; $T(164)$
⁴¹⁹ $= 1.91$, $p = 0.06$; Figure 5A and B, lower panel). As in humans, mice showed larger biases
⁴²⁰ during internal mode ($0.14 \pm 7.96 \times 10^{-3}$) as compared to external mode ($0.07 \pm 8.7 \times 10^{-3}$;
⁴²¹ $\beta_0 = -0.18 \pm 0.03$, $T = -6.38$, $p = 1.77 \times 10^{-9}$; controlling for differences in lapses and
⁴²² thresholds).

⁴²³ Lower and upper lapses amounted to $\gamma = 0.1 \pm 4.35 \times 10^{-3}$ and $\delta = 0.11 \pm 4.65 \times 10^{-3}$
⁴²⁴ (see Figure 5A, C and D). Lapse rates were higher in internal mode ($\gamma = 0.15 \pm 5.14 \times 10^{-3}$,

⁴²⁵ $\delta = 0.16 \pm 5.79 \times 10^{-3}$) as compared to external mode ($\gamma = 0.06 \pm 3.11 \times 10^{-3}$, $\delta = 0.07$
⁴²⁶ $\pm 3.34 \times 10^{-3}$; $\beta_0 = -0.11 \pm 4.39 \times 10^{-3}$, $T = -24.8$, $p = 4.91 \times 10^{-57}$; controlling for
⁴²⁷ differences in biases and thresholds).

⁴²⁸ For $y_{t-1} = 0$, the difference between internal and external mode was more pronounced for
⁴²⁹ higher lapses δ ($T(164) = 21.44$, $p = 1.93 \times 10^{-49}$). Conversely, for $y_{t-1} = 1$, the difference
⁴³⁰ between internal and external mode was more pronounced for lower lapses γ ($T(164) = -$
⁴³¹ 18.24 , $p = 2.68 \times 10^{-41}$). In contrast to the human data, higher lapses δ and lower lapses
⁴³² γ were significantly elevated during internal mode irrespective of the preceding perceptual
⁴³³ choice (higher lapses δ for $y_{t-1} = 1$: $T(164) = -2.65$, $p = 8.91 \times 10^{-3}$; higher lapses δ for
⁴³⁴ $y_{t-1} = 0$: $T(164) = -28.29$, $p = 5.62 \times 10^{-65}$; lower lapses γ for $y_{t-1} = 1$: $T(164) = -32.44$,
⁴³⁵ $p = 2.92 \times 10^{-73}$; lower lapses γ for $y_{t-1} = 0$: $T(164) = -2.5$, $p = 0.01$).

⁴³⁶ In mice, thresholds t amounted to $0.15 \pm 6.52 \times 10^{-3}$ (see Figure 5A and E) and were higher
⁴³⁷ in internal mode (0.27 ± 0.01) as compared to external mode ($0.09 \pm 4.44 \times 10^{-3}$; $\beta_0 =$
⁴³⁸ -0.28 ± 0.04 , $T = -7.26$, $p = 1.53 \times 10^{-11}$; controlling for differences in biases and lapses).
⁴³⁹ Thresholds t were not modulated by perceptual history ($T(164) = 0.94$, $p = 0.35$).

⁴⁴⁰ In sum, the above analyses of the psychometric function in mice corroborated our findings in
⁴⁴¹ humans. Higher thresholds indicated a reduced sensitivity to external information during in-
⁴⁴² ternal mode. Additionally, internally-biased processing was characterized history-dependent
⁴⁴³ modulation of biases and lapses.

⁴⁴⁴ **5.7 Fluctuations in mode result from coordinated changes in the 445 impact of external and internal information on perception**

⁴⁴⁶ The empirical data presented above indicate that, for both humans and mice, perception
⁴⁴⁷ fluctuates between internal and external modes, i.e., multi-trial epochs that are characterized
⁴⁴⁸ by enhanced sensitivity toward either internal or external information. Since natural envi-
⁴⁴⁹ ronments typically show high temporal redundancy³⁴, previous experiences are often good

450 predictors of new stimuli^{30,31,35,41}. Serial dependencies may therefore induce autocorrelations in perception by serving as an internal prediction (or *memory* processes^{9,13}) about the environment that actively integrates noisy sensory information over time⁵³.

453 Previous work has shown that such internal predictions are built by dynamically updating the estimated probability of being in a particular perceptual state from the sequence of preceding experiences^{35,48,54}. The integration of sequential inputs may lead to accumulating effects of perceptual history that progressively override incoming sensory information, enabling internal mode processing¹⁹. However, since such a process would lead to internal biases that may eventually become impossible to overcome⁵⁵, we assumed that changes in mode may additionally be driven by ongoing wave-like fluctuations^{9,13} in the perceptual impact of external and internal information that occur *irrespective* of the sequence of previous experiences and temporarily de-couple the decision variable from implicit internal representations of the environment¹⁹.

463 Following Bayes' theorem, we reasoned that binary perceptual decisions depend on the posterior log ratio L of the two alternative states of the environment that participants learn about via noisy sensory information⁵⁴. We computed the posterior by combining the sensory evidence available at time-point t (i.e., the log likelihood ratio LLR) with the prior probability ψ , **weighted by the respective precision terms ω_{LLR} and ω_ψ** :

$$L_t = LLR_t * \omega_{LLR} + \psi_t(L_{t-1}, H) * \omega_\psi \quad (2)$$

468 We derived the prior probability ψ at timepoint t from the posterior probability of perceptual outcomes at timepoint L_{t-1} . Since a switch between the two states can occur at any time, the effect of perceptual history varies according to both the sequence of preceding experiences and the estimated stability of the external environment (i.e., the *hazard rate* H ⁵⁴):

$$\psi_t(L_{t-1}, H) = L_{t-1} + \log\left(\frac{1-H}{H} + \exp(-L_{t-1})\right) - \log\left(\frac{1-H}{H} + \exp(L_{t-1})\right) \quad (3)$$

472 The *LLR* was computed from inputs s_t by applying a sigmoid function defined by parameter
473 α that controls the sensitivity of perception to the available sensory information (see Methods
474 for detailed equations on humans and mice):

$$u_t = \frac{1}{1 + \exp(-\alpha * s_t)} \quad (4)$$

$$LLR_t = \log\left(\frac{u_t}{1 - u_t}\right) \quad (5)$$

475 To allow for *bimodal inference*, i.e., alternating periods of internally- and externally-biased
476 modes of perceptual processing that occur irrespective of the sequence of preceding experi-
477 ences, we assumed that the relative influences of likelihood and prior show coherent anti-
478 phase fluctuations governed by ω_{LLR} and ω_ψ that are determined by amplitude a , frequency
479 f and phase p . **This implements a hyperprior in which the sensory and prior**
480 **precisions fluctuate at a particular time scale:**

$$\omega_{LLR} = a_{LLR} * \sin(f * t + p) + 1 \quad (6)$$

$$\omega_\psi = a_\psi * \sin(f * t + p + \pi) + 1 \quad (7)$$

481 Finally, a sigmoid transform of the posterior L_t yields the probability of observing the
482 perceptual decision y_t at a temperature determined by ζ^{-1} :

$$P(y_t = 1) = 1 - P(y_t = 0) = \frac{1}{1 + \exp(-\zeta * L_t)} \quad (8)$$

483 Fitting the bimodal inference model outlined above to behavioral data (see Methods for
484 details) characterizes each subject by a sensitivity parameter α that captures how strongly
485 perception is driven by the available sensory information, and a hazard rate parameter H
486 that controls how heavily perception is biased by perceptual history. As a sanity check for
487 model fit, we tested whether the frequency of stimulus- and history-congruent trials in the
488 Confidence database²⁰ and IBL database²¹ correlate with the estimated parameters α and
489 H , respectively. As expected, the estimated sensitivity toward stimulus information α was
490 positively correlated with the frequency of stimulus-congruent perceptual choices (humans:
491 $\beta = 8.4 \pm 0.26$, $T(4.31 \times 10^3) = 32.87$, $p = 1.3 \times 10^{-211}$; mice: $\beta = 1.93 \pm 0.12$, $T(2.07 \times 10^3)$
492 $= 16.21$, $p = 9.37 \times 10^{-56}$). Likewise, H was negatively correlated with the frequency of
493 history-congruent perceptual choices (humans: $\beta = -11.84 \pm 0.5$, $T(4.29 \times 10^3) = -23.5$,
494 $p = 5.16 \times 10^{-115}$; mice: $\beta = -6.18 \pm 0.66$, $T(2.08 \times 10^3) = -9.37$, $p = 1.85 \times 10^{-20}$).

495 Our behavioral analyses have shown that humans and mice showed significant ef-
496 fects of perceptual history that impaired performance in randomized psychophysical
497 experiments^{24,28,30,31,43} (Figure 2A and 3A). We therefore expected that humans and mice
498 underestimated the true hazard rate \hat{H} of the experimental environments (Confidence
499 database²⁰: $\hat{H}_{Humans} = 0.5 \pm 1.58 \times 10^{-5}$); IBL database²¹: $\hat{H}_{Mice} = 0.49 \pm 6.47 \times 10^{-5}$).
500 Indeed, when fitting the bimodal inference model outlined above to the trial-wise perceptual
501 choices (see Methods), we found that the estimated (i.e., subjective) hazard rate H was
502 lower than \hat{H} for both humans ($H = 0.45 \pm 4.8 \times 10^{-5}$, $\beta = -6.87 \pm 0.94$, $T(61.87) =$
503 -7.33 , $p = 5.76 \times 10^{-10}$) and mice ($H = 0.46 \pm 2.97 \times 10^{-4}$, $\beta = -2.91 \pm 0.34$, $T(112.57)$
504 $= -8.51$, $p = 8.65 \times 10^{-14}$).

505 Simulations from the bimodal inference model (based on the posterior model parameters
506 obtained in humans; see Methods for details) closely matched the empirical results outlined
507 above: Simulated perceptual decisions resulted from a competition of perceptual history with
508 incoming sensory signals (Figure 6A). Stimulus- and history-congruence were significantly

509 auto-correlated (Figure 6B-C), fluctuating in anti-phase as a scale-invariant process with a
510 1/f power law (Figure 6D-F). Simulated posterior certainty^{28,30,50} (i.e., the absolute of the
511 posterior log ratio $|L_t|$) showed a quadratic relationship to the mode of sensory processing
512 (Figure 6H), mirroring the relation of RTs and confidence reports to external and internal
513 biases in perception (Figure 2G-H and Figure 4G-H). Crucially, the overlap between empirical
514 and simulated data broke down when we removed the anti-phase oscillations (ω_{LLR} and/or
515 ω_ψ) or the accumulation of evidence over time (i.e., setting H to 0.5) from the bimodal
516 inference model (see Supplemental Figure S7-10).

517 To further probe the validity of the bimodal inference model, we tested whether posterior
518 model quantities could explain aspects of the behavioral data that the model was not fitted
519 to. First, we predicted that the posterior decision variable L_t not only encodes perceptual
520 choices (i.e., the variable used for model estimation), but should also predict the speed of
521 response and subjective confidence^{30,50}. Indeed, the estimated trial-wise posterior decision
522 certainty $|L_t|$ correlated negatively with RTs in humans ($\beta = -4.36 \times 10^{-3} \pm 4.64 \times 10^{-4}$,
523 $T(1.98 \times 10^6) = -9.41$, $p = 5.19 \times 10^{-21}$) and TDs mice ($\beta = -35.45 \pm 0.86$, $T(1.28 \times 10^6) =$
524 -41.13 , $p = 0$). Likewise, subjective confidence was positively correlated with the estimated
525 posterior decision certainty in humans ($\beta = 7.63 \times 10^{-3} \pm 8.32 \times 10^{-4}$, $T(2.06 \times 10^6) =$
526 9.18 , $p = 4.48 \times 10^{-20}$).

527 Second, the dynamic accumulation of information inherent to our model entails that biases
528 toward perceptual history are stronger when the posterior decision certainty at the preceding
529 trial is high^{30,31,54}. Due to the link between posterior decision certainty and confidence, we
530 reasoned that confident perceptual choices should be more likely to induce history-congruent
531 perception at the subsequent trial^{30,31}. Indeed, logistic regression indicated that history-
532 congruence was predicted by the posterior decision certainty $|L_{t-1}|$ (humans: $\beta = 8.22 \times 10^{-3}$
533 $\pm 1.94 \times 10^{-3}$, $z = 4.25$, $p = 2.17 \times 10^{-5}$; mice: $\beta = -3.72 \times 10^{-3} \pm 1.83 \times 10^{-3}$, $z =$
534 -2.03 , $p = 0.04$) and subjective confidence (humans: $\beta = 0.04 \pm 1.62 \times 10^{-3}$, $z = 27.21$, p

⁵³⁵ $= 4.56 \times 10^{-163}$) at the preceding trial.

⁵³⁶ In sum, computational modeling thus suggested that between-mode fluctuations are best
⁵³⁷ explained by two interlinked processes (Figure 1E): (i), the dynamic accumulation of infor-
⁵³⁸ mation across successive trials (i.e., following the estimated hazard rate H) and, (ii), ongoing
⁵³⁹ anti-phase oscillations in the impact of external and internal information (i.e., as determined
⁵⁴⁰ by ω_ψ and ω_{LLR}).

⁵⁴¹ **5.8 Bimodal inference improves learning and perceptual metacog-
542 nition in the absence of feedback**

⁵⁴³ Is there a computational benefit to be gained from temporarily down-regulating biases to-
⁵⁴⁴ ward preceding choices (Figure 2-3 B and C), instead of combining them with external
⁵⁴⁵ sensory information at a constant weight (Supplemental Figure S7)? In their adaptive func-
⁵⁴⁶ tion for perceptual decision-making, internal predictions critically depend on error-driven
⁵⁴⁷ learning to remain aligned with the current state of the world⁵⁶. Yet when the same network
⁵⁴⁸ processes external and internal information in parallel, inferences may become circular and
⁵⁴⁹ maladaptive⁵⁷: Ongoing decision-related activity may be distorted by noise in external sen-
⁵⁵⁰ sory signals that are fed forward from the periphery or, alternatively, by aberrant internal
⁵⁵¹ predictions about the environment that are fed back from higher cortical levels^{18,57}.

⁵⁵² Purely parallel processing therefore creates at least two challenges for perception: First,
⁵⁵³ due to the sequential integration of inputs over time, internal predictions may progressively
⁵⁵⁴ override sensory information⁵⁵, leading to false inferences about the presented stimuli¹⁹. As a
⁵⁵⁵ consequence, purely parallel processing may also lead to false inferences about the statistical
⁵⁵⁶ regularities of volatile environments, where the underlying hazard rate $\hat{H} = P(s_t \neq s_{t-1})$
⁵⁵⁷ (i.e., the probability of a change in the state of the environment between two trials) may
⁵⁵⁸ change over time. In the absence of feedback, agents have to update the estimate about \hat{H}
⁵⁵⁹ solely on the grounds of their experience, which is determined by the posterior log ratio L_t .

560 Yet L_t depends not only on external information from the environment (the log likelihood
561 ratio LLR_t), but also on internal predictions, i.e., the log prior ratio L_{t-1} and the assumed
562 hazard rate H_t . This circularity may impair the ability to learn about changes in H that
563 occur in volatile environments (Figure 7A).

564 Second, purely parallel processing may also reduce the capacity to calibrate metacognitive
565 beliefs about ongoing changes in the precision at which sensory signals are encoded. In the
566 absence of feedback, agents depend on internal confidence signals⁵⁸ (i.e., the absolute of
567 the posterior log ratio $|L_t|$) to update beliefs M_t about the precision of sensory encoding
568 $\hat{M} = 1 - |s_t - u_t|$. While \hat{M} depends only on the likelihood LLR_t , the estimate M_t is
569 informed by the posterior L_t , which, in turn, is additionally modulated by the prior L_{t-1}
570 and H_t . Relying on internal predictions may thus distort metacognitive beliefs about the
571 precision of sensory encoding (Figure 7B). This problem becomes particularly relevant when
572 agents do not have full insight into the strength at which external and internal sources of
573 information contribute to perceptual inference (i.e., when confidence is high during both
574 internally- and externally-biased processing; Figure 2I-J; Figure 6G-H).

575 Here, we propose that bimodal inference may provide potential solutions to these problems
576 of circular inference. By intermittently decoupling the decision variable L_t from internal
577 predictions, between-mode fluctuations may create unambiguous error signals that adaptively
578 update estimates about the hazard rate \hat{H} and the precision of sensory encoding \hat{M} .

579 To illustrate this hypothesis, we simulated data for a total of 1000 participants who performed
580 binary perceptual decisions for a total of 20 blocks of 100 trials each. Each block differed
581 with respect to the true hazard rate \hat{H} (either 0.1, 0.3, 0.5, 0.7 or 0.9) and the sensitivity
582 parameter α (either 2, 3, 4, 5 or 6, determining \hat{M} via the absolute of the log likelihood ratio
583 $|LLR_t|$, Figure 7A-B, upper panel). Importantly, the synthetic participants did not receive
584 feedback on whether their perceptual decisions were correct.

585 We initialized each participant at a random value of H'_t (ranging from -0.25 to 0) and M'_t

586 (ranging from 0.25 to 2), which were transformed into the unit interval to yield trial-wise
587 estimates for H_t and M_t :

$$H_t = \frac{1}{1 + \exp(-(H'_t))} \quad (9)$$

$$M_t = \frac{1}{1 + \exp(-(M'_t))} \quad (10)$$

588 For each block, we generated stimuli s_t using the true hazard rate \hat{H} . Detected inputs u_t
589 were computed according to the block-wise sensitivity parameter α . Perceptual decisions
590 y_t were generated using the bimodal inference model with ($a_\psi = a_{LLR} = 1$, $\zeta = 1$ and f
591 between 0.05 and 0.15) and a unimodal control model ($a_\psi = a_{LLR} = 0$, $\zeta = 1$).

592 Leaning about H was driven by the error-term ϵ_H (Figure 7A, lower panel), reflecting the
593 difference between H_t and presence of a perceived change in the environment $|y_t - y_{t-1}|$:

$$\epsilon_H = |y_t - y_{t-1}| - H_t \quad (11)$$

594 Trial-wise updates to H were provided by a Resorla-Wagner-rule with learning rate β_H
595 (ranging from 0.05 to 0.25). Since y_t is more likely to accurately reflect the state of the
596 environment during external mode, updates to H were additionally modulated by ω_{LLR} :

$$H'_t = H'_{t-1} + \beta_H * \omega_{LLR} * \epsilon_H \quad (12)$$

597 Learning about \hat{M} was driven by error-term ϵ_M (Figure 7B, lower panel), reflecting the
598 difference between M_t and the posterior decision-certainty ($1 - |y_t - P(y_t = 1)|$):

$$\epsilon_M = (1 - |y_t - P(y_t = 1)|) - M_t \quad (13)$$

599 In analogy to H , we modeled trial-wise updates to M using a Rescorla-Wagner-rule with
 600 learning rate β_M (ranging from 0.05 to 0.25). Since y_t reflects the log likelihood ratio LLR_t
 601 (and therefore the precision of sensory encoding) more closely during external mode, updates
 602 to P were additionally modulated by ω_{LLR} :

$$M'_t = M'_{t-1} + \beta_M * \omega_{LLR} * \epsilon_M \quad (14)$$

603 For each participant, we simulated data using both the bimodal inference model described
 604 above and a unimodal control model, in which the between-mode fluctuations were removed
 605 by setting the amplitude parameter a to zero ($a_\psi = a_{LLR} = 0$). We compared the bimodal
 606 model of perceptual inference to the unimodal control model in terms of three dependent
 607 variables: the probability of stimulus-congruent perceptual choices, the error in the estimate
 608 about H (i.e., $|H - \hat{H}|$) and the error in the estimate about M (i.e., $|M - \hat{M}|$, with $\hat{M} =$
 609 $1 - (|s_t - u_t|)$).

610 We found that the bimodal inference model achieved lower stimulus-congruence in compar-
 611 ison to the unimodal control model ($\beta_1 = -6.71 \pm 0.03$, $T(8.42 \times 10^3) = -234.31$, $p =$
 612 0, Figure 7C). At the same time, the bimodal inference model yielded lower errors in the
 613 estimated hazard rate H ($\beta_1 = -2.94 \times 10^{-3} \pm 2.89 \times 10^{-4}$, $T(4.96 \times 10^3) = -10.18$, $p =$
 614 4.11×10^{-24}) and probability of stimulus-congruent choices P ($\beta_1 = -0.03 \pm 1.86 \times 10^{-4}$,
 615 $T(6.07 \times 10^3) = -137.75$, $p = 0$, Figure 7E). This suggests that between-mode fluctuations
 616 may play an adaptive role for learning and perceptual metacognition by supporting robust
 617 inferences about the statistical regularities of volatile environments and ongoing changes in
 618 the precision of sensory encoding.

619 Finally, we asked whether differences between the bimodal inference model the unimodal
 620 control model depend on the presence of external feedback. We predicted that the benefits
 621 of the bimodal inference model over the unimodal control model should be lost when feedback
 622 is provided: With feedback, the error terms that induce updates in H and P can be informed

623 by the true state of the environment s_t instead of posterior stimulus probabilities that are
624 distorted by circular inferences:

$$\epsilon_H = |s_t - s_{t-1}| - H_t \quad (15)$$

$$\epsilon_M = (1 - (|y_t - s_t|)) - M_t \quad (16)$$

625 We repeated the above simulation for each participant while providing feedback on a subset
626 of trials (10%, 20%, 30%, 40%, 50%, 60%, 70%, 80%, 90% and 100%). With increasing
627 availability of external feedback, the bimodal inference model lost its advantage over the
628 unimodal control model in terms of, (i), the estimated hazard rate H ($\beta_2 = 1.43 \times 10^{-3} \pm$
629 3.71×10^{-5} , $T(10 \times 10^3) = 38.58$, $p = 9.44 \times 10^{-304}$) and, (ii), the estimated probability of
630 stimulus-congruent choices M ($\beta_2 = 3.91 \times 10^{-3} \pm 2.51 \times 10^{-5}$, $T(10 \times 10^3) = 156.18$, $p =$
631 0, Figure 7F). This indicates that the benefits of bimodal inference are limited to situations
632 in which external feedback is sparse.

633 **6 Discussion**

634 This work investigates the behavioral and computational characteristics of ongoing fluctuations
635 in perceptual decision-making using two large-scale datasets in humans²⁰ and mice²¹.
636 We found that humans and mice cycle through recurring intervals of reduced sensitivity to
637 external sensory information, during which they relied more strongly on perceptual history,
638 i.e., an internal prediction that is provided by the sequence of preceding choices. Computational
639 modeling indicated that these slow periodicities are governed by two interlinked
640 factors: (i), the dynamic integration of sensory inputs over time and, (ii), anti-phase os-
641 cillations in the strength at which perception is driven by internal versus external sources
642 of information. These cross-species results suggest that ongoing fluctuations in perceptual
643 decision-making arise not merely as a noise-related epiphenomenon of limited processing
644 capacity, but result from a structured and adaptive mechanism that fluctuates between
645 internally- and externally-oriented modes of sensory analysis.

646 **6.1 Serial dependencies represent a pervasive and adaptive aspect
647 of perceptual decision-making in humans and mice**

648 A growing body of literature has highlighted that perception is modulated by preceding
649 choices^{22–28,30,32,33}. Our work provides converging cross-species evidence supporting the no-
650 tion that such serial dependencies are a pervasive and general phenomenon of perceptual
651 decision-making (Figures 2 and 4, Supplemental Figures 1 and 3). While introducing errors
652 in randomized psychophysical designs^{24,28,30,31,43} (Figures 2 and 4A), we found that percep-
653 tual history facilitates post-perceptual processes such as speed of response⁴² (Figure 2G) and
654 subjective confidence in humans (Figure 2I).

655 At the level of individual traits, increased biases toward preceding choices were associated
656 with reduced sensitivity to external information (Supplemental Figure 1C-D) and lower
657 metacognitive efficiency. When investigating how serial dependencies evolve over time, we

658 observed dynamic changes in strength of perceptual history (Figures 2 and 4B) that cre-
659 ated wavering biases toward internally- and externally-biased modes of sensory processing.
660 Between-mode fluctuations may thus provide a new explanation for ongoing changes in per-
661 ceptual performance⁶⁻¹¹.

662 In computational terms, serial dependencies may leverage the temporal autocorrelation of
663 natural environments^{31,48} to increase the efficiency of decision-making^{35,43}. Such temporal
664 smoothing⁴⁸ of sensory inputs may be achieved by updating dynamic predictions about the
665 world based on the sequence of noisy perceptual experiences^{22,31}, using algorithms such as
666 Kalman filtering³⁵, Hierarchical Gaussian filtering⁵⁹ or sequential Bayes^{25,42,54}. At the level
667 of neural mechanisms, the integration of internal with external information may be realized
668 by combining feedback from higher levels in the cortical hierarchy with incoming sensory
669 signals that are fed forward from lower levels⁶⁰.

670 Yet relying too strongly on serial dependencies may come at a cost: When accumulating over
671 time, internal predictions may eventually override external information, leading to circular
672 and false inferences about the state of the environment. In this work, we used model simula-
673 tions to show that, akin to the wake-sleep-algorithm in machine learning⁶¹, bimodal inference
674 may help to determine whether errors result from external input or from internally-stored pre-
675 dictions (Figure 7): During internal mode, sensory processing is more strongly constrained by
676 predictive processes that auto-encode the agent’s environment. Conversely, during external
677 mode, the network is driven predominantly by sensory inputs¹⁸. Between-mode fluctua-
678 tions may thus generate an unambiguous error signal that aligns internal predictions with
679 the current state of the environment in iterative test-update-cycles⁶¹. On a broader scale,
680 between-mode fluctuations may thus regulate the balance between feedforward versus feed-
681 back contributions to perception and thereby play a adaptive role in metacognition and
682 reality monitoring⁶².

683 **6.2 Arousal, attentional lapses, general response biases, insuffi-**
684 **cient training and metacognitive strategies as alternative ex-**
685 **planations for between-mode fluctuations**

686 These functional explanations for external and internal modes share the idea that, in order
687 to form stable internal predictions about the statistical properties of the world (e.g., tracking
688 the hazard rate of the environment) or metacognitive beliefs about processes occurring within
689 the agent (e.g., monitoring ongoing changes in the reliability of feedback and feedforward
690 processing), perception needs to temporarily disengage from internal predictions. By the
691 same token, they presuppose that fluctuations in mode occur at the level of perceptual
692 processing^{26,30,48,49}, and are not a passive phenomenon that is primarily driven by factors
693 situated up- or downstream of sensory analysis.

694 First, it may be argued that agents stereotypically repeat preceding choices when less alert.
695 Our analyses address this alternative driver of serial dependencies by building on the as-
696 sociation between RTs and arousal^{45,47}. We found that RTs do not map linearly onto the
697 mode of sensory processing, but become shorter for stronger biases toward both externally-
698 and internally-oriented mode (Figure 2G-H; Figure 4I). These observations argue against
699 the view that biases toward internal mode can be explained solely on the ground of ongoing
700 changes in tonic arousal or fatigue⁴⁴.

701 However, internal modes of sensory processing may also be attributed to attentional lapses⁶³,
702 which are caused by mind-wandering or mind-blanking and show a more complex relation to
703 RTs⁶³: While episodes of mind-blanking are characterized by an absence of subjective mental
704 activity, more frequent misses, a relative increase in slow waves over posterior EEG electrodes
705 and increased RTs, episodes of mind-wandering come along which rich inner experiences,
706 more frequent false alarms, a relative increase of slow-wave amplitudes over frontal electrodes
707 and decreased RTs⁶³.

708 Yet in contrast to gradual between-mode fluctuations, engaging in mind-wandering as
709 opposed to on-task attention seems to be an all-or-nothing phenomenon⁶³. In addition,
710 internally-biased processing did not increase either false alarms or misses, but induced
711 choice errors through an enhanced impact of perceptual history (Figure 2 and 4A) that
712 unfolded in alternating *streaks*^{9,13} of elevated stimulus- and history-congruence. Finally, the
713 increase in lapse rates during internal mode was not general, but history-dependent (Figures
714 3 and 5). While these observations clearly distinguishes between-mode fluctuations from
715 unspecific effects of lapses on decision-making, it remains an intriguing question for future
716 research how mind-wandering and -blanking can be differentiated from internally-oriented
717 modes of sensory processing in terms of their phenomenology, behavioral characteristics,
718 neural signatures and noise profiles^{10,63}.

719 Second, it may be proposed that humans and mice apply a metacognitive response strategy
720 that repeats preceding choices when less confident about their responses or when insufficiently
721 trained on the task. In humans, however, confidence increased for stronger biases toward
722 both external and internal mode (Figure 2I-J). For humans and mice, history-effects grew
723 stronger with increasing exposure to (and expertise in) the task (Supplemental Figure S6). In
724 addition, the existence of external and internal modes in murine perceptual decision-making
725 (Figure 4) implies that between-mode fluctuations do not depend exclusively on the rich
726 cognitive functions associated with human prefrontal cortex⁶⁴.

727 Third, our computational modeling results provide further evidence against both of the above
728 caveats: Simulations based on estimated model parameters closely matched the empirical
729 data (Figure 6), reproduced aspects of behavior it was not fitted to (such as trial-wise con-
730 fidence reports and RTs/TD for human and mice, respectively), and predicted that history-
731 congruent choices occur more frequently after high-confidence trials^{30,31}. These findings
732 suggest that perceptual choices and post-perceptual processes such as response behavior or
733 metacognition are jointly driven by a dynamic decision variable⁵⁰ that encodes uncertainty³¹

734 and is affected by ongoing changes in the integration of external versus internal information.

735 Of note, a recent computational study⁶⁵ has used a Hidden Markov Model (HMM) to in-

736 vestigate perceptual decision-making in the IBL database²¹. In analogy to our findings, the

737 authors observed that mice switch between temporally extended *strategies* that last for more

738 than 100 trials: During *engaged* states, perception was highly sensitive to external sensory

739 information. During *disengaged* states, in turn, choice behavior was prone to errors due

740 to enhanced biases toward one of the two perceptual outcomes⁶⁵. Despite the conceptual

741 differences to our approach (discrete states in a HMM that correspond to switches between

742 distinct decision-making strategies⁶⁵ vs. gradual changes in mode that emerge from sequen-

743 tial Bayesian inference and ongoing fluctuations in the impact of external relative to internal

744 information), it is tempting to speculate that engaged/disengaged states and between-mode

745 fluctuations might tap into the same underlying phenomenon.

746 **6.3 Dopamine-dependent changes in E-I-balance as a neural mech-**
747 **anism of between-mode fluctuations**

748 The link to self-organized criticality suggests that balanced cortical excitation and

749 inhibition⁶⁶ (E-I), which may enable efficient coding⁶⁶ by maintaining neural networks in

750 critical states⁶⁷, could provide a potential neural mechanism of between-mode fluctuations.

751 Previous work has proposed that the balance between glutamatergic excitation and GABA-

752 ergic inhibition is regulated by activity-dependent feedback through NMDA receptors⁶⁸.

753 Such NMDA-mediated feedback has been related to the integration of external inputs over

754 time⁶⁶ (model component (i), Figure 1E), thereby generating serial dependencies in decision-

755 making^{69–72}. Intriguingly, slow neuromodulation by dopamine enhances NMDA-dependent

756 signaling^{69,73,74} and fluctuates at slow frequencies^{75,76} that match the temporal dynamics of

757 between-mode fluctuations observed in humans (Figure 2) and mice (Figure 4). Ongoing

758 fluctuations in the impact of external versus internal information (model component (ii))

⁷⁵⁹ may thus be caused by phasic changes in E-I-balance that are induced by dopaminergic
⁷⁶⁰ neuromodulation.

⁷⁶¹ 6.4 Limitations and open questions

⁷⁶² In this study, we show that perception is attracted toward preceding choices in mice²¹ (Figure
⁷⁶³ 4A) and humans (Figure 2A; see Supplemental Figure S1 for analyses within individual
⁷⁶⁴ studies of the Confidence database²⁰). Of note, previous work has shown that perceptual
⁷⁶⁵ decision-making is concurrently affected by both attractive and repulsive serial biases that op-
⁷⁶⁶ erate on distinct time-scales and serve complementary functions for sensory processing^{27,77,78}.
⁷⁶⁷ Short-term attraction may serve the decoding of noisy sensory inputs and increase the stabil-
⁷⁶⁸ ity of perception, whereas long-term repulsion may enable efficient encoding and sensitivity
⁷⁶⁹ to change²⁷.

⁷⁷⁰ Importantly, repulsive biases operate in parallel to attractive biases²⁷ and are therefore
⁷⁷¹ unlikely to account for the ongoing changes in mode that occur in alternating cycles of
⁷⁷² internally- and externally-oriented processing. To elucidate whether attraction and repulsion
⁷⁷³ both fluctuate in their impact on perceptual decision-making will be an important task for
⁷⁷⁴ future research, since this would help to understand whether attractive and repulsive biases
⁷⁷⁵ are linked in terms of their computational function and neural implementation²⁷.

⁷⁷⁶ A second open question concerns the neurobiological underpinnings of ongoing changes in
⁷⁷⁷ mode. Albeit purely behavioral, our results tentatively suggest dopaminergic neuromodula-
⁷⁷⁸ tion of NMDA-mediated feedback as one potential mechanism of externally- and internally-
⁷⁷⁹ biased modes. Since between-mode fluctuations were found in both humans and mice, future
⁷⁸⁰ studies can apply both non-invasive and invasive neuro-imaging and electrophysiology to bet-
⁷⁸¹ ter understand the neural mechanisms that generate ongoing changes in mode in terms of
⁷⁸² neuro-anatomy, -chemistry and -circuitry.

⁷⁸³ Finally, establishing the neural correlates of externally- an internally-biased modes will en-

⁷⁸⁴ able exiting opportunities to investigate their role for adaptive perception and decision-
⁷⁸⁵ making. Causal interventions via pharmacological challenges, optogenetic manipulations or
⁷⁸⁶ (non-)invasive brain stimulation will help to understand whether between-mode fluctuations
⁷⁸⁷ are implicated in resolving credit-assignment problems^{18,79} or in calibrating metacognition
⁷⁸⁸ and reality monitoring⁶². Addressing these questions may therefore provide new insight
⁷⁸⁹ into the pathophysiology of hallucinations and delusions, which have been characterized by
⁷⁹⁰ an imbalance in the impact of external versus internal information^{60,80,81} and are typically
⁷⁹¹ associated with metacognitive failures and a departure from consensual reality⁸¹.

792 **7 Methods**

793 **7.1 Ressource availability**

794 **7.1.1 Lead contact**

795 Further information and requests for resources should be directed to and will be fulfilled by
796 the lead contact, Veith Weilnhammer (veith.weilnhammer@gmail.com).

797 **7.1.2 Materials availability**

798 This study did not generate new unique reagents.

799 **7.1.3 Data and code availability**

800 All custom code and behavioral data are available on <https://github.com/veithweilnhamer/Modes>. This manuscript was created using the *R Markdown* framework, which
801 integrates all data-related computations and the formatted text within one document. With
802 this, we wish to make our approach fully transparent and reproducible for reviewers and
803 future readers.

805 **7.2 Experimental model and subject details**

806 **7.2.1 Confidence database**

807 We downloaded the human data from the Confidence database²⁰ on 21/10/2020, limiting our
808 analyses to the database category *perception*. Within this category, we selected studies in
809 which participants made binary perceptual decision between two alternative outcomes (see
810 Supplemental Table 1). We excluded two studies in which the average perceptual accuracy
811 fell below 50%. After excluding these studies, our sample consisted of 21.05 million trials
812 obtained from 4317 human participants and 66 individual studies.

813 **7.2.2 IBL database**

814 We downloaded the murine data from the IBL database²¹ on 28/04/2021. We limited our
815 analyses to the *basic task*, during which mice responded to gratings that appeared with
816 equal probability in the left or right hemifield. Within each mouse, we excluded sessions in
817 which perceptual accuracy was below 80% for stimuli presented at a contrast $\geq 50\%$. After
818 exclusion, our sample consisted of 1.46 million trials obtained from $N = 165$ mice.

819 **7.3 Method details**

820 **7.3.1 Variables of interest**

821 **Primary variables of interest:** We extracted trial-wise data on the presented stimulus and
822 the associated perceptual decision. Stimulus-congruent choices were defined by perceptual
823 decisions that matched the presented stimuli. History-congruent choices were defined by
824 perceptual choices that matched the perceptual choice at the immediately preceding trial.
825 The dynamic probabilities of stimulus- and history-congruence were computed in sliding
826 windows of ± 5 trials.

827 The *mode* of sensory processing was derived by subtracting the dynamic probability of history-
828 congruence from the dynamic probability of stimulus-congruence, such that positive values
829 indicate externally-oriented processing, whereas negative values indicate internally-oriented
830 processing. When visualizing the relation of the mode of sensory processing to confidence,
831 response times or trial duration (see below), we binned the mode variable in 10% intervals.
832 We excluded bins than contained less than 0.5% of the total number of available data-points.

833 **Secondary variables of interest:** From the Confidence Database²⁰, we furthermore ex-
834 tracted trial-wise confidence reports and response times (RTs; if RTs were available for both
835 the perceptual decision and the confidence report, we only extracted the RT associated with
836 the perceptual decision). To enable comparability between studies, we normalized RTs and
837 confidence reports within individual studies using the *scale* R function. If not available for

838 a particular study, RTs and confidence reports were treated as missing variables. From the
839 IBL database²¹, we extracted trial durations (TDs) as defined by interval between stimulus
840 onset and feedback, which represents a coarse measure of RT²¹.

841 **Exclusion criteria for individual data-points:** For non-normalized data (TDs from the
842 IBL database²¹; d-prime, meta-dprime and M-ratio from the Confidence database²⁰ and
843 simulated confidence reports), we excluded data-points that differed from the median by
844 more than 3 x MAD (median absolute distance⁵²). For normalized data (RTs and confidence
845 reports from the Confidence database²⁰), we excluded data-points that differed from the
846 mean by more than 3 x SD (standard deviation).

847 7.3.2 Control variables

848 Next to the sequence of presented stimuli, we assessed the autocorrelation of task difficulty
849 as an alternative explanation for any autocorrelation in stimulus- and history-congruence.
850 For the Confidence Database²⁰, task difficulty was indicated by one of the following labels:
851 *Difficulty, Difference, Signal-to-Noise, Dot-Difference, Congruency, Coherence(-Level), Dot-*
852 *Proportion, Contrast(-Difference), Validity, Setsize, Noise-Level(-Degree) or Temporal Dis-*
853 *tance.* When none of the above was available for a given study, task difficulty was treated
854 as a missing variable. In analogy to RTs and confidence, difficulty levels were normalized
855 within individual studies. For the IBL Database²¹, task difficulty was defined by the contrast
856 of the presented grating.

857 7.3.3 Autocorrelations

858 For each participant, trial-wise autocorrelation coefficients were estimated using the R-
859 function *acf* with a maximum lag defined by the number of trials available per subject.
860 Autocorrelation coefficients are displayed against the lag (in numbers of trials, ranging from
861 1 to 20) relative to the index trial ($t = 0$, see Figure 2B-C, 4B-C and 6B-C). To account
862 for spurious autocorrelations that occur due to imbalances in the analyzed variables, we

863 estimated autocorrelations for randomly permuted data (100 iterations). For group-level
864 autocorrelations, we computed the differences between the true autocorrelation coefficients
865 and the mean autocorrelation observed for randomly permuted data and averaged across
866 participants.

867 At a given trial, group-level autocorrelation coefficients were considered significant when
868 linear mixed effects modeling indicated that the difference between real and permuted au-
869 tocorrelation coefficients was above zero at an alpha level of 0.05%. To test whether the
870 autocorrelation of stimulus- and history-congruence remained significant when controlling
871 for task difficulty and the sequence of presented stimuli, we added the respective autocorre-
872 lation as an additional factor to the linear mixed effects model that computed the group-level
873 statistics (see also *Mixed effects modeling*).

874 To assess autocorrelations at the level of individual participants, we counted the number of
875 subsequent trials (starting at the first trial after the index trial) for which less than 50% of
876 the permuted autocorrelation coefficients exceeded the true autocorrelation coefficient. For
877 example, a count of zero indicates that the true autocorrelation coefficients exceeded *less*
878 *than 50%* of the autocorrelation coefficients computed for randomly permuted data at the
879 first trial following the index trial. A count of five indicates that, for the first five trials
880 following the index trial, the true autocorrelation coefficients exceeded *more than 50%* of
881 the respective autocorrelation coefficients for the randomly permuted data; at the 6th trial
882 following the index trial, however, *less than 50%* of the autocorrelation coefficients exceeded
883 the respective permuted autocorrelation coefficients.

884 7.3.4 Spectral analysis

885 We used the R function *spectrum* to compute the spectral densities for the dynamic proba-
886 bilities of stimulus- and history-congruence as well as the phase (i.e., frequency-specific shift
887 between the two time-series ranging from 0 to 2π) and squared coherence (frequency-specific
888 variable that denotes the degree to which the shift between the two time-series is constant,

889 ranging from 0 to 100%). Periodograms were smoothed using modified Daniell smoothers at
890 a width of 50.

891 Since the dynamic probabilities of history- and stimulus-congruence were computed using
892 a sliding windows of ± 5 trials (i.e., intervals containing a total of 11 trials), we report the
893 spectral density, coherence and phase for frequencies below $1/11 \text{ } 1/N_{trials}$. Spectral densities
894 have one value per subject and frequency (data shown in Figures 2D and 4D). To assess the
895 relation between stimulus- and history-congruence in this frequency range, we report average
896 phase and average squared coherence for all frequencies below $1/11 \text{ } 1/N_{trials}$ (i.e., one value
897 per subject; data shown in Figure 2E-F and 4E-F).

898 Since the data extracted from the Confidence Database²⁰ consist of a large set of individual
899 studies that differ with respect to inter-trial intervals, we defined the variable *frequency* in the
900 dimension of cycles per trial $1/N_{trials}$ rather than cycles per second (Hz). For consistency,
901 we chose $1/N_{trials}$ as the unit of frequency for the IBL database²¹ as well.

902 7.4 Quantification and statistical procedures

903 All aggregate data are reported and displayed with errorbars as mean \pm standard error of
904 the mean.

905 7.4.1 Mixed effects modeling

906 Unless indicated otherwise, we performed group-level inference using the R-packages *lmer*
907 and *afex* for linear mixed effects modeling and *glmer* with a binomial link-function for logistic
908 regression. We compared models based on Akaike Information Criteria (AIC). To account for
909 variability between the studies available from the Confidence Database²⁰, mixed modeling
910 was conducted using random intercepts defined for each study. To account for variability
911 across experimental session within the IBL database²¹, mixed modeling was conducted using
912 random intercepts defined for each individual session. When multiple within-participant

913 datapoints were analyzed, we estimated random intercepts for each participant that were
914 *nested* within the respective study of the Confidence database²⁰. By analogy, for the IBL
915 database²¹, we estimated random intercepts for each session that were nested within the
916 respective mouse. We report β values referring to the estimates provided by mixed effects
917 modeling, followed by the respective T statistic (linear models) or z statistic (logistic models).

918 The effects of stimulus- and history-congruence on RTs and confidence reports (Figure 2,
919 4 and 6, subpanels G-I) were assessed in linear mixed effects models that tested for main
920 effects of both stimulus- and history-congruence as well as the between-factor interaction.
921 Thus, the significance of any effect of history-congruence on RTs and confidence reports was
922 assessed while controlling for the respective effect of stimulus-congruence (and vice versa).

923 **7.4.2 Psychometric function**

924 We obtained psychometric curves by fitting the following error function to the behavioral
925 data:

$$y_p = \gamma + (1 - \gamma - \delta) * (\operatorname{erf}(\frac{s_w + \mu}{t}) + 1)/2 \quad (17)$$

926 We used a maximum likelihood procedure to predict individual choices y (outcome A: $y = 0$;
927 outcome B: $y = 1$) from the choice probability y_p . In humans, we computed s_w multiplying
928 the inputs s (stimulus A: 0; outcome B: 1) with the task difficulty D_b (binarized across 7
929 levels):

$$s_w = (s - 0.5) * D_b \quad (18)$$

930 In mice, s_w was defined by the respective stimulus contrast in the two hemifields:

$$s_w = \operatorname{Contrast}_{Right} - \operatorname{Contrast}_{Left} \quad (19)$$

931 Parameters of the psychometric error function were fitted using the R-package *optimx*. The
932 psychometric error function was defined via the parameters γ (lower lapse; lower bound =
933 0, upper bound = 0.5), δ (upper lapse; lower bound = 0, upper bound = 0.5), μ (bias; lower
934 bound humans = -5; upper bound humans = 5, lower bound mice = -0.5, upper bound mice
935 = 0.5) and threshold t (lower bound humans = 0.5, upper bound humans = 25; lower bound
936 mice = 0.01, upper bound mice = 1.5).

937 **7.4.3 Computational modeling**

938 **Model definition:** Our modeling analysis is an extension of a model proposed by Glaze
939 et al.⁵⁴, who defined a normative account of evidence accumulation for decision-making. In
940 this model, trial-wise choices are explained by applying Bayes theorem to infer moment-
941 by-moment changes in the state of environment from trial-wise noisy observations across
942 trials.

943 Following Glaze et al.⁵⁴, we applied Bayes rule to compute the posterior evidence for the
944 two alternative choices (i.e., the log posterior ratio L) from the sensory evidence available
945 at time-point t (i.e., the log likelihood ratio LLR) with the prior probability ψ , **weighted**
946 **by the respective precision terms ω_{LLR} and ω_ψ :**

$$L_t = LLR_t * \omega_{LLR} + \psi_t(L_{t-1}, H) * \omega_\psi \quad (20)$$

947 In the trial-wise design studied here, a transition between the two states of the environment
948 (i.e., the sources generating the noisy observations available to the participant) can occur
949 at any time. Despite the random nature of the psychophysical paradigms studied here^{20,21},
950 humans and mice showed significant biases toward preceding choices (Figure 2A and 4A).
951 We thus assumed that the prior probability of the two possible outcomes depends on the
952 posterior choice probability at the preceding trial and the hazard rate H assumed by the
953 participant. Following Glaze et al.⁵⁴, the prior ψ is thus computed as follows:

$$\psi_t(L_{t-1}, H) = L_{t-1} + \log\left(\frac{1-H}{H} + \exp(-L_{t-1})\right) - \log\left(\frac{1-H}{H} + \exp(L_{t-1})\right) \quad (21)$$

954 In this model, humans, mice and simulated agents make perceptual choices based on noisy
 955 observations u . These are computed by applying a sensitivity parameter α to the content of
 956 external sensory information s . For humans, we defined the input s by the two alternative
 957 states of the environment (stimulus A: $s = 0$; stimulus B: $s = 1$), which generated the
 958 observations u through a sigmoid function that applied a sensitivity parameter α :

$$u_t = \frac{1}{1 + \exp(-\alpha * (s_t - 0.5))} \quad (22)$$

959 In mice, the inputs s were defined by the respective stimulus contrast in the two hemifields:

$$s_t = \text{Contrast}_{Right} - \text{Contrast}_{Left} \quad (23)$$

960 As in humans, we derived the input u by applying a sigmoid function with a sensitivity
 961 parameter α to input s :

$$u_t = \frac{1}{1 + \exp(-\alpha * s_t)} \quad (24)$$

962 For humans, mice and in simulations, the log likelihood ratio LLR was computed from u as
 963 follows:

$$LLR_t = \log\left(\frac{u_t}{1 - u_t}\right) \quad (25)$$

964 To allow for long-range autocorrelation in stimulus- and history-congruence (Figure 2B and
 965 4B), our modeling approach differed from Glaze et al.⁵⁴ in that it allowed for systematic
 966 fluctuation in the impact of sensory information (i.e., LLR) and the prior probability of

967 choices ψ on the posterior probability L . This was achieved by multiplying the log likelihood
 968 ratio and the log prior ratio with coherent anti-phase fluctuations according to $\omega_{LLR} =$
 969 $a_{LLR} * \sin(f * t + phase) + 1$ and $\omega_\psi = a_\psi * \sin(f * t + phase + \pi) + 1$.

970 **Model fitting:** In model fitting, we predicted the trial-wise choices y_t (option A: 0; option
 971 B: 1) from inputs s . To this end, we minimized the log loss between y_t and the choice
 972 probability y_{pt} in the unit interval. y_{pt} was derived from L_t using a sigmoid function defined
 973 by the inverse decision temperature ζ :

$$y_{pt} = \frac{1}{1 + \exp(-\zeta * L_t)} \quad (26)$$

974 This allowed us to infer the free parameters H (lower bound = 0, upper bound = 1; human
 975 posterior = $0.45 \pm 4.8 \times 10^{-5}$; murine posterior = $0.46 \pm 2.97 \times 10^{-4}$), α (lower bound
 976 = 0, upper bound = 5; human posterior = $0.5 \pm 1.12 \times 10^{-4}$; murine posterior = $1.06 \pm$
 977 2.88×10^{-3}), a_ψ (lower bound = 0, upper bound = 10; human posterior = $1.44 \pm 5.27 \times 10^{-4}$;
 978 murine posterior = $1.71 \pm 7.15 \times 10^{-3}$), amp_{LLR} (lower bound = 0, upper bound = 10;
 979 human posterior = $0.5 \pm 2.02 \times 10^{-4}$; murine posterior = $0.39 \pm 1.08 \times 10^{-3}$), frequency f
 980 (lower bound = 1/40, upper bound = 1/5; human posterior = $0.11 \pm 1.68 \times 10^{-5}$; murine
 981 posterior = $0.11 \pm 1.63 \times 10^{-4}$), p (lower bound = 0, upper bound = $2*\pi$; human posterior =
 982 $2.72 \pm 4.41 \times 10^{-4}$; murine posterior = $2.83 \pm 3.95 \times 10^{-3}$) and inverse decision temperature
 983 ζ (lower bound = 1, upper bound = 10; human posterior = $4.63 \pm 1.95 \times 10^{-4}$; murine
 984 posterior = $4.82 \pm 3.03 \times 10^{-3}$) using the R-function *optimx*.

985 To validate our model, we correlated individual posterior parameter estimates with the re-
 986 spective conventional variables. We assumed that, (i), the estimated hazard rate H should
 987 correlate negatively with the frequency of history-congruent choices and that, (ii), the es-
 988 timated α should correlate positively with the frequency of stimulus-congruent choices. In
 989 addition, we tested whether the posterior decision certainty (i.e. the absolute of the pos-
 990 terior log ratio) correlated negatively with RTs and positively with subjective confidence.

991 This allowed us to assess whether our model could explain aspects of the data it was not
992 fitted to (i.e., RTs and confidence). Finally, we used simulations (see below) to show that
993 all model components, including the anti-phase oscillations governed by a_ψ , a_{LLR} , f and p ,
994 were necessary for our model to reproduce the empirical data observed for the Confidence
995 database²⁰ and IBL database²¹.

996 **Model simulation 1: Data recovery:** We used the posterior model parameters observed
997 for humans (H , α , a_ψ , a_{LLR} and f) to define individual parameters for simulation in 4317
998 simulated participants (i.e., equivalent to the number of human participants). For each
999 participant, the number of simulated choices was drawn from a uniform distribution ranging
1000 from 300 to 700 trials. Inputs s were drawn at random for each trial, such that the sequence
1001 of inputs to the simulation did not contain any systematic seriality. Noisy observations u
1002 were generated by applying the posterior parameter α to inputs s , thus generating stimulus-
1003 congruent choices in $71.36 \pm 2.6 \times 10^{-3}\%$ of trials. Choices were simulated based on the
1004 trial-wise choice probabilities y_p . Simulated data were analyzed in analogy to the human
1005 and murine data. As a substitute of subjective confidence, we computed the absolute of the
1006 trial-wise posterior log ratio $|L|$ (i.e., the posterior decision certainty).

1007 **Model simulation 2: Testing the adaptive benefits of bimodal inference:** In contrast
1008 to the model applied to the behavioral data, our second set of simulations considered a
1009 situation in which agents learn about the properties of the environment from experience.
1010 We modeled dynamic updates in the trial-wise estimates H_t about the true hazard rate
1011 $\hat{H} = P(s_t \neq s_{t-1})$ and trial-wise estimates M_t about the precision of sensory encoding
1012 $\hat{M} = 1 - (|s_t - u_t|)$.

1013 In the absence of feedback, leaning about \hat{H} was driven by the error-term ϵ_H , which reflected
1014 the difference between the currently assumed hazard rate H_t and the presence of a *perceived*
1015 change in the environment $|y_t - y_{t-1}|$:

$$\epsilon_H = |y_t - y_{t-1}| - H_t \quad (27)$$

1016 In the presence of feedback, ϵ_H reflected the difference between the currently assumed hazard
 1017 rate H_t and an presence of a *true* change in the environment $|s_t - s_{t-1}|$:

$$\epsilon_H = |s_t - s_{t-1}| - H_t \quad (28)$$

1018 In the absence of feedback, learning about \hat{M} was driven by the error-term ϵ_M , reflecting
 1019 the difference between M_t and the posterior decision-certainty $(1 - |y_t - P(y_t = 1)|)$:

$$\epsilon_M = (1 - |y_t - P(y_t = 1)|) - M_t \quad (29)$$

1020 In the presence of feedback, ϵ_M reflected the difference between M_t and the stimulus-
 1021 congruence of the current response $(1 - (|y_t - s_t|))$:

$$\epsilon_M = (1 - (|y_t - s_t|)) - M_t \quad (30)$$

1022 Updates to H and M were computed in logit-space using a Rescorla-Wagner-rule with learn-
 1023 ing rates defined by the product of $\beta_{H/M}$ and ω_{LLR} . H_t and M_t are computed by trans-
 1024 forming H'_t and M'_t into the unit interval using a sigmoid function:

$$H'_t = H'_{t-1} + \beta_H * \omega_{LLR} * \epsilon_H \quad (31)$$

$$H_t = \frac{1}{1 + \exp(-(H'_t))} \quad (32)$$

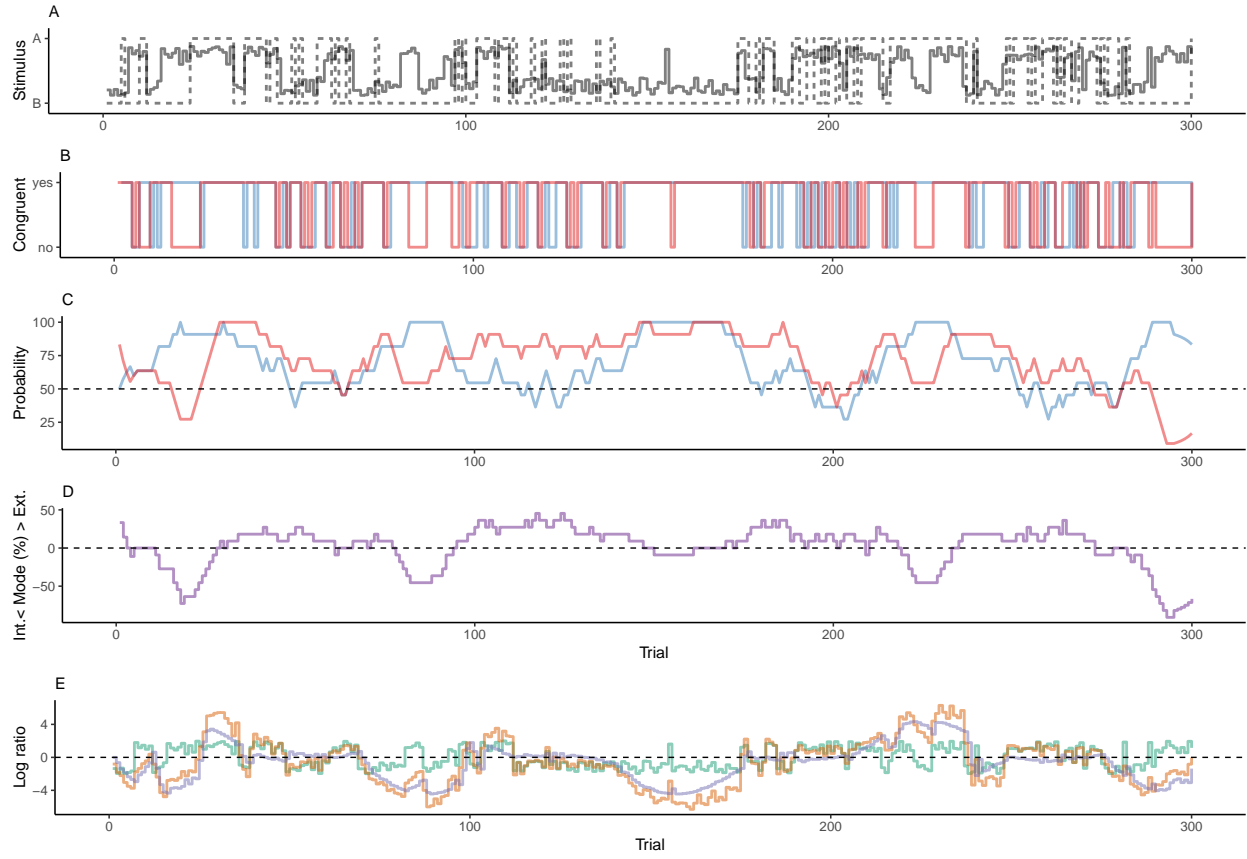
$$M'_t = M'_{t-1} + \beta_M * \omega_{LLR} * \epsilon_M \quad (33)$$

$$M_t = \frac{1}{1 + \exp(-(M'_t))} \quad (34)$$

1025 We simulated data for a total of 1000 participants for a total of 20 blocks of 100 trials each.
 1026 Each block differed with respect to the true hazard rate \hat{H} (either 0.1, 0.3, 0.5, 0.7 or 0.9)
 1027 and the sensitivity parameter α (either 2, 3, 4, 5 or 6, corresponding to values of \hat{M} of 0.73,
 1028 0.82, 0.88, 0.92 or 0.95). Across participants, model parameters were set as follows: H'_1
 1029 initialized at random in a unit interval between -0.25 to 0; P'_1 initialized at random in a
 1030 unit interval between 0.25 to 2; $a = 1$; f between 0.05 and 0.15 $1/N_{trials}$; $\zeta = 1$; β_H and
 1031 β_M between 0.05 and 0.25. For each participant, we ran separate simulations with external
 1032 feedback provided in 0%, 10%, 20%, 30%, 40%, 50%, 60%, 70%, 80%, 90% and 100% of
 1033 trials.

1034 **8 Figures**

1035 **8.1 Figure 1**



1036

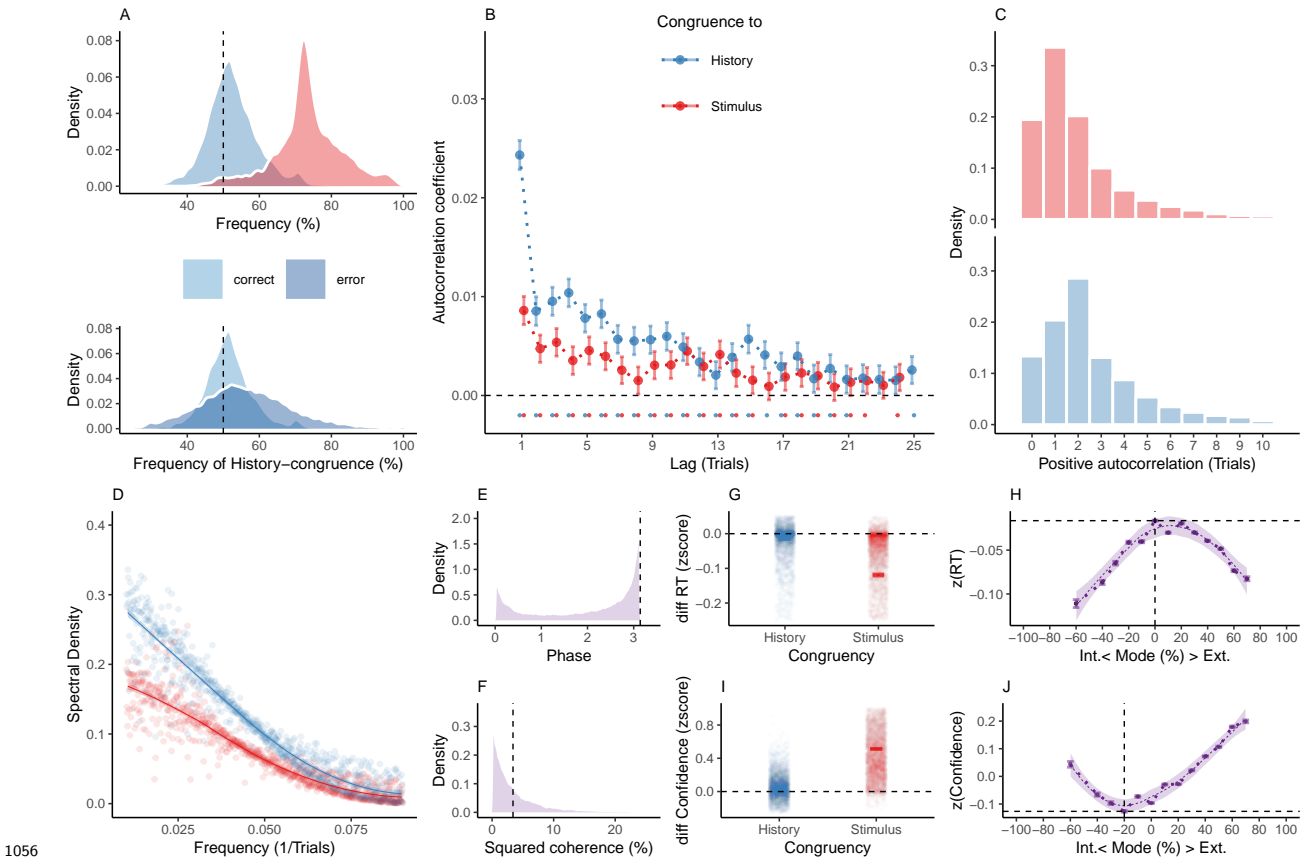
1037 **Figure 1. Concept.**

- 1038 A. In binary perceptual decision-making, a participant is presented with stimuli from two
1039 categories (A vs. B; dotted line) and reports consecutive perceptual choices via button presses
1040 (solid line). All panels below refer to this example data.
- 1041 B. When the response matched the external stimulus information (i.e., overlap between
1042 dotted and solid line in panel A), perceptual choices are *stimulus-congruent* (red line). When
1043 the response matches the response at the preceding trial, perceptual choices are *history-
1044 congruent* (blue line).
- 1045 C. The dynamic probabilities of stimulus- and history-congruence (i.e., computed in sliding
1046 windows of ± 5 trials) fluctuate over time.

₁₀₄₇ D. The *mode* of perceptual processing is derived by computing the difference between the
₁₀₄₈ dynamic probabilities of stimulus- and history-congruence. Values above 0% indicate a
₁₀₄₉ bias toward external information, whereas values below 0% indicate a bias toward internal
₁₀₅₀ information.

₁₀₅₁ E. In computational modeling, internal mode is caused by an enhanced impact of perceptual
₁₀₅₂ history. This causes the posterior (black line) to be close to the prior (blue line). Conversely,
₁₀₅₃ during external mode, the posterior is close to the sensory information (log likelihood ratio,
₁₀₅₄ red line).

1055 **8.2 Figure 2**



1056 **Figure 2. Internal and external modes in human perceptual decision-making.**

1057 A. In humans, perception was stimulus-congruent in $73.46\% \pm 0.15\%$ (in red) and history-congruent in $52.7\% \pm 0.12\%$ of trials (in blue; upper panel). History-congruent perceptual choices were more frequent when perception was stimulus-incongruent (i.e., on *error* trials; lower panel), indicating that history effects impair performance in randomized psychophysical designs.

1058 B. Relative to randomly permuted data, we found highly significant autocorrelations of stimulus-congruence and history-congruence (dots indicate intercepts $\neq 0$ in trial-wise linear mixed effects modeling at $p < 0.05$). Across trials, the autocorrelation coefficients were best fit by an exponential function (adjusted R^2 for stimulus-congruence: 0.53; history-congruence: 0.71) as compared to a linear function (adjusted R^2 for stimulus-congruence: 0.52; history-congruence: 0.49).

1069 C. Here, we depict the number of consecutive trials at which autocorrelation coefficients
1070 exceeded the respective autocorrelation of randomly permuted data within individual partic-
1071 ipants. For stimulus-congruence (upper panel), the lag of positive autocorrelation amounted
1072 to $3.24 \pm 2.39 \times 10^{-3}$ on average, showing a peak at trial t+1 after the index trial. For
1073 history-congruence (lower panel), the lag of positive autocorrelation amounted to $4.87 \pm$
1074 3.36×10^{-3} on average, peaking at trial t+2 after the index trial.

1075 D. The smoothed probabilities of stimulus- and history-congruence (sliding windows of ± 5
1076 trials) fluctuated as **a scale-invariant process with a 1/f power law**, i.e., at power
1077 densities that were inversely proportional to the frequency.

1078 E. The distribution of phase shift between fluctuations in stimulus- and history-congruence
1079 peaked at half a cycle (π denoted by dotted line).

1080 F. The average squared coherence between fluctuations in stimulus- and history-congruence
1081 (black dottet line) amounted to $6.49 \pm 2.07 \times 10^{-3}\%$

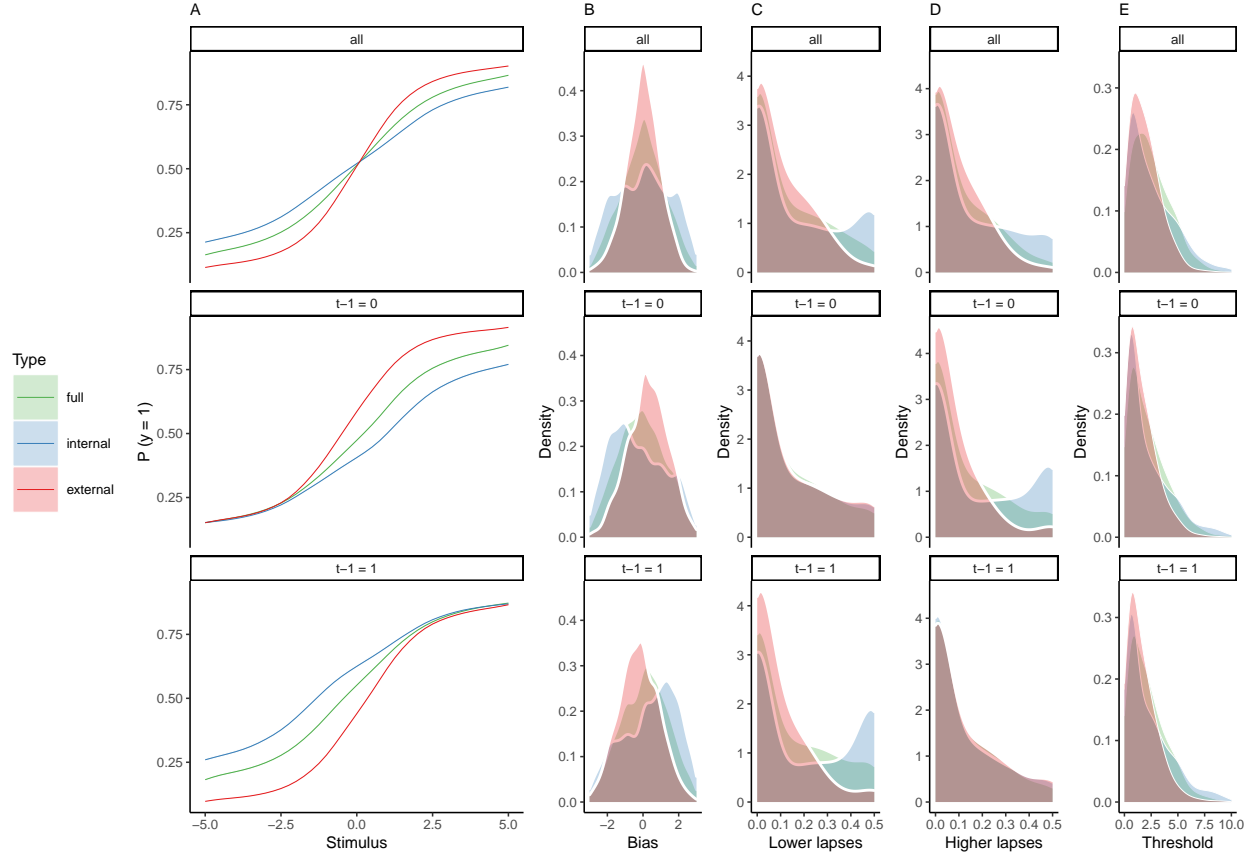
1082 G. We observed faster response times (RTs) for both stimulus-congruence (as opposed to
1083 stimulus-incongruence, $\beta = -0.14 \pm 1.61 \times 10^{-3}$, $T(1.99 \times 10^6) = -85.91$, $p = 0$) and history-
1084 congruence ($\beta = -9.73 \times 10^{-3} \pm 1.38 \times 10^{-3}$, $T(1.99 \times 10^6) = -7.06$, $p = 1.66 \times 10^{-12}$).

1085 H. The mode of perceptual processing (i.e., the difference between the smoothed probability
1086 of stimulus- vs. history-congruence) showed a quadratic relationship to RTs, with faster
1087 response times for stronger biases toward both external sensory information and internal
1088 predictions provided by perceptual history ($\beta_2 = -19.86 \pm 0.52$, $T(1.98 \times 10^6) = -38.43$,
1089 $p = 5 \times 10^{-323}$). The horizontal and vertical dotted lines indicate maximum RT and the
1090 associated mode, respectively.

1091 I. Confidence was enhanced for both stimulus-congruence (as opposed to stimulus-
1092 incongruence, $\beta = 0.48 \pm 1.38 \times 10^{-3}$, $T(2.06 \times 10^6) = 351.89$, $p = 0$) and history-congruence
1093 ($\beta = 0.04 \pm 1.18 \times 10^{-3}$, $T(2.06 \times 10^6) = 36.86$, $p = 2.93 \times 10^{-297}$).

¹⁰⁹⁴ J. In analogy to RTs, we found a quadratic relationship between the mode of perceptual pro-
¹⁰⁹⁵ cessing and confidence, which increased when both externally- and internally-biased modes
¹⁰⁹⁶ grew stronger ($\beta_2 = 39.3 \pm 0.94$, $T(2.06 \times 10^6) = 41.95$, $p = 0$). The horizontal and vertical
¹⁰⁹⁷ dotted lines indicate minimum confidence and the associated mode, respectively.

1098 **8.3 Figure 3**



1099 **Figure 3. Full and history-conditioned psychometric functions across modes in**
1100 **humans.**

1102 A. Here, we show average psychometric functions for the full dataset (upper panel) and
1103 conditioned on perceptual history ($y_{t-1} = 1$ and $y_{t-1} = 0$; middle and lower panel) across
1104 modes (green line) and for internal mode (blue line) and external mode (red line) separately.

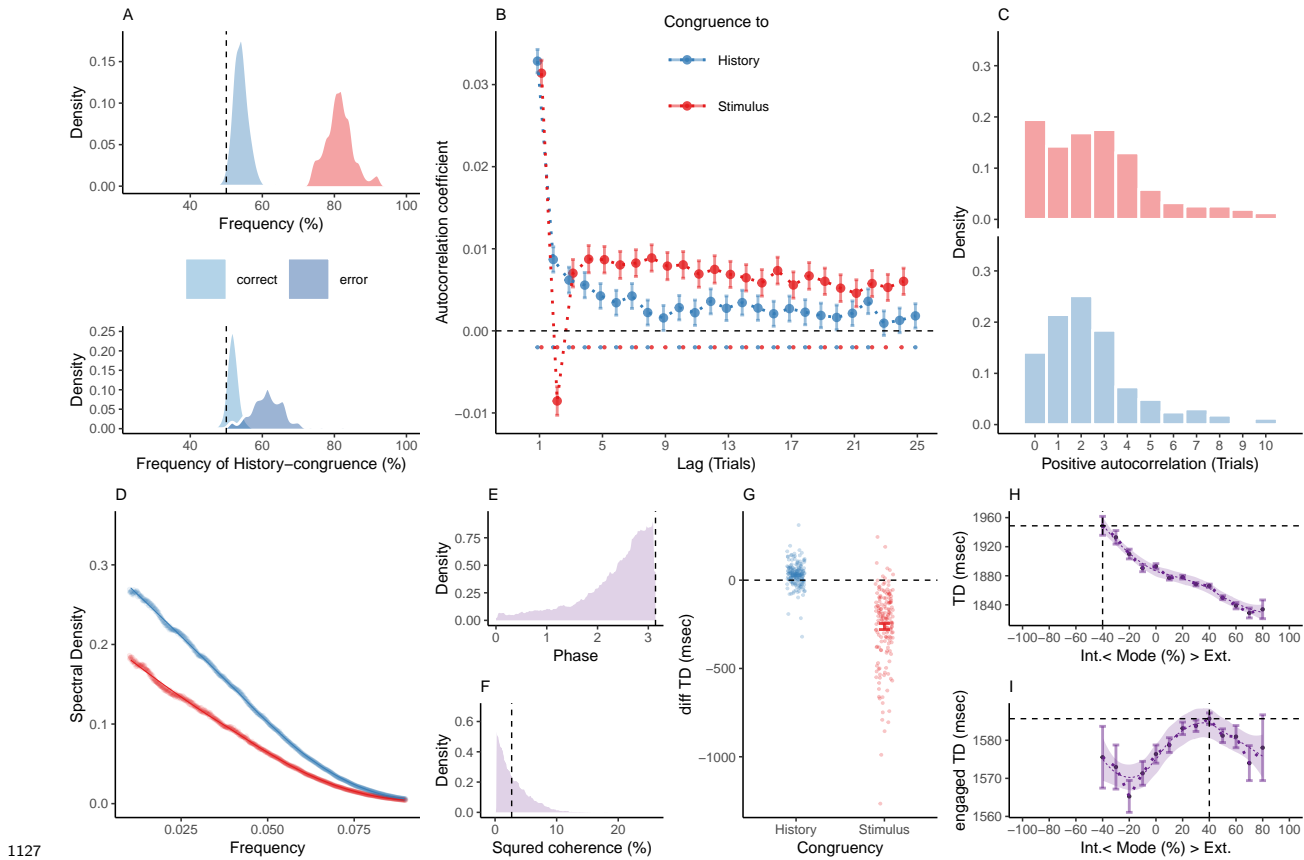
1105 B. Across the full dataset, biases μ were distributed around zero ($\beta_0 = 7.37 \times 10^{-3} \pm$
1106 0.09, $T(36.8) = 0.08$, $p = 0.94$; upper panel), with larger absolute biases $|\mu|$ for internal
1107 as compared to external mode ($\beta_0 = -0.62 \pm 0.07$, $T(45.62) = -8.38$, $p = 8.59 \times 10^{-11}$;
1108 controlling for differences in lapses and thresholds). When conditioned on perceptual history,
1109 we observed negative biases for $y_{t-1} = 0$ ($\beta_0 = 0.56 \pm 0.12$, $T(43.39) = 4.6$, $p = 3.64 \times 10^{-5}$;
1110 middle panel) and positive biases for $y_{t-1} = 1$ ($\beta_0 = 0.56 \pm 0.12$, $T(43.39) = 4.6$, $p =$
1111 3.64×10^{-5} ; lower panel).

₁₁₁₂ C. Lapse rates were higher in internal mode as compared to external mode ($\beta_0 = -0.05 \pm$
₁₁₁₃ 5.73×10^{-3} , $T(47.03) = -9.11$, $p = 5.94 \times 10^{-12}$; controlling for differences in biases and
₁₁₁₄ thresholds; see upper panel and subplot D). Importantly, the between-mode difference in
₁₁₁₅ lapses depended on perceptual history: We found no significant difference in lower lapses
₁₁₁₆ γ for $y_{t-1} = 0$ ($\beta_0 = 0.01 \pm 7.77 \times 10^{-3}$, $T(33.1) = 1.61$, $p = 0.12$; middle panel), but a
₁₁₁₇ significant difference for $y_{t-1} = 1$ ($\beta_0 = -0.11 \pm 0.01$, $T(40.11) = -9.59$, $p = 6.14 \times 10^{-12}$;
₁₁₁₈ lower panel).

₁₁₁₉ D. Conversely, higher lapses δ were significantly increased for $y_{t-1} = 0$ ($\beta_0 = -0.1 \pm 9.58 \times$
₁₁₂₀ 10^{-3} , $T(36.87) = -10.16$, $p = 3.06 \times 10^{-12}$; middle panel), but not for $y_{t-1} = 1$ ($\beta_0 = 0.01$
₁₁₂₁ $\pm 7.74 \times 10^{-3}$, $T(33.66) = 1.58$, $p = 0.12$; lower panel).

₁₁₂₂ E. The thresholds t were larger in internal as compared to external mode ($\beta_0 = -1.77 \pm$
₁₁₂₃ 0.25 , $T(50.45) = -7.14$, $p = 3.48 \times 10^{-9}$; controlling for differences in biases and lapses)
₁₁₂₄ and were not modulated by perceptual history ($\beta_0 = 0.04 \pm 0.06$, $T(2.97 \times 10^3) = 0.73$, p
₁₁₂₅ $= 0.47$).

1126 **8.4 Figure 4**



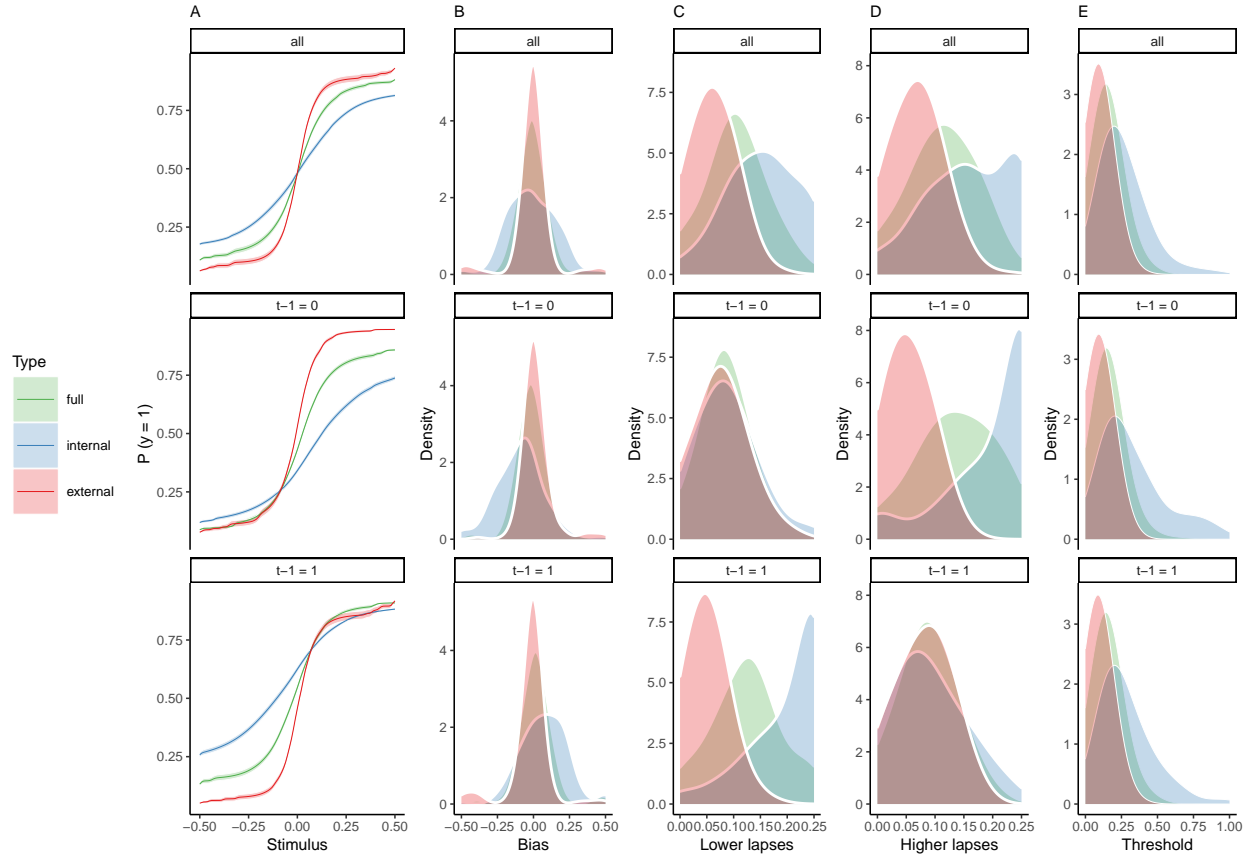
1127 **Figure 4. Internal and external modes in murine perceptual decision-making.**

1129 A. In mice, $81.37\% \pm 0.3\%$ of trials were stimulus-congruent (in red) and $54.03\% \pm 0.17\%$ of
1130 trials were history-congruent (in blue; upper panel). History-congruent perceptual choices
1131 were not a consequence of the experimental design, but a source of error, as they were more
1132 frequent on stimulus-incongruent trials (lower panel).

1133 B. Relative to randomly permuted data, we found highly significant autocorrelations of
1134 stimulus-congruence and history-congruence (dots indicate intercepts $\neq 0$ in trial-wise lin-
1135 ear mixed effects modeling at $p < 0.05$). Please note that the negative autocorrelation of
1136 stimulus-congruence at trial 2 was a consequence of the experimental design (see Supplemen-
1137 tal Figure 2D-F). As in humans, autocorrelation coefficients were best fit by an exponential
1138 function (adjusted R^2 for stimulus-congruence: 0.44; history-congruence: 0.52) as compared
1139 to a linear function (adjusted R^2 for stimulus-congruence: 3.16×10^{-3} ; history-congruence:

- ₁₁₄₀ 0.26).
- ₁₁₄₁ C. For stimulus-congruence (upper panel), the lag of positive autocorrelation was longer
₁₁₄₂ in comparison to humans (4.59 ± 0.06 on average). For history-congruence (lower panel),
₁₁₄₃ the lag of positive autocorrelation was slightly shorter relative to humans (2.58 ± 0.01 on
₁₁₄₄ average, peaking at trial $t+2$ after the index trial).
- ₁₁₄₅ D. In mice, the dynamic probabilities of stimulus- and history-congruence (sliding windows
₁₁₄₆ of ± 5 trials) fluctuated as **a scale-invariant process with a $1/f$ power law**.
- ₁₁₄₇ E. The distribution of phase shift between fluctuations in stimulus- and history-congruence
₁₁₄₈ peaked at half a cycle (π denoted by dotted line).
- ₁₁₄₉ F. The average squared coherence between fluctuations in stimulus- and history-congruence
₁₁₅₀ (black dotted line) amounted to $3.45 \pm 0.01\%$
- ₁₁₅₁ G. We observed shorter trial durations (TDs) for stimulus-congruence (as opposed to
₁₁₅₂ stimulus-incongruence, $\beta = -1.12 \pm 8.53 \times 10^{-3}$, $T(1.34 \times 10^6) = -131.78$, $p = 0$), but
₁₁₅₃ longer TDs for history-congruence ($\beta = 0.06 \pm 6.76 \times 10^{-3}$, $T(1.34 \times 10^6) = 8.52$, $p =$
₁₁₅₄ 1.58×10^{-17}).
- ₁₁₅₅ H. TDs decreased monotonically for stronger biases toward external mode ($\beta_1 = -4.16 \times 10^4$
₁₁₅₆ $\pm 1.29 \times 10^3$, $T(1.35 \times 10^6) = -32.31$, $p = 6.03 \times 10^{-229}$). The horizontal and vertical dotted
₁₁₅₇ lines indicate maximum TD and the associated mode, respectively.
- ₁₁₅₈ I. For TDs that differed from the median TD by no more than $1.5 \times \text{MAD}$ (median absolute
₁₁₅₉ distance⁵²), mice exhibited a quadratic component in the relationship between the mode
₁₁₆₀ of sensory processing and TDs ($\beta_2 = -1.97 \times 10^3 \pm 843.74$, $T(1.19 \times 10^6) = -2.34$, $p =$
₁₁₆₁ 0.02, Figure 4I). This explorative post-hoc analysis focuses on trials at which mice engage
₁₁₆₂ more swiftly with the experimental task. The horizontal and vertical dotted lines indicate
₁₁₆₃ maximum TD and the associated mode, respectively.

1164 **8.5 Figure 5**



1165 **Figure 5. Full and history-conditioned psychometric functions across modes in**
1166 **mice.**

1167 A. Here, we show average psychometric functions for the full IBL dataset (upper panel) and
1168 conditioned on perceptual history ($y_{t-1} = 1$ and $y_{t-1} = 0$; middle and lower panel) across
1169 modes (green line) and for internal mode (blue line) and external mode (red line) separately.
1170

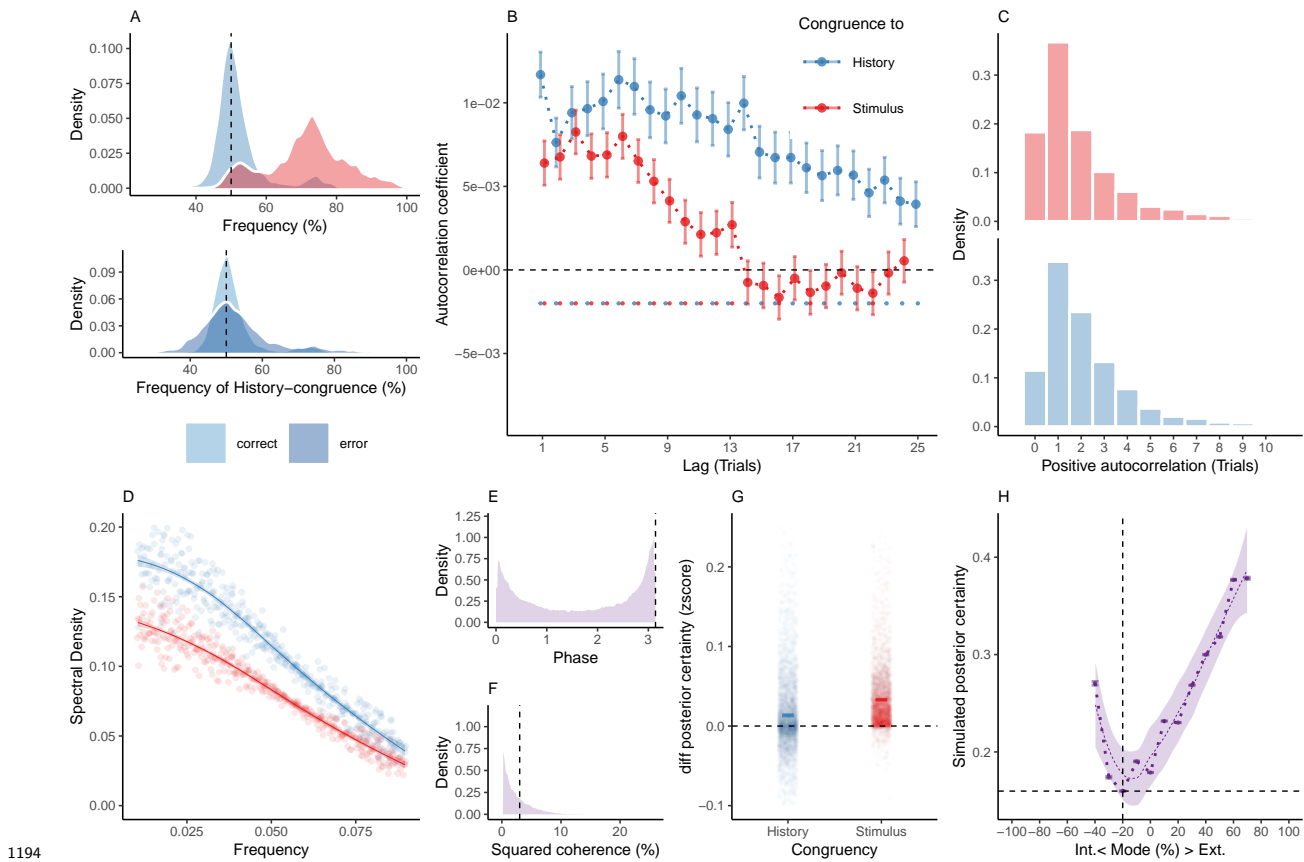
1171 B. Across the full dataset, biases μ were distributed around zero ($T(164) = 0.39$, $p = 0.69$;
1172 upper panel), with larger absolute biases $|\mu|$ for internal as compared to external mode ($\beta_0 =$
1173 -0.18 ± 0.03 , $T = -6.38$, $p = 1.77 \times 10^{-9}$; controlling for differences in lapses and thresholds).
1174 When conditioned on perceptual history, we observed negative biases for $y_{t-1} = 0$ ($T(164)$
1175 $= -1.99$, $p = 0.05$; middle panel) and positive biases for $y_{t-1} = 1$ ($T(164) = 1.91$, $p = 0.06$;
1176 lower panel).

₁₁₇₇ C. Lapse rates were higher in internal as compared to external mode ($\beta_0 = -0.11 \pm 4.39 \times$
₁₁₇₈ 10^{-3} , $T = -24.8$, $p = 4.91 \times 10^{-57}$; controlling for differences in biases and thresholds; upper
₁₁₇₉ panel, see also subplot D). For $y_{t-1} = 1$, the difference between internal and external mode
₁₁₈₀ was more pronounced for lower lapses γ ($T(164) = -18.24$, $p = 2.68 \times 10^{-41}$) as compared
₁₁₈₁ to higher lapses δ (see subplot D). In mice, lower lapses γ were significantly elevated during
₁₁₈₂ internal mode irrespective of the preceding perceptual choice (middle panel: lower lapses γ
₁₁₈₃ for $y_{t-1} = 0$; $T(164) = -2.5$, $p = 0.01$, lower panel: lower lapses γ for $y_{t-1} = 1$; $T(164) =$
₁₁₈₄ -32.44 , $p = 2.92 \times 10^{-73}$).

₁₁₈₅ D. For $y_{t-1} = 0$, the difference between internal and external mode was more pronounced
₁₁₈₆ for higher lapses δ ($T(164) = 21.44$, $p = 1.93 \times 10^{-49}$, see subplot C). Higher lapses were
₁₁₈₇ significantly elevated during internal mode irrespective of the preceding perceptual choice
₁₁₈₈ (middle panel: higher lapses δ for $y_{t-1} = 0$; $T(164) = -28.29$, $p = 5.62 \times 10^{-65}$ lower panel:
₁₁₈₉ higher lapses δ for $y_{t-1} = 1$; $T(164) = -2.65$, $p = 8.91 \times 10^{-3}$;).

₁₁₉₀ E. Thresholds t were higher in internal as compared to external mode ($\beta_0 = -0.28 \pm 0.04$,
₁₁₉₁ $T = -7.26$, $p = 1.53 \times 10^{-11}$; controlling for differences in biases and lapses) and were not
₁₁₉₂ modulated by perceptual history ($T(164) = 0.94$, $p = 0.35$).

1193 **8.6 Figure 6**



1194 **Figure 6. Internal and external modes in simulated perceptual decision-making.**

1195 A. Simulated perceptual choices were stimulus-congruent in $71.36\% \pm 0.17\%$ (in red) and
 1196 history-congruent in $51.99\% \pm 0.11\%$ of trials (in blue; $T(4.32 \times 10^3) = 17.42, p = 9.89 \times 10^{-66}$;
 1197 upper panel). Due to the competition between stimulus- and history-congruence, history-
 1198 congruent perceptual choices were more frequent when perception was stimulus-incongruent
 1199 (i.e., on *error* trials; $T(4.32 \times 10^3) = 11.19, p = 1.17 \times 10^{-28}$; lower panel) and thus impaired
 1200 performance in the randomized psychophysical design simulated here.

1201 B. At the simulated group level, we found significant autocorrelations in both stimulus-
 1202 congruence (13 consecutive trials) and history-congruence (30 consecutive trials).

1203 C. On the level of individual simulated participants, autocorrelation coefficients exceeded the
 1204 autocorrelation coefficients of randomly permuted data within a lag of $2.46 \pm 1.17 \times 10^{-3}$

₁₂₀₆ trials for stimulus-congruence and $4.24 \pm 1.85 \times 10^{-3}$ trials for history-congruence.

₁₂₀₇ D. The smoothed probabilities of stimulus- and history-congruence (sliding windows of ± 5
₁₂₀₈ trials) fluctuated as a **scale-invariant process with a $1/f$ power law**, i.e., at power den-
₁₂₀₉ sities that were inversely proportional to the frequency (power $\sim 1/f^\beta$; stimulus-congruence:
₁₂₁₀ $\beta = -0.81 \pm 1.18 \times 10^{-3}$, $T(1.92 \times 10^5) = -687.58$, $p = 0$; history-congruence: $\beta = -0.83$
₁₂₁₁ $\pm 1.27 \times 10^{-3}$, $T(1.92 \times 10^5) = -652.11$, $p = 0$).

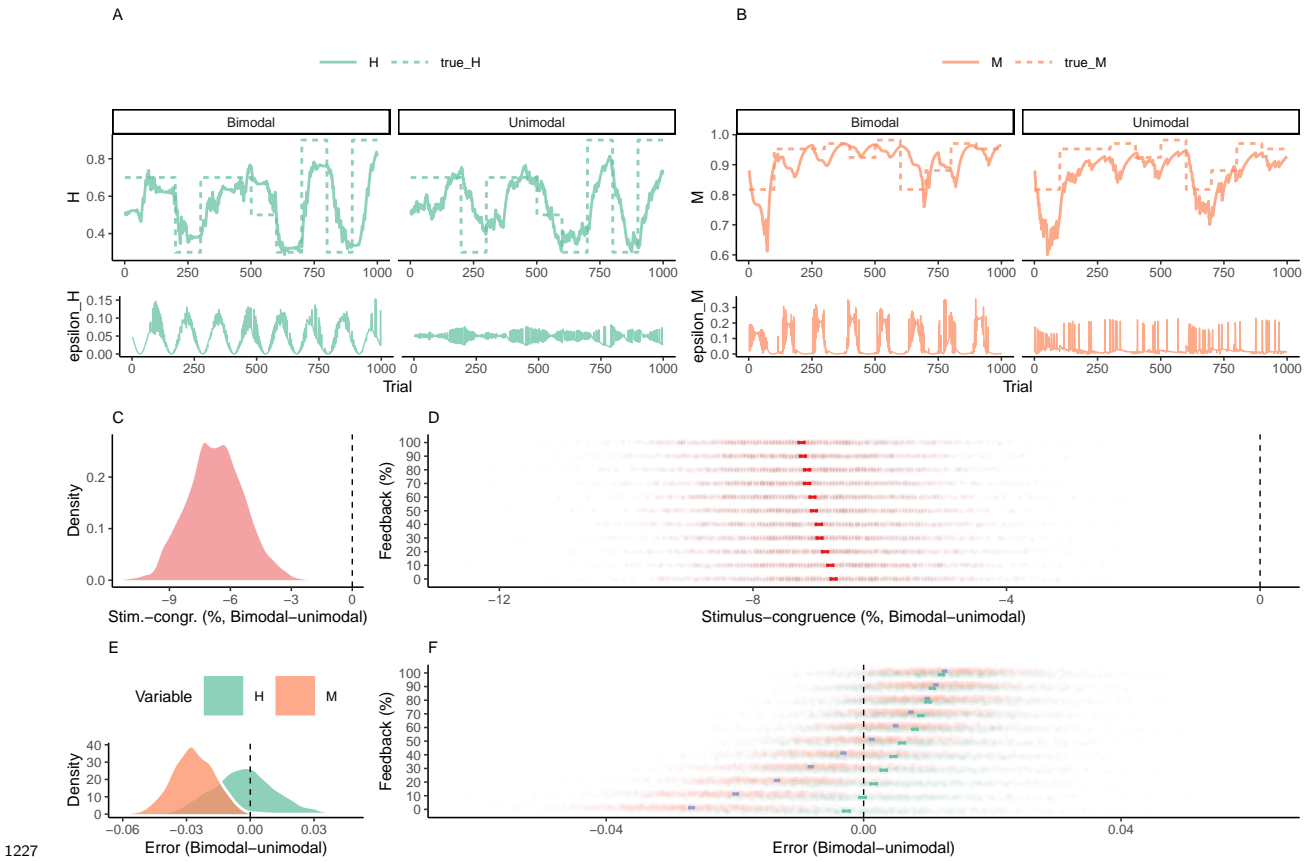
₁₂₁₂ E. The distribution of phase shift between fluctuations in simulated stimulus- and history-
₁₂₁₃ congruence peaked at half a cycle (π denoted by dotted line). The dynamic probabilities of
₁₂₁₄ simulated stimulus- and history-congruence were therefore were strongly anti-correlated (β
₁₂₁₅ $= -0.03 \pm 8.22 \times 10^{-4}$, $T(2.12 \times 10^6) = -40.52$, $p = 0$).

₁₂₁₆ F. The average squared coherence between fluctuations in simulated stimulus- and history-
₁₂₁₇ congruence (black dotted line) amounted to $6.49 \pm 2.07 \times 10^{-3}\%$.

₁₂₁₈ G. Simulated confidence was enhanced for stimulus-congruence ($\beta = 0.03 \pm 1.71 \times 10^{-4}$,
₁₂₁₉ $T(2.03 \times 10^6) = 178.39$, $p = 0$) and history-congruence ($\beta = 0.01 \pm 1.5 \times 10^{-4}$, $T(2.03 \times 10^6)$
₁₂₂₀ $= 74.18$, $p = 0$).

₁₂₂₁ H. In analogy to humans, the simulated data showed a quadratic relationship between the
₁₂₂₂ mode of perceptual processing and posterior certainty, which increased for stronger external
₁₂₂₃ and internal biases ($\beta_2 = 31.03 \pm 0.15$, $T(2.04 \times 10^6) = 205.95$, $p = 0$). The horizontal
₁₂₂₄ and vertical dotted lines indicate minimum posterior certainty and the associated mode,
₁₂₂₅ respectively.

1226 **8.7 Figure 7**



1228 **Figure 7. Adaptive benefits of bimodal inference.**

1229 A. When the sensory environment changes unpredictably over time, agents have to update
 1230 estimates H_t (solid green line, upper panel) about the true hazard rate \hat{H}_t from experience
 1231 (dotted green line, upper panel). Updates to H_t are driven by an error term ϵ_H (solid
 1232 green line, lower panel) that is defined by the difference between H_t and the presence of a
 1233 perceived change in the environment. In contrast to the unimodal model (right panels), ϵ_H
 1234 of the bimodal model (left panels) is modulated by a phasic component reflecting ongoing
 1235 fluctuations between internal and external mode.

1236 B. When the precision of sensory encoding changes unpredictably over time, agents have
 1237 to update estimates M_t (solid orange line, upper panel) about the true precision of sensory
 1238 encoding \hat{M}_t from experience (dotted orange line, upper panel). Updates to M_t are driven
 1239 by an error term ϵ_M (red line, lower panel) that is defined by the difference between M_t

₁₂₄₀ and the posterior decision-certainty. In contrast to the unimodal model (right panels), ϵ_M
₁₂₄₁ of the bimodal model (left panels) is modulated by a phasic component reflecting ongoing
₁₂₄₂ fluctuations between internal and external mode.

₁₂₄₃ C. In the absence of feedback, the bimodal inference model achieved lower stimulus-
₁₂₄₄ congruence as compared the unimodal control model ($\beta_1 = -6.71 \pm 0.03$, $T(8.42 \times 10^3) =$
₁₂₄₅ -234.31 , $p = 0$).

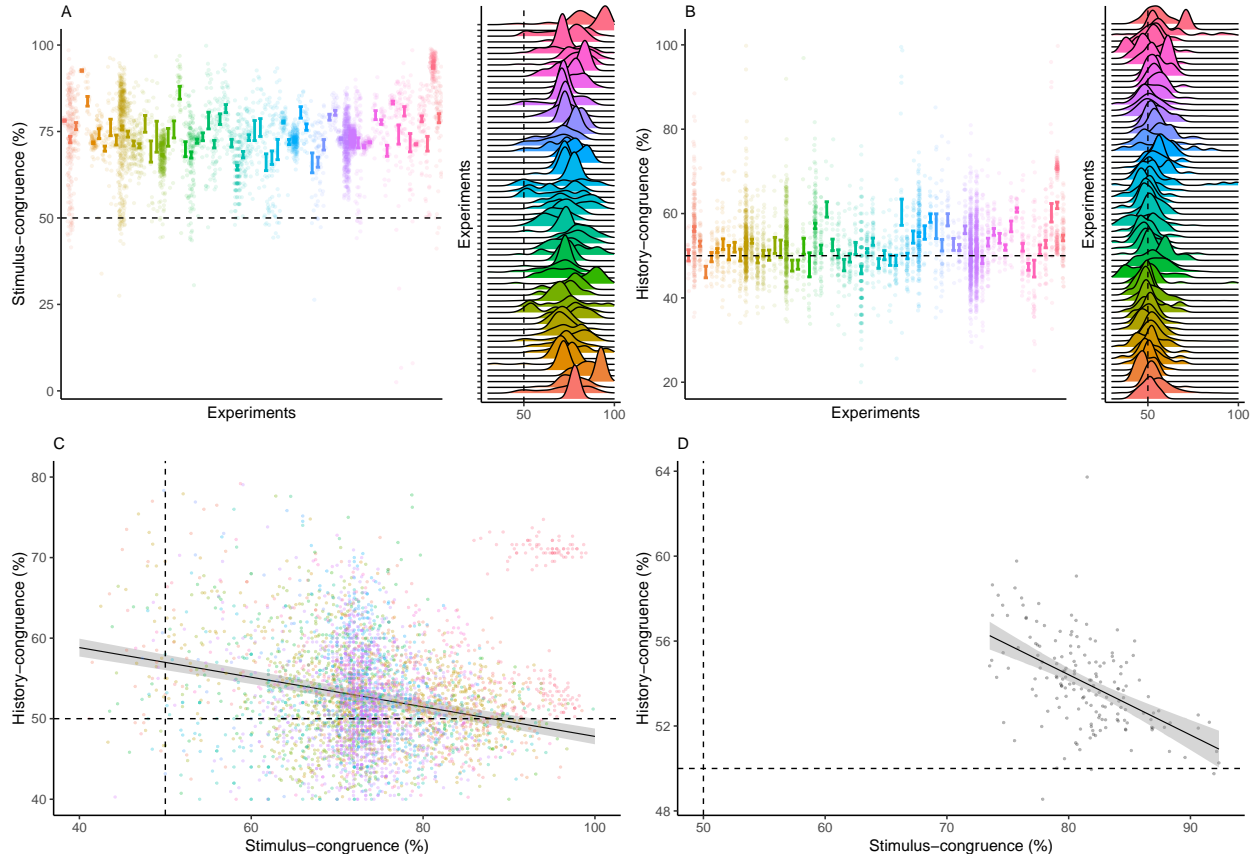
₁₂₄₆ D. The unimodal control model benefited more strongly from the presence of external feed-
₁₂₄₇ back, leading to a relative decrease in stimulus-congruence for the bimodal inference model at
₁₂₄₈ higher feedback levels ($\beta_2 = -0.05 \pm 4.13 \times 10^{-3}$, $T(10 \times 10^3) = -12.32$, $p = 1.25 \times 10^{-34}$).

₁₂₄₉ E. In the absence of feedback, the bimodal inference model achieved lower errors in the
₁₂₅₀ estimated hazard rate H ($\beta_1 = -2.94 \times 10^{-3} \pm 2.89 \times 10^{-4}$, $T(4.96 \times 10^3) = -10.18$, p
₁₂₅₁ $= 4.11 \times 10^{-24}$) as well as lower errors in the estimated probability of stimulus-congruent
₁₂₅₂ choices M ($\beta_1 = -0.03 \pm 1.86 \times 10^{-4}$, $T(6.07 \times 10^3) = -137.75$, $p = 0$).

₁₂₅₃ F. With an increasing availability of feedback, the advantage of the bimodal inference model
₁₂₅₄ was lost with respect to H ($\beta_2 = 1.43 \times 10^{-3} \pm 3.71 \times 10^{-5}$, $T(10 \times 10^3) = 38.58$, $p =$
₁₂₅₅ 9.44×10^{-304}) and M ($\beta_2 = 3.91 \times 10^{-3} \pm 2.51 \times 10^{-5}$, $T(10 \times 10^3) = 156.18$, $p = 0$).

1256 **9 Supplemental Items**

1257 **9.1 Supplemental Figure S1**



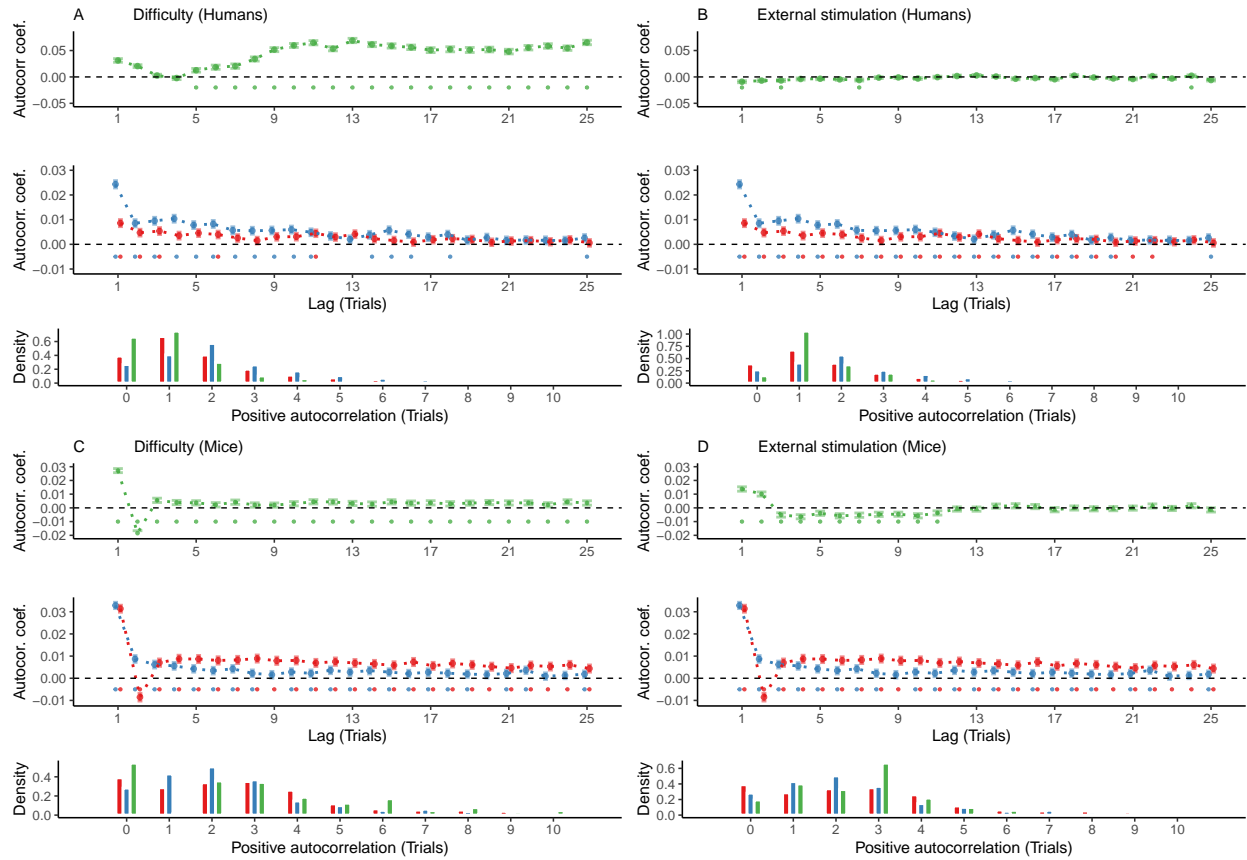
1258 **Supplemental Figure S1. Stimulus- and history-congruence.**

- 1259 A. Stimulus-congruent choices in humans amounted to $73.46\% \pm 0.15\%$ of trials and were
1260 highly consistent across the experiments selected from the Confidence Database.
1261
- 1262 B. History-congruent choices in humans amounted to $52.7\% \pm 0.12\%$ of trials. In analogy to
1263 stimulus-congruence, the prevalence of history-congruence was highly consistent across the
1264 experiments selected from the Confidence Database. 48.48% of experiments showed signif-
1265 icant ($p < 0.05$) attractive biases toward preceding choices, whereas 3.03% of experiments
1266 showed significant repulsive biases.
1267
- C. In humans, we found an enhanced impact of perceptual history in participants who were

₁₂₆₈ less sensitive to external sensory information ($T(4.3 \times 10^3) = -14.27$, $p = 3.78 \times 10^{-45}$),
₁₂₆₉ suggesting that perception results from the competition of external with internal information.

₁₂₇₀ D. In analogy to humans, mice that were less sensitive to external sensory information
₁₂₇₁ showed stronger biases toward perceptual history ($T(163) = -7.52$, $p = 3.44 \times 10^{-12}$, Pearson
₁₂₇₂ correlation).

1273 **9.2 Supplemental Figure S2**



1274

1275 **Supplemental Figure S2. Controlling for task difficulty and external stimulation.**

1276 In this study, we found highly significant autocorrelations of stimulus- and history-
 1277 congruence in humans as well as in mice. Here, we show that these autocorrelations are not
 1278 a trivial consequence of task difficulty or the sequence external stimulation. In addition, we
 1279 computed trial-wise logistic regression coefficients as an alternative approach to assessing
 1280 serial dependencies in stimulus- and history-congruence.

1281 A. In humans, task difficulty (in green) showed a significant autocorrelated starting at the
 1282 5th trial (upper panel, dots at the bottom indicate intercepts $\neq 0$ in trial-wise linear mixed
 1283 effects modeling at $p < 0.05$). When controlling for task difficulty, linear mixed effects
 1284 modeling indicated a significant auto-correlation of stimulus-congruence (in red) for the first
 1285 3 consecutive trials (middle panel). 20% of trials within the displayed time window remained
 1286 significantly autocorrelated. The autocorrelation of history-congruence (in blue) remained

1287 significant for the first 11 consecutive trials (64% significantly autocorrelated trials within
1288 the displayed time window). At the level of individual participants, the autocorrelation of
1289 task difficulty exceeded the respective autocorrelation of randomly permuted within a lag of
1290 $21.66 \pm 8.37 \times 10^{-3}$ trials (lower panel).

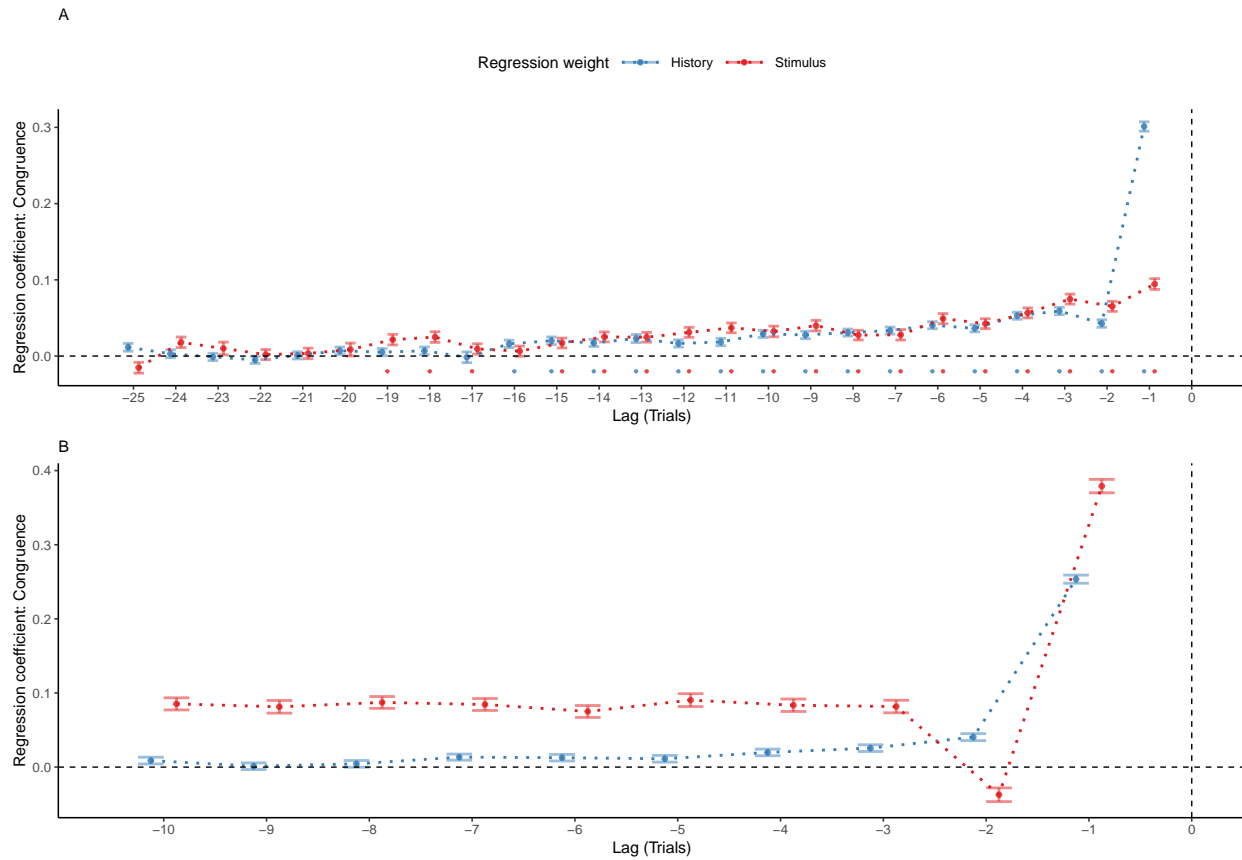
1291 B. The sequence of external stimulation (i.e., which of the two binary outcomes was sup-
1292 ported by the presented stimuli; depicted in green) was negatively autocorrelated for 1 trial.
1293 When controlling for the autocorrelation of external stimulation, stimulus-congruence re-
1294 mained significantly autocorrelated for 22 consecutive trials (88% of trials within the dis-
1295 played time window; lower panel) and history-congruence remained significantly autocor-
1296 related for 20 consecutive trials (84% of trials within the displayed time window). At the level
1297 of individual participants, the autocorrelation of external stimulation exceeded the respective
1298 autocorrelation of randomly permuted within a lag of $2.94 \pm 4.4 \times 10^{-3}$ consecutive trials
1299 (lower panel).

1300 C. In mice, task difficulty showed an significant autocorrelated for the first 25 consecutive
1301 trials (upper panel). When controlling for task difficulty, linear mixed effects modeling indi-
1302 cated a significant auto-correlation of stimulus-congruence for the first 36 consecutive trials
1303 (middle panel). In total, 100% of trials within the displayed time window remained signif-
1304 icantly autocorrelated. The autocorrelation of history-congruence remained significant for
1305 the first 8 consecutive trials, with 84% significantly autocorrelated trials within the displayed
1306 time window. At the level of individual mice, autocorrelation coefficients for difficulty were
1307 elevated above randomly permuted data within a lag of 15.13 ± 0.19 consecutive trials (lower
1308 panel).

1309 D. In mice, the sequence of external stimulation (i.e., which of the two binary outcomes was
1310 supported by the presented stimuli) was negatively autocorrelated for 11 consecutive trials
1311 (upper panel). When controlling for the autocorrelation of external stimulation, stimulus-
1312 congruence remained significantly autocorrelated for 86 consecutive trials (100% of trials

₁₃₁₃ within the displayed time window; middle) and history-congruence remained significantly
₁₃₁₄ autocorrelated for 8 consecutive trials (84% of trials within the displayed time window). At
₁₃₁₅ the level of individual mice, autocorrelation coefficients for external stimulation were elevated
₁₃₁₆ above randomly permuted data within a lag of $2.53 \pm 9.8 \times 10^{-3}$ consecutive trials (lower
₁₃₁₇ panel).

1318 **9.3 Supplemental Figure S3**



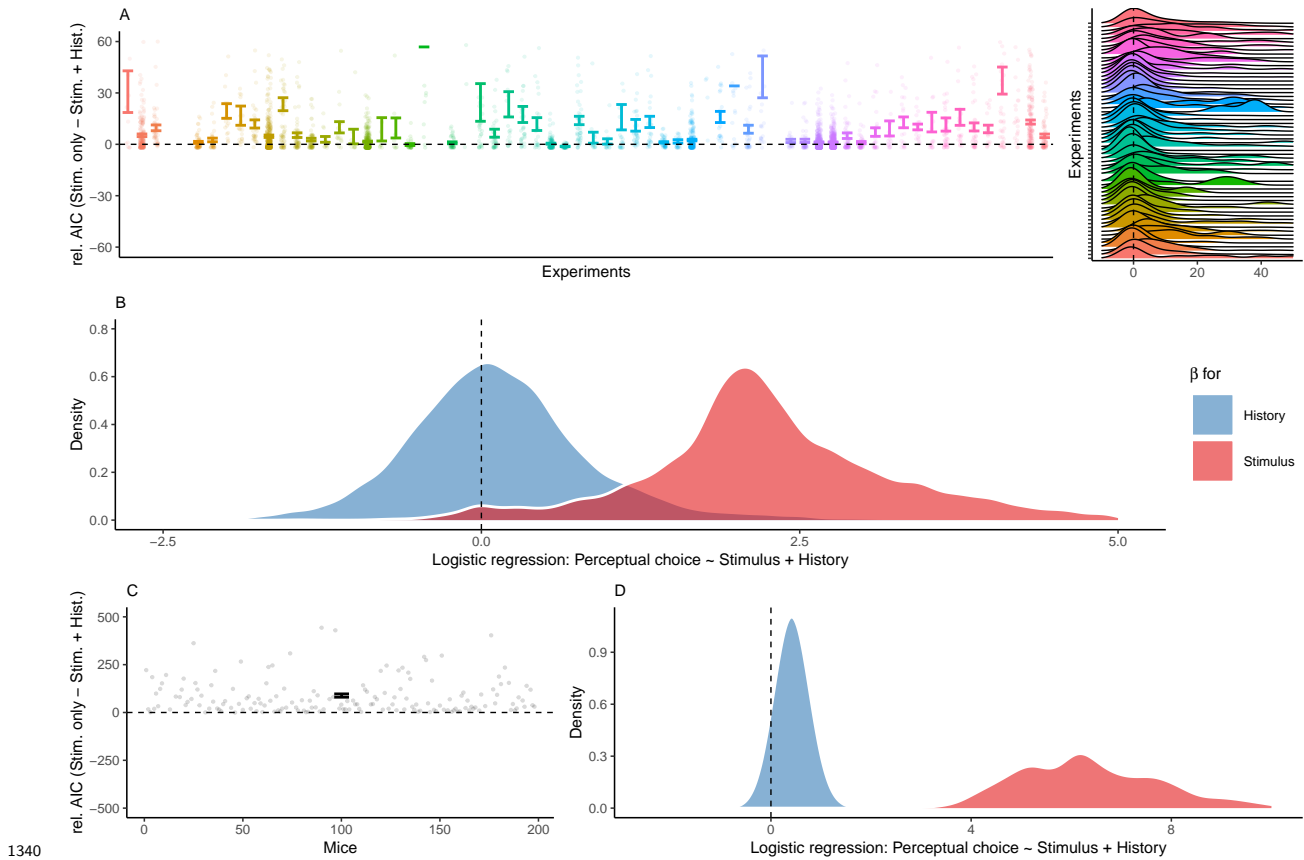
1319 **Supplemental Figure S3. Reproducing group-level autocorrelations using logistic
1320 regression.**

1321 A. As an alternative to group-level autocorrelation coefficients, we used trial-wise logistic
1322 regression to quantify serial dependencies in stimulus- and history-congruence. This analysis
1323 predicted stimulus- and history-congruence at the index trial (trial $t = 0$, vertical line)
1324 based on stimulus- and history-congruence at the 25 preceding trials. Mirroring the shape of
1325 the group-level autocorrelations, trial-wise regression coefficients (depicted as mean \pm SEM,
1326 dots mark trials with regression weights significantly greater than zero at $p < 0.05$) increased
1327 toward the index trial $t = 0$ for the human data.

1328 B. Following our results in human data, regression coefficients that predicted history-
1329 congruence at the index trial (trial $t = 0$, vertical line) increased exponentially for trials
1330 closer to the index trial in mice. In contrast to history-congruence, stimulus-congruence
1331

¹³³² showed a negative regression weight (or autocorrelation coefficient, see Figure 4B) at trial
¹³³³ -2. This was due to the experimental design (see also the autocorrelations of difficulty and
¹³³⁴ external stimulation in Supplemental Figure S2C and D): When mice made errors at easy
¹³³⁵ trials (contrast $\geq 50\%$), the upcoming stimulus was shown at the same spatial location and
¹³³⁶ at high contrast. This increased the probability of stimulus-congruent perceptual choices
¹³³⁷ after stimulus-incongruent perceptual choices at easy trials, thereby creating a negative
¹³³⁸ regression weight (or autocorrelation coefficient) of stimulus-congruence at trial -2.

1339 **9.4 Supplemental Figure S4**



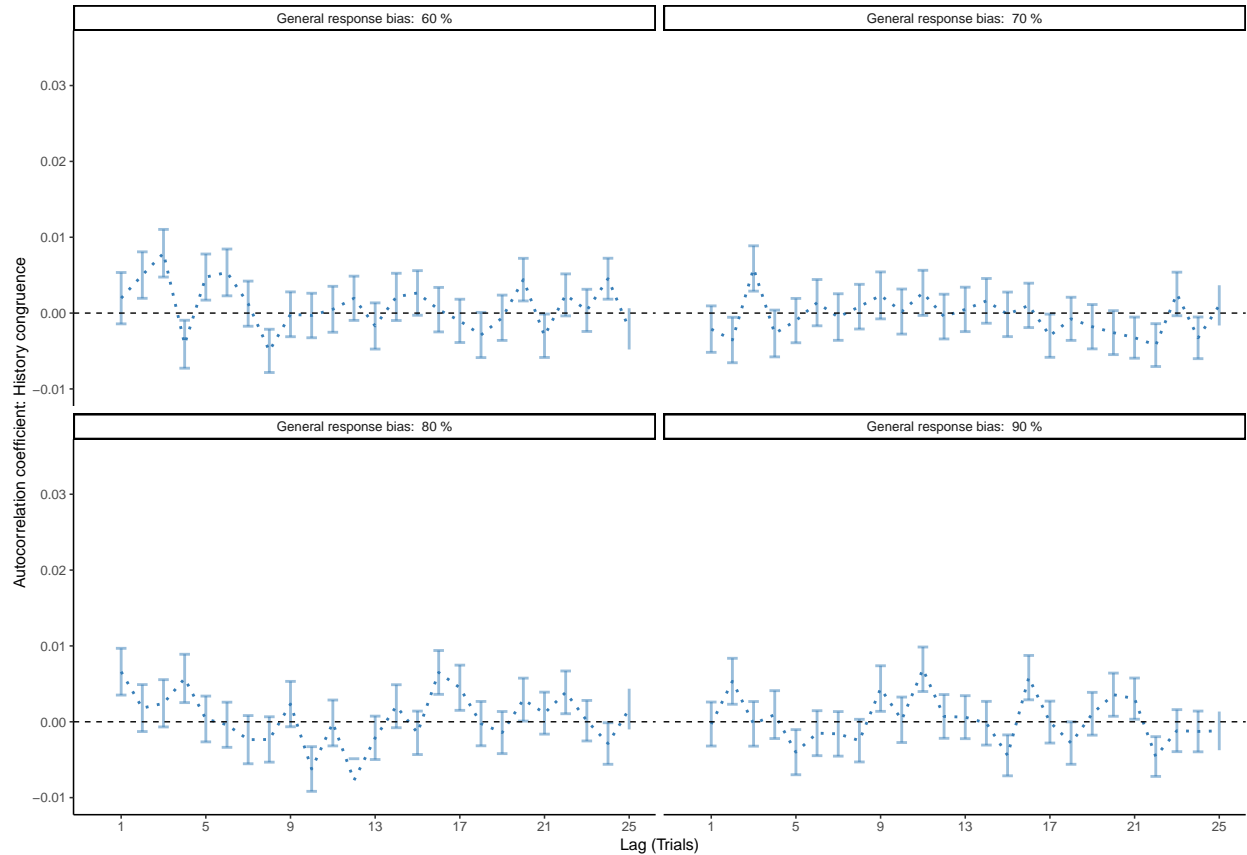
1340 **Supplemental Figure S4. History-congruence in logistic regression.**

1341 A. To ensure that perceptual history played a significant role in perception despite the ongoing stream of external information, we tested whether human perceptual decision-making was better explained by the combination of external and internal information or, alternatively, by external information alone. To this end, we compared Akaike information criteria between logistic regression models that predicted trial-wise perceptual responses either by both current external sensory information and the preceding percept, or by external sensory information alone (values above zero indicate a superiority of the full model). With high consistency across the experiments selected from the Confidence Database, this model-comparison confirmed that perceptual history contributed significantly to perception (difference in AIC = 8.07 ± 0.53 , $T(57.22) = 4.1$, $p = 1.31 \times 10^{-4}$).

1352 B. Participant-wise regression coefficients amount to 0.18 ± 0.02 for the effect of perceptual

- ₁₃₅₃ history and 2.51 ± 0.03 for external sensory stimulation.
- ₁₃₅₄ C. In mice, an AIC-based model comparison indicated that perception was better explained
₁₃₅₅ by logistic regression models that predicted trial-wise perceptual responses based on both
₁₃₅₆ current external sensory information and the preceding percept (difference in AIC = 88.62
₁₃₅₇ ± 8.57 , $T(164) = -10.34$, $p = 1.29 \times 10^{-19}$).
- ₁₃₅₈ D. In mice, individual regression coefficients amounted to 0.42 ± 0.02 for the effect of per-
₁₃₅₉ ceptual history and 6.91 ± 0.21 for external sensory stimulation.

1360 **9.5 Supplemental Figure S5**

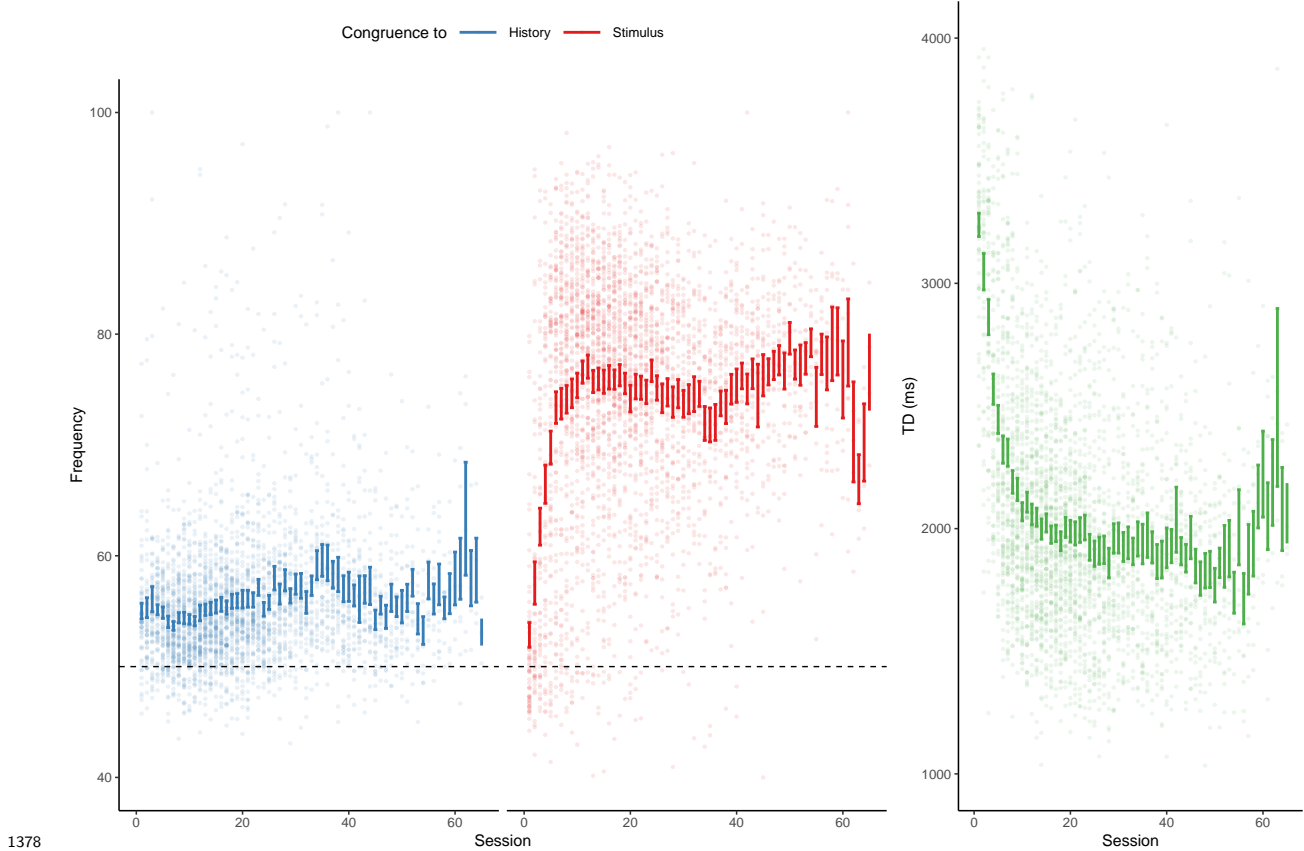


1361 **1362 Supplemental Figure S5. Correcting for general response biases.**

1363 Here, we ask whether the autocorrelation of history-congruence (as shown in Figure 2-3C)
1364 may be driven by general response biases (i.e., a general propensity to choose one of the
1365 two possible outcomes more frequently than the alternative). To this end, we generated
1366 sequences of 100 perceptual choices with general response biases ranging from 60 to 90%
1367 for 1000 simulated participants each. We then computed the autocorrelation of history-
1368 congruence for these simulated data. Crucially, we used the correction procedure that is
1369 applied to all autocorrelation curves shown in this manuscript: All reported autocorrelation
1370 coefficients are computed relative to the average autocorrelation coefficients obtained for
1371 100 iterations of randomly permuted trial sequences. The above simulation show that this
1372 correction procedure removes any potential contribution of general response biases to the
1373 auto-correlation of history-congruence. This indicates that the autocorrelation of history-

¹³⁷⁴ congruence (as shown in Figure 2-3C) is not driven by general response biases that were
¹³⁷⁵ present in the empirical data at a level of $58.71\% \pm 0.22\%$ in humans and $54.6\% \pm 0.3\%$ in
¹³⁷⁶ mice.

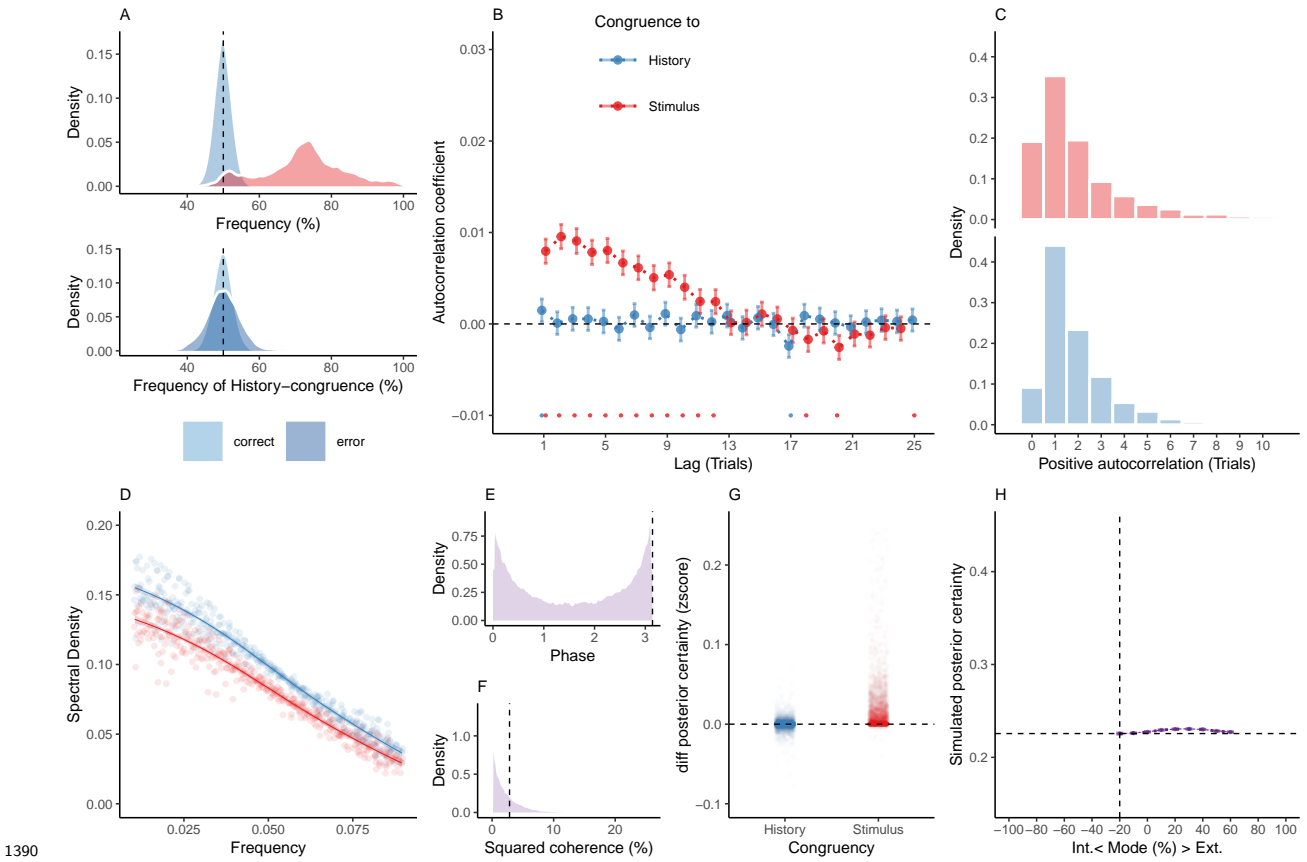
1377 **9.6 Supplemental Figure S6**



1379 **Supplemental Figure S6. History-/stimulus-congruence and TDs during training**
1380 **of the basic task.**

1381 Here, we depict the progression of history- and stimulus-congruence (depicted in blue and
1382 red, respectively; left panel) as well as TDs (in green; right panel) across training sessions in
1383 mice that achieved proficiency (i.e., stimulus-congruence $\geq 80\%$) in the *basic* task of the IBL
1384 dataset. We found that both history-congruent perceptual choices ($\beta = 0.13 \pm 4.67 \times 10^{-3}$,
1385 $T(8.4 \times 10^3) = 27.04$, $p = 1.96 \times 10^{-154}$) and stimulus-congruent perceptual choices ($\beta =$
1386 $0.34 \pm 7.13 \times 10^{-3}$, $T(8.51 \times 10^3) = 47.66$, $p = 0$) became more frequent with training.
1387 As in humans, mice showed shorter TDs with increase exposure to the task ($\beta = -22.14 \pm$
1388 17.06 , $T(1.14 \times 10^3) = -1.3$, $p = 0$).

1389 **9.7 Supplemental Figure S7**



1390 **Supplemental Figure S7. Reduced Control Model 1: No accumulation of information across trials.** When simulating data for the *no-accumulation model*, we removed the accumulation of information across trials by setting the Hazard rate H to 0.5. Simulated data thus depended only on the participant-wise estimates for the amplitudes $a_{LLR/\psi}$, frequency f , phase p and inverse decision temperature ζ .

1391 A. Similar to the full model (Figure 6), simulated perceptual choices were stimulus-congruent in $72.14\% \pm 0.17\%$ of trials (in red). History-congruent amounted to $49.89\% \pm 0.03\%$ of trials (in blue). In contrast to the full model, the no-accumulation model showed a significant bias against perceptual history $T(4.32 \times 10^3) = -3.28$, $p = 1.06 \times 10^{-3}$; upper panel). In contrast to the full model, there was no difference in the frequency of history-congruent choices between correct and error trials ($T(4.31 \times 10^3) = 0.76$, $p = 0.44$; lower panel).

1402 B. In the no-accumulation model, we found no significant autocorrelation of history-

¹⁴⁰³ congruence beyond the first trial, whereas the autocorrelation of stimulus-congruence was
¹⁴⁰⁴ preserved.

¹⁴⁰⁵ C. In the no-accumulation model, the number of consecutive trials at which true autocor-
¹⁴⁰⁶ relation coefficients exceeded the autocorrelation coefficients for randomly permuted data
¹⁴⁰⁷ increased with respect to stimulus-congruence ($2.83 \pm 1.49 \times 10^{-3}$ trials; $T(4.31 \times 10^3) =$
¹⁴⁰⁸ 3.45 , $p = 5.73 \times 10^{-4}$) and decreased with respect to history-congruence ($1.85 \pm 3.49 \times 10^{-4}$
¹⁴⁰⁹ trials; $T(4.32 \times 10^3) = -19.37$, $p = 3.49 \times 10^{-80}$) relative to the full model.

¹⁴¹⁰ D. In the no-accumulation model, the smoothed probabilities of stimulus- and history-
¹⁴¹¹ congruence (sliding windows of ± 5 trials) fluctuated as **a scale-invariant process with a**
¹⁴¹² **1/f power law**, i.e., at power densities that were inversely proportional to the frequency
¹⁴¹³ (power $\sim 1/f^\beta$; stimulus-congruence: $\beta = -0.82 \pm 1.2 \times 10^{-3}$, $T(1.92 \times 10^5) = -681.98$, p
¹⁴¹⁴ = 0; history-congruence: $\beta = -0.78 \pm 1.11 \times 10^{-3}$, $T(1.92 \times 10^5) = -706.57$, $p = 0$).

¹⁴¹⁵ E. In the no-accumulation model, the distribution of phase shift between fluctuations in
¹⁴¹⁶ simulated stimulus- and history-congruence peaked at half a cycle (π denoted by dotted
¹⁴¹⁷ line). In contrast to the full model, the dynamic probabilities of simulated stimulus- and
¹⁴¹⁸ history-congruence were not significantly anti-correlated ($\beta = 6.39 \times 10^{-4} \pm 7.22 \times 10^{-4}$,
¹⁴¹⁹ $T(8.89 \times 10^5) = 0.89$, $p = 0.38$).

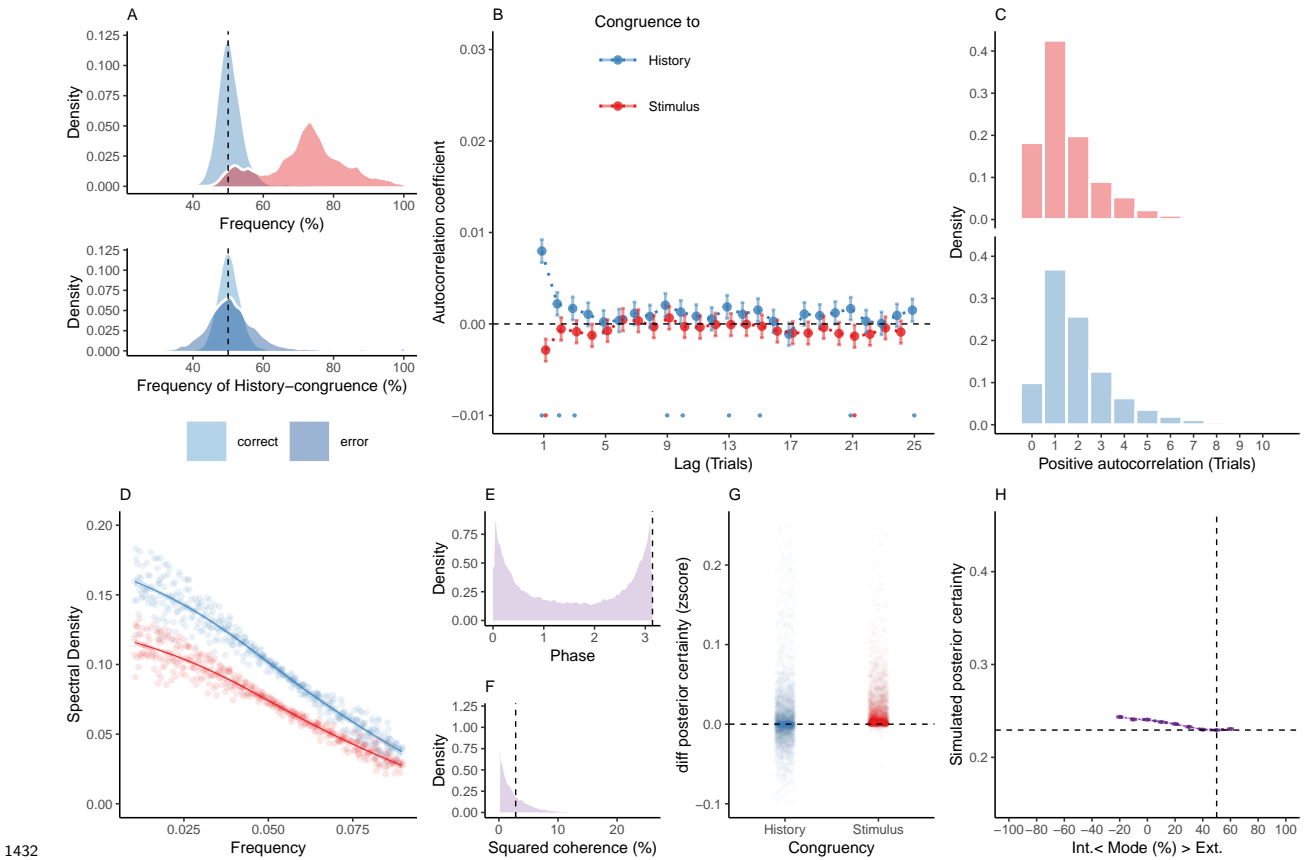
¹⁴²⁰ F. In the no-accumulation model, the average squared coherence between fluctuations in
¹⁴²¹ simulated stimulus- and history-congruence (black dotted line) was reduced in comparison to
¹⁴²² the full model ($T(3.56 \times 10^3) = -9.96$, $p = 4.63 \times 10^{-23}$) and amounted to $2.8 \pm 7.29 \times 10^{-4}\%$.

¹⁴²³ G. Similar to the full model, confidence simulated from the no-accumulation model was
¹⁴²⁴ enhanced for stimulus-congruent choices ($\beta = 0.01 \pm 9.4 \times 10^{-5}$, $T(2.11 \times 10^6) = 158.1$, $p =$
¹⁴²⁵ 0). In contrast to the full model (Figure 6), history-congruent choices were not characterized
¹⁴²⁶ by enhanced confidence ($\beta = 8.78 \times 10^{-5} \pm 8.21 \times 10^{-5}$, $T(2.11 \times 10^6) = 1.07$, $p = 0.29$).

¹⁴²⁷ H. In the no-accumulation model, the positive quadratic relationship between the mode of
¹⁴²⁸ perceptual processing and confidence was markedly reduced in comparison to the full model

₁₄₂₉ $(\beta_2 = 0.19 \pm 0.06, T(2.11 \times 10^6) = 3, p = 2.69 \times 10^{-3})$. The horizontal and vertical dotted
₁₄₃₀ lines indicate minimum posterior certainty and the associated mode, respectively.

1431 **9.8 Supplemental Figure S8**



1432 **Supplemental Figure S8. Reduced Control Model 2: No oscillations.** When
 1433 simulating data for the *no-oscillation model*, we removed the oscillation from the likelihood
 1434 and prior terms by setting the amplitudes a_{LLR} and a_ψ to zero. Simulated data thus
 1435 depended only on the participant-wise estimates for hazard rate H and inverse decision
 1436 temperature ζ .

1437 A. Similar to the full model (Figure 6), simulated perceptual choices were stimulus-congruent
 1438 in $71.97\% \pm 0.17\%$ of trials (in red). History-congruent amounted to $50.73\% \pm 0.07\%$ of
 1439 trials (in blue). As in the full model, the no-oscillation model showed a significant bias
 1440 toward perceptual history $T(4.32 \times 10^3) = 9.94$, $p = 4.88 \times 10^{-23}$; upper panel). Similarly,
 1441 history-congruent choices were more frequent at error trials ($T(4.31 \times 10^3) = 10.59$, $p =$
 1442 7.02×10^{-26} ; lower panel).

1443 B. In the no-oscillation model, we did not find significant autocorrelations for stimulus-

¹⁴⁴⁵ congruence. Likewise, we did not observe any autocorrelation of history-congruence beyond
¹⁴⁴⁶ the first three consecutive trials.

¹⁴⁴⁷ C. In the no-oscillation model, the number of consecutive trials at which true autocorrelation
¹⁴⁴⁸ coefficients exceeded the autocorrelation coefficients for randomly permuted data decreased
¹⁴⁴⁹ with respect to both stimulus-congruence ($1.8 \pm 1.59 \times 10^{-3}$ trials; $T(4.31 \times 10^3) = -5.21$,
¹⁴⁵⁰ $p = 2 \times 10^{-7}$) and history-congruence ($2.18 \pm 5.48 \times 10^{-4}$ trials; $T(4.32 \times 10^3) = -17.1$, p
¹⁴⁵¹ $= 1.75 \times 10^{-63}$) relative to the full model.

¹⁴⁵² D. In the no-oscillation model, the smoothed probabilities of stimulus- and history-
¹⁴⁵³ congruence (sliding windows of ± 5 trials) fluctuated as **a scale-invariant process with a**
¹⁴⁵⁴ **1/f power law**, i.e., at power densities that were inversely proportional to the frequency
¹⁴⁵⁵ (power $\sim 1/f^\beta$; stimulus-congruence: $\beta = -0.78 \pm 1.1 \times 10^{-3}$, $T(1.92 \times 10^5) = -706.93$, p
¹⁴⁵⁶ $= 0$; history-congruence: $\beta = -0.79 \pm 1.12 \times 10^{-3}$, $T(1.92 \times 10^5) = -702.46$, $p = 0$).

¹⁴⁵⁷ E. In the no-oscillation model, the distribution of phase shift between fluctuations in sim-
¹⁴⁵⁸ uulated stimulus- and history-congruence peaked at half a cycle (π denoted by dotted line).
¹⁴⁵⁹ In contrast to the full model, the dynamic probabilities of simulated stimulus- and history-
¹⁴⁶⁰ congruence were positively correlated ($\beta = 4.3 \times 10^{-3} \pm 7.97 \times 10^{-4}$, $T(1.98 \times 10^6) = 5.4$,
¹⁴⁶¹ $p = 6.59 \times 10^{-8}$).

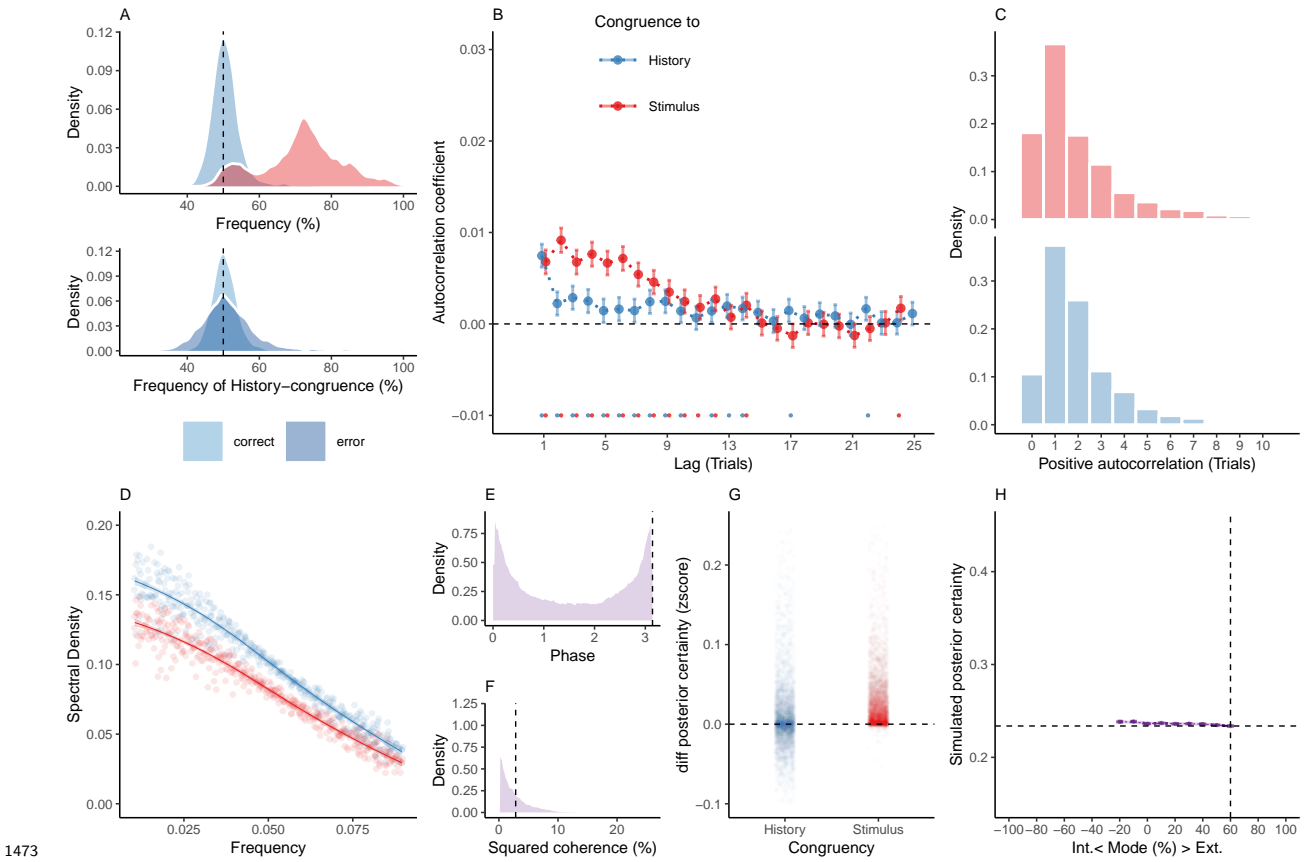
¹⁴⁶² F. In the no-oscillation model, the average squared coherence between fluctuations in simu-
¹⁴⁶³ lated stimulus- and history-congruence (black dottet line) was reduced in comparison to the
¹⁴⁶⁴ full model ($T(3.52 \times 10^3) = -6.27$, $p = 3.97 \times 10^{-10}$) and amounted to $3.26 \pm 8.88 \times 10^{-4}\%$.

¹⁴⁶⁵ G. Similar to the full model, confidence simulated from the no-oscillation model was enhanced
¹⁴⁶⁶ for stimulus-congruent choices ($\beta = 0.01 \pm 1.05 \times 10^{-4}$, $T(2.1 \times 10^6) = 139.17$, $p = 0$) and
¹⁴⁶⁷ history-congruent choices ($\beta = 8.05 \times 10^{-3} \pm 9.2 \times 10^{-5}$, $T(2.1 \times 10^6) = 87.54$, $p = 0$).

¹⁴⁶⁸ H. In the no-oscillation model, the positive quadratic relationship between the mode of
¹⁴⁶⁹ perceptual processing and confidence was markedly reduced in comparison to the full model
¹⁴⁷⁰ ($\beta_2 = 0.14 \pm 0.07$, $T(2.1 \times 10^6) = 1.95$, $p = 0.05$). The horizontal and vertical dotted lines

₁₄₇₁ indicate minimum posterior certainty and the associated mode, respectively.

1472 **9.9 Supplemental Figure S9**



1474 **Supplemental Figure S9. Reduced Control Model 3: Only oscillation of the**
 1475 **likelihood.** When simulating data for the *likelihood-oscillation-only model*, we removed
 1476 the oscillation from the prior term by setting the amplitude a_ψ to zero. Simulated data
 1477 thus depended only on the participant-wise estimates for hazard rate H , amplitude a_{LLR} ,
 1478 frequency f , phase p and inverse decision temperature ζ .

1479 A. Similar to the full model (Figure 6), simulated perceptual choices were stimulus-congruent
 1480 in $71.97\% \pm 0.17\%$ of trials (in red). History-congruent amounted to $50.76\% \pm 0.07\%$ of trials
 1481 (in blue). As in the full model, the likelihood-oscillation-only model showed a significant bias
 1482 toward perceptual history $T(4.32 \times 10^3) = 10.29$, $p = 1.54 \times 10^{-24}$; upper panel). Similarly,
 1483 history-congruent choices were more frequent at error trials ($T(4.32 \times 10^3) = 9.71$, $p =$
 1484 4.6×10^{-22} ; lower panel).

1485 B. In the likelihood-oscillation-only model, we observed that the autocorrelation coeffi-

1486 cients for history-congruence were reduced below the autocorrelation coefficients of stimulus-
1487 congruence. This is an approximately five-fold reduction relative to the empirical results
1488 observed in humans (Figure 2B), where the autocorrelation of history-congruence was above
1489 the autocorrelation of stimulus-congruence. Moreover, in the reduced model shown here, the
1490 number of consecutive trials that showed significant autocorrelation of history-congruence
1491 was reduced to 11.

1492 C. In the likelihood-oscillation-only model, the number of consecutive trials at which true
1493 autocorrelation coefficients exceeded the autocorrelation coefficients for randomly permuted
1494 data did not differ with respect to stimulus-congruence ($2.62 \pm 1.39 \times 10^{-3}$ trials; $T(4.32 \times$
1495 $10^3) = 1.85$, $p = 0.06$), but decreased with respect to history-congruence ($2.4 \pm 8.45 \times 10^{-4}$
1496 trials; $T(4.32 \times 10^3) = -15.26$, $p = 3.11 \times 10^{-51}$) relative to the full model.

1497 D. In the likelihood-oscillation-only model, the smoothed probabilities of stimulus- and
1498 history-congruence (sliding windows of ± 5 trials) fluctuated as **a scale-invariant pro-**
1499 **cess with a 1/f power law**, i.e., at power densities that were inversely proportional to the
1500 frequency (power $\sim 1/f^\beta$; stimulus-congruence: $\beta = -0.81 \pm 1.17 \times 10^{-3}$, $T(1.92 \times 10^5) =$
1501 -688.65 , $p = 0$; history-congruence: $\beta = -0.79 \pm 1.14 \times 10^{-3}$, $T(1.92 \times 10^5) = -698.13$, p
1502 $= 0$).

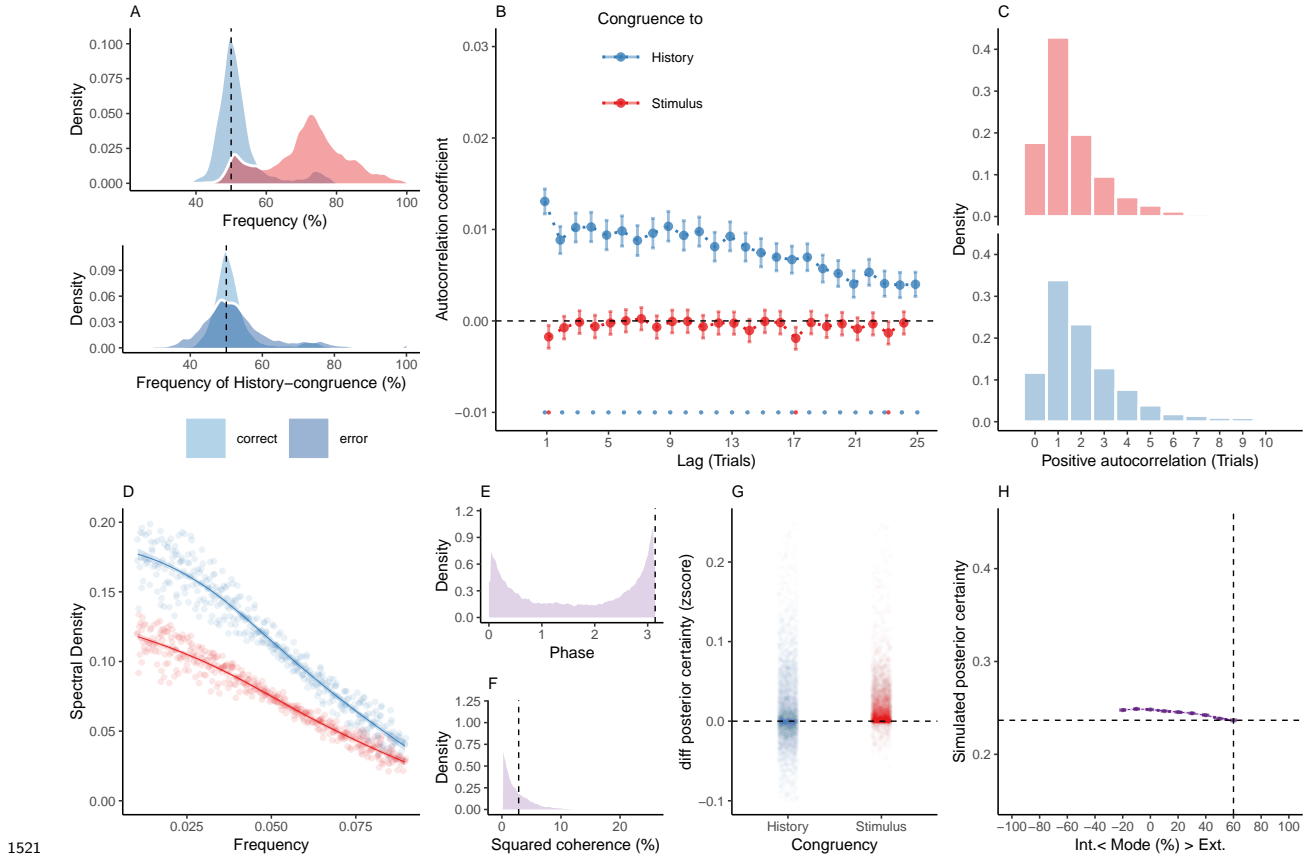
1503 E. In the likelihood-oscillation-only model, the distribution of phase shift between fluctua-
1504 tions in simulated stimulus- and history-congruence peaked at half a cycle (π denoted by
1505 dotted line). In contrast to the full model, the dynamic probabilities of simulated stimulus-
1506 and history-congruence were positively correlated ($\beta = 2.7 \times 10^{-3} \pm 7.6 \times 10^{-4}$, $T(2.02 \times 10^6)$
1507 $= 3.55$, $p = 3.8 \times 10^{-4}$).

1508 F. In the likelihood-oscillation-only model, the average squared coherence between fluctu-
1509 ations in simulated stimulus- and history-congruence (black dottet line) was reduced in
1510 comparison to the full model ($T(3.51 \times 10^3) = -4.56$, $p = 5.27 \times 10^{-6}$) and amounted to 3.43
1511 $\pm 1.02 \times 10^{-3}\%$.

₁₅₁₂ G. Similar to the full model, confidence simulated from the likelihood-oscillation-only model
₁₅₁₃ was enhanced for stimulus-congruent choices ($\beta = 0.03 \pm 1.42 \times 10^{-4}$, $T(2.1 \times 10^6) = 191.78$,
₁₅₁₄ $p = 0$) and history-congruent choices ($\beta = 9.1 \times 10^{-3} \pm 1.25 \times 10^{-4}$, $T(2.1 \times 10^6) = 72.51$,
₁₅₁₅ $p = 0$).

₁₅₁₆ H. In the likelihood-oscillation-only model, the positive quadratic relationship between the
₁₅₁₇ mode of perceptual processing and confidence was markedly reduced in comparison to the full
₁₅₁₈ model ($\beta_2 = 0.34 \pm 0.1$, $T(2.1 \times 10^6) = 3.49$, $p = 4.78 \times 10^{-4}$). The horizontal and vertical
₁₅₁₉ dotted lines indicate minimum posterior certainty and the associated mode, respectively.

1520 **9.10 Supplemental Figure S10**



1521 **Supplemental Figure S10. Reduced Control Model 4: Only oscillation of the prior.** When simulating data for the *prior-oscillation-only model*, we removed the oscillation from the prior term by setting the amplitude a_{LLR} to zero. Simulated data thus depended only on the participant-wise estimates for hazard rate H , amplitude a_ψ , frequency f , phase p and inverse decision temperature ζ .

1522 A. Similar to the full model (Figure 6), simulated perceptual choices were stimulus-congruent
 1523 in $71.97\% \pm 0.17\%$ of trials (in red). History-congruent amounted to $52.1\% \pm 0.11\%$ of trials
 1524 (in blue). As in the full model, the prior-oscillation-only showed a significant bias toward
 1525 perceptual history $T(4.32 \times 10^3) = 18.34, p = 1.98 \times 10^{-72}$; upper panel). Similarly, history-
 1526 congruent choices were more frequent at error trials ($T(4.31 \times 10^3) = 12.35, p = 1.88 \times 10^{-34}$;
 1527 lower panel).

1528 B. In the prior-oscillation-only model, we did not observe any significant positive autocor-

1534 relation of stimulus-congruence , whereas the autocorrelation of history-congruence was pre-
1535 served.

1536 C. In the prior-oscillation-only model, the number of consecutive trials at which true au-
1537 tocorrelation coefficients exceeded the autocorrelation coefficients for randomly permuted
1538 data did was decreased with respect to stimulus-congruence relative to the full model ($1.8 \pm$
1539 1.01×10^{-3} trials; $T(4.31 \times 10^3) = -6.48$, $p = 1.03 \times 10^{-10}$), but did not differ from the full
1540 model with respect to history-congruence ($4.25 \pm 1.84 \times 10^{-3}$ trials; $T(4.32 \times 10^3) = 0.07$,
1541 $p = 0.95$).

1542 D. In the prior-oscillation-only model, the smoothed probabilities of stimulus- and history-
1543 congruence (sliding windows of ± 5 trials) fluctuated as **a scale-invariant process with a**
1544 **1/f power law**, i.e., at power densities that were inversely proportional to the frequency
1545 (power $\sim 1/f^\beta$; stimulus-congruence: $\beta = -0.78 \pm 1.11 \times 10^{-3}$, $T(1.92 \times 10^5) = -706.62$, p
1546 = 0; history-congruence: $\beta = -0.83 \pm 1.27 \times 10^{-3}$, $T(1.92 \times 10^5) = -651.6$, $p = 0$).

1547 E. In the prior-oscillation-only model, the distribution of phase shift between fluctuations
1548 in simulated stimulus- and history-congruence peaked at half a cycle (π denoted by dotted
1549 line). Similar to the full model, the dynamic probabilities of simulated stimulus- and history-
1550 congruence were anti-correlated ($\beta = -0.03 \pm 8.61 \times 10^{-4}$, $T(2.12 \times 10^6) = -34.03$, $p =$
1551 8.17×10^{-254}).

1552 F. In the prior-oscillation-only model, the average squared coherence between fluctuations in
1553 simulated stimulus- and history-congruence (black dottet line) was reduced in comparison to
1554 the full model ($T(3.54 \times 10^3) = -3.22$, $p = 1.28 \times 10^{-3}$) and amounted to $3.52 \pm 1.04 \times 10^{-3}\%$.

1555 G. Similar to the full model, confidence simulated from the prior-oscillation-only model was
1556 enhanced for stimulus-congruent choices ($\beta = 0.02 \pm 1.44 \times 10^{-4}$, $T(2.03 \times 10^6) = 128.53$,
1557 $p = 0$) and history-congruent choices ($\beta = 0.01 \pm 1.26 \times 10^{-4}$, $T(2.03 \times 10^6) = 88.24$, $p =$
1558 0).

1559 H. In contrast to the full model, the prior-oscillation-only model did not yield a positive

₁₅₆₀ quadratic relationship between the mode of perceptual processing and confidence ($\beta_2 =$
₁₅₆₁ -0.17 ± 0.1 , $T(2.04 \times 10^6) = -1.66$, $p = 0.1$). The horizontal and vertical dotted lines
₁₅₆₂ indicate minimum posterior certainty and the associated mode, respectively.

1563 9.11 Supplemental Table T1

Authors	Journal	Year
Bang, Shekhar, Rahnev	JEP:General	2019
Bang, Shekhar, Rahnev	JEP:General	2019
Calder-Travis, Charles, Bogacz, Yeung	Unpublished	NA
Clark & Merfeld	Journal of Neurophysiology	2018
Clark	Unpublished	NA
Faivre, Filevich, Solovey, Kuhn, Blanke	Journal of Neuroscience	2018
Faivre, Vuillaume, Blanke, Cleeremans	bioRxiv	2018
Filevich & Fandakova	Unplublished	NA
Gajdos, Fleming, Saez Garcia, Weindel, Davranche	Neuroscience of Consciousness	2019
Gherman & Philiastides	eLife	2018
Haddara & Rahnev	PsyArXiv	2020
Haddara & Rahnev	PsyArXiv	2020
Hainguierlot, Vergnaud, & de Gardelle	Scientific Reports	2018
Hainguierlot, Gajdos, Vergnaud, & de Gardelle	Unpublished	NA
Jachs, Blanco, Grantham-Hill, Soto	JEP:HPP	2015
Jachs, Blanco, Grantham-Hill, Soto	JEP:HPP	2015
Jachs, Blanco, Grantham-Hill, Soto	JEP:HPP	2015
Jaquiere, Yeung	Unpublished	NA
Kvam, Pleskac, Yu, Busemeyer	PNAS	2015
Kvam, Pleskac, Yu, Busemeyer	PNAS	2015
Kvam and Pleskac	Cognition	2016
Law, Lee	Unpublished	NA
Lebreton, et al.	Sci. Advances	2018
Lempert, Chen, & Fleming	PlosOne	2015
Locke*, Gaffin-Cahn*, Hosseiniavah, Mamassian, & Landy	Attention, Perception, & Psychophysics	2020
Maniscalco, McCurdy,Odegaard, & Lau	J Neurosci	2017
Maniscalco, McCurdy,Odegaard, & Lau	J Neurosci	2017
Maniscalco, McCurdy,Odegaard, & Lau	J Neurosci	2017
Maniscalco, McCurdy,Odegaard, & Lau	J Neurosci	2017
Martin, Hsu	Unpublished	NA
Massoni & Roux	Journal of Mathematical Psychology	2017
Massoni	Unpublished	NA
Mazor, Friston & Fleming	eLife	2020
Mei, Rankine,Olafsson, Soto	bioRxiv	2019
Mei, Rankine,Olafsson, Soto	bioRxiv	2019
O'Hora, Zgonnikov, Kenny, Wong-Lin	Fechner Day proceedings	2017
O'Hora, Zgonnikov, CiChocki	Unpublished	NA

(continued)

Authors	Journal	Year
O'Hora, Zgonnikov, Neverauskaite	Unpublished	NA
Palser et al	Consciousness & Cognition	2018
Pereira, Faivre, Iturrate et al.	bioRxiv	2018
Prieto et al.	Submitted	NA
Rahnev et al	J Neurophysiol	2013
Rausch & Zehetleitner	Front Psychol	2016
Rausch et al	Attention, Perception, & Psychophysics	2018
Rausch et al	Attention, Perception, & Psychophysics	2018
Rausch, Zehetleitner, Steinhauser, & Maier	NeuroImage	2020
Recht, de Gardelle & Mamassian	Unpublished	NA
Reyes et al.	PlosOne	2015
Reyes et al.	Submitted	NA
Rouault, Seow, Gillan, Fleming	Biol. Psychiatry	2018
Rouault, Seow, Gillan, Fleming	Biol. Psychiatry	2018
Rouault, Dayan, Fleming	Nat Commun	2019
Sadeghi et al	Scientific Reports	2017
Schmidt et al.	Consc Cog	2019
Shekhar & Rahnev	J Neuroscience	2018
Shekhar & Rahnev	PsyArXiv	2020
Sherman et al	Journal of Neuroscience	2016
Sherman et al	Journal of Cognitive Neuroscience	2016
Sherman et al	Unpublished	NA
Sherman et al	Unpublished	NA
Siedlecka, Wereszczyski, Paulewicz, Wierzchon	bioRxiv	2019
Song et al	Consciousness & Cognition	2011
van Boxtel, Orchard, Tsuchiya	bioRxiv	2019
van Boxtel, Orchard, Tsuchiya	bioRxiv	2019
Wierzchon, Paulewicz, Asanowicz, Timmermans & Cleeremans	Consciousness and Cognition	2014
Wierzchon, Anzulewicz, Hobot, Paulewicz & Sackur	Consciousness and Cognition	2019

1564 **10 Response to Reviewers**

1565 **10.1 Reviewer 1:**

1566 This was an interesting and thought-provoking submission. I note that it is
1567 a revision: I am therefore supposing that the authors have already responded
1568 to one round of reviewer comments and that you are potentially interested in
1569 publishing this work. In brief, I think there are many elements of this report that
1570 warrant publication; however, there are some parts that are less compelling and
1571 could be deferred to a subsequent paper. The paper is far too long and would
1572 benefit greatly from being streamlined. Furthermore, some of the modelling is
1573 overengineered and is difficult to follow. I have tried to suggest how the authors
1574 might improve the presentation of their work in my comments to authors.

1575 I enjoyed reading this long but thought-provoking report of fluctuations in the
1576 sensitivity to sensory evidence in perceptual decision-making tasks. There were
1577 some parts of this report that were compelling and interesting. Other parts were
1578 less convincing and difficult to understand. Overall, this paper is far too long.
1579 An analogy that might help here is that a dinner guest is very entertaining for the
1580 first hour or so - and then overstays their welcome; until you start wishing they
1581 would leave. Another analogy, which came to mind, was that the modelling—
1582 and its interpretation—was a bit autistic (i.e., lots of fascinating if questionable
1583 detail with a lack of central coherence).

1584 I think that both issues could be resolved by shortening the paper and removing
1585 (or, at least, greatly simplifying) the final simulation studies of metacognition.
1586 I try to unpack this suggestion in the following.

1587 We would like to thank Prof. Friston for the very insightful and helpful comments on our
1588 manuscript. We fully agree that our ideas about the computational function of between-

1589 mode fluctuations and the associated simulation may be presented in a more accessible form
1590 in a standalone paper. As we outline below in more detail, we have followed the suggestion
1591 of streamlining our findings and rewrote the paper to reduce it's length by shortening the
1592 sections on computational modeling.

1593 **Major points:**

1594 **As I understand it, you have used publicly available data on perceptual decision-**
1595 **making to demonstrate slow fluctuations in the tendency to predicate perceptual**
1596 **decisions on the stimuli and on the history of recent decisions. You find scale-free**
1597 **fluctuations in this tendency — that are anti-correlated — and interpret this as**
1598 **fluctuations in the precision afforded sensory evidence, relative to prior beliefs.**
1599 **This interpretation is based upon a model of serial dependencies (parameterised**
1600 **with a hazard function).**

1601 **The stimulus and history (i.e., likelihood and prior) sensitivities are anti-**
1602 **correlated and both show scale free behaviour. This is reproduced in men and**
1603 **mice. You then proceed to model this with periodic fluctuations in the precisions**
1604 **or weights applied to the likelihood and prior that are in anti-phase - and then**
1605 **estimate the parameters of the ensuing model. Finally, you then simulate the**
1606 **learning of the hazard parameter — and something called metacognition - to**
1607 **show that periodic fluctuations improve estimates of metacognition (based upon**
1608 **a Rescorla-Wagner model of learning). You motivate this by suggesting that**
1609 **the fluctuations in sensitivity are somehow necessary to elude circular inference**
1610 **and provide better estimates of precision.**

1611 **Note that I am reading the parameters omega_LL and omega_ as the preci-**
1612 **sion of the likelihood and prior, where the precision of the likelihood is called**
1613 **sensory precision. This contrasts with your use of sensory precision, which seems**
1614 **to be attributed to a metacognitive construct M.**

₁₆₁₅ As noted above, all of this is fascinating but there are too many moving parts
₁₆₁₆ that do not fit together comfortably. I will list a few examples:

₁₆₁₇ **10.1.1 Comment 1**

₁₆₁₈ If, empirically, the fluctuations in sensitivity are scale-free with a 1/f power law,
₁₆₁₉ why did you elect to model fluctuations in precision as a periodic function with
₁₆₂₀ one unique timescale (i.e., f).?

₁₆₂₁ The reason for choosing a unique timescale f was to enable our model to depict the the
₁₆₂₂ dominant timescale at which prior and likelihood precision are temporarily suspended, giving
₁₆₂₃ rise to what we believe constitutes between-mode fluctuations. In line with the shape of the
₁₆₂₄ autocorrelation curves, the value for f lies at approximately $0.11 \sqrt{1/N_{trials}}$. Simulating from
₁₆₂₅ our model (Figure 6) replicates the 1/f feature of the empirical data. Please note that the
₁₆₂₆ individual trial is the smallest unit of *measurement* for these fluctuations, such that our
₁₆₂₇ analysis only deals with frequencies below 1 ($1/N_{trials}$). We have added a paragraph on f
₁₆₂₈ to the results section:

- ₁₆₂₉ • value of f , reason for only one variable

₁₆₃₀ **10.1.2 Comment 2**

₁₆₃₁ At present, the estimates of meta-cognition (M) play the role of accumulated
₁₆₃₂ estimates of (sensory or prior) precision. Why are these not used in your model
₁₆₃₃ of perceptual decisions in Equation 2.

₁₆₃₄ We would like to thank Prof. Friston for this comment. In our model, the parameter α
₁₆₃₅ controls the encoding precision by governing the transformation from sensory stimuli to the
₁₆₃₆ log likelihood ratio (LLR) via the following equations, which is closer to zero for lower values
₁₆₃₇ of α .

$$u_t = \frac{1}{1 + \exp(-\alpha * s_t)} \quad (35)$$

$$LLR_t = \log\left(\frac{u_t}{1 - u_t}\right) \quad (36)$$

1638 Our model simulations on the adaptive benefits of bimodal inference rest on the assumption
 1639 that α may change unpredictably. The construct M is a belief about α that may be useful
 1640 for, e.g., communicating the precision of sensory encoding to other cognitive domains or
 1641 agents. To our mind, α is a feature of low-level sensory encoding that cannot be modulated
 1642 by top-down beliefs such as M . This is why we did not include M in equation (2).

1643 **10.1.3 Comment 3**

1644 **Why do you assume that non-specific increases in attention and arousal will
 1645 increase reaction times? If one has very precise prior beliefs (and is not attending
 1646 to stimuli), would you not expect a decrease in reaction time?**

1647 Thanks a lot for pointing this out (see also the comment below and comment X.X.X by
 1648 Reviewer 3). As we understand, both high prior and high likelihood precision lead to higher
 1649 absolute values of the posterior log ratio (reflecting decision certainty), and thus faster re-
 1650 sponse times (RTs). This is reflected empirically by RTs in humans (Figure 2) and to a
 1651 lesser degree in mice (Figure 4) and to a lesser degree in mice): RTs tended to be shorter for
 1652 stronger biases toward both external and internal mode. Our full model, which incorporates
 1653 (i), the accumulation of information across trials, and (ii), antiphase fluctuations, recapitu-
 1654 lates this feature of the data, which is lost or greatly attenuated when eliminating (i) and/or
 1655 (ii). Our data thus confirm the hypothesis that both high prior and likelihood precision lead
 1656 to faster RTs.

1657 At the same time, we included the relation between mode and RTs and confidence as a

1658 defensive analysis. One might argue that fluctuations in perceptual performance are not
1659 influenced at all by periods of enhanced prior precision (which decrease performance in fully
1660 randomized designs), but by periods where participants may not attend to the task at all,
1661 i.e., neither to sensory information nor to prior precision. We think that analysis of response
1662 times and confidence can give some insight into whether such alternative mechanisms may
1663 be at play, as we would assume longer response times and lower confidence if participants
1664 failed to attend to the task at all (e.g., due to low arousal).

1665 We realize that, due to the potential non-linearity in their relation to arousal (see also
1666 comment X.X.X by Reviewer 3), RTs and confidence cannot provide a definitive map of
1667 where fluctuations in mode are situated in relation to arousal/attention. This can potentially
1668 be provided by eye-tracking, motor behavior or neural data, which is not available for the
1669 studies in the Confidence Database, but was recently published for the IBL database. We
1670 will assess the relation of pupil diameter, motor behavior (turning of the response wheel)
1671 and LFPs to between-mode fluctuations in a future publication.

1672 In light of the above, we have adapted the manuscript in the following ways:

- 1673 • explanation of how fluctuations in prior and likelihood precision may impact RTs and
1674 confidence: *TODO*
- 1675 • reference to the potential non-linearity: *TODO*
- 1676 • reference to future work that will use pupillometry, video tracking and neural signals
1677 to discern between-mode fluctuations from global and?or unspecific flucations in perfor-
1678 mance: *TODO*

1679 10.1.4 Comment 4

1680 **In the predictive processing literature, attention is thought to correspond to**
1681 **fluctuations in sensory and prior precision. Why did you then consider attention**
1682 **as some additional or unrelated confound?**

1683 We feel that this point is closely related to the comment above. We realize that, in the
1684 predictive coding field, attention is equated the precision of factors that contribute to the
1685 perceptual decision, such that an observer can attend strongly to sensory information (high
1686 likelihood precision) or to internal predictions derived from the sequence of preceding per-
1687 cepts (high prior precision). Therefore, when following the above predictive coding definition,
1688 fluctuations in attention can be equated with fluctuations in mode.

1689 However, we feel that outside of the predictive coding field, attention is not always conceived
1690 in that way, such that low attention may reflect low engagement with the task, relating to
1691 low likelihood and low prior precision. Is it against this notion that we have included the
1692 analysis of attention as a separate control analysis (with the caveats outlined in our response
1693 to the comment above).

1694 We now provide a more nuanced interpretation of our findings of RTs and confidence in
1695 relation to attention, with a specific focus on predictive coding and precision:

- 1696 • attention and precision in PC: *TODO*

1697 **10.1.5 Comment 5**

1698 **What licences the assumption that “agents depend upon internal confidence**
1699 **signals” in the absence of feedback?**

1700 In the absence of feedback, observers can only rely on internal estimates of performance to
1701 guide updates to their model of the reliability of their sensory apparatus (inferences about
1702 M). Previous work (e.g. Guggenmos et al., Elife 2106, <https://doi.org/10.7554/eLife.13388>)
1703 has shown that confidence signals can provide signals that drive perceptual learning in the
1704 absence of feedback. This has motivated our model simulation on the adaptive benefits of
1705 bimodal inference for metacognition, where the learning signal ϵ_M drives inferences about
1706 M :

$$\epsilon_M = (1 - |y_t - P(y_t = 1)|) - M_t \quad (37)$$

₁₇₀₇ **10.1.6 Comment 6**

₁₇₀₈ **And what licences the assumption that internal confidence feedback corresponds**
₁₇₀₉ **to “the absolute of the posterior log ratio” (did you mean the log of the posterior**
₁₇₁₀ **ratio)?**

₁₇₁₁ We mean the log of the posterior ratio. Following first order models (see e.g., Fleming &
₁₇₁₂ Daw, Self-evaluation of decision-making: A general Bayesian framework for metacognitive
₁₇₁₃ computation, Psychol. Rev. 2017, <https://doi.org/10.1037/rev0000045>), the perceptual
₁₇₁₄ decision and the confidence report rely on the posterior. The distance of the log of the
₁₇₁₅ posterior ratio L_t from zero becomes a measure of decision-certainty or confidence.

₁₇₁₆ **10.1.7 Comment 7**

₁₇₁₇ **I got a bit lost here when you say that “the precision of sensory coding M a**
₁₇₁₈ **function of u_t. This is largely because I couldn’t find a definition of u_t.**

₁₇₁₉ We apologize for this lack of clarity. In the model simulations on the adaptive benefits of
₁₇₂₀ bimodal inference, we generated stimuli s_t from a Bernoulli-distribution with $p + q + 0.5$.
₁₇₂₁ The value of u_t was then defined via equation (22), following our modeling of the human
₁₇₂₂ data:

$$u_t = \frac{1}{1 + \exp(-\alpha * (s_t - 0.5))} \quad (38)$$

₁₇₂₃ **10.1.8 Comment 8**

₁₇₂₄ **What licences an application of Rescorla-Wagner to learning the parameters (as**
₁₇₂₅ **in Equation 11) and, learning sensory precision as described by M_T (Equation**

1726 **13). Are you moving from a Bayesian framework to a reinforcement learning**
1727 **framework?**

1728 We would like to thank the reviewer for pointing out this inconsistency. We chose the a
1729 Rescorla-Wagner learning rule for simplicity: In our model, the speed of learning about H
1730 and M varies according to the current mode of perceptual processing and a constant learning
1731 rate:

$$H'_t = H'_{t-1} + \beta_H * \omega_{LLR} * \epsilon_H \quad (39)$$

$$M'_t = M'_{t-1} + \beta_M * \omega_{LLR} * \epsilon_M \quad (40)$$

1732 Allowing the learning rate itself to vary as a function of preceding experiences would add
1733 an additional level of complexity that we sought to omit in this analysis. However, we fully
1734 agree that choosing a Bayesian framework (e.g., a three-level HGF) would indeed be more
1735 consistent.

1736 **10.1.9 Comment 9**

1737 **I am sure you have answers to these questions - but with each new question**
1738 **the reader is left more and more skeptical that there is a coherent story behind**
1739 **your analyses. It would have been more convincing had you just committed to**
1740 **a Bayesian filter and made your points using one update scheme, under ideal**
1741 **Bayesian observer assumptions.**

1742 **Unlike your piecemeal scheme, things like the hierarchical Gaussian filter esti-**
1743 **mates the sensory and prior decisions explicitly and these estimates underwrite**
1744 **posterior inference. In your scheme, the sensory precision M appears to have no**
1745 **influence on perceptual inference (which is why, presumably you call it metacog-**

1746 nition). The problem with this is that your motivation for systematic fluctuations
1747 in precision is weakened. This is because improved metacognition does not
1748 improve perception — it only improves the perception of perception.

1749 In light of the above, can I suggest that you remove Section 5.8 and use your
1750 model in the preceding section to endorse your hypothesis along the following
1751 lines:

1752 “In summary, we hypothesized that subjects have certain hyperpriors that are
1753 apt for accommodating fluctuations in the predictability of their environment;
1754 i.e., people believe that their world is inherently volatile. This means that to be
1755 Bayes optimal it is necessary to periodically re-evaluate posterior beliefs about
1756 model parameters. One way to do this is to periodically suspend the precision
1757 of prior beliefs and increase the precision afforded to sensory evidence that up-
1758 dates (Bayesian) beliefs about model parameters. The empirical evidence above
1759 suggests that the timescale of this periodic scheduling of evidence accumulation
1760 is scale invariant. This means there exists a timescale of periodic fluctuations in
1761 precision over every window or length of perceptual decision-making. In what
1762 follows, we model perceptual decisions under a generative model (based upon
1763 a hazard function to model historical or serial dependencies) with, a periodic
1764 fluctuation in the precision of sensory evidence relative to prior beliefs at a
1765 particular timescale. Remarkably—using Bayesian model comparison—we find
1766 that a model with fluctuating precisions has much greater evidence, relative to
1767 a model in the absence of fluctuating precisions. Furthermore, we were able to
1768 quantify the dominant timescale of periodic fluctuations; appropriate for these
1769 kinds of paradigm.”

1770 Note, again, I am reading your ω_{LLR} and ω_{prior} as precisions and that
1771 the periodic modulation is the hyperprior that you are characterizing—and have

1772 discovered.

1773 We would like to thank Prof. Friston for these very helpful and precise suggestions. In the
1774 light of our response to Comments 1 - 9, we agree that a complete and extensive investigation
1775 of the relation between bimodal inference, learning about changes in the environment and
1776 the relation to metacognition may be beyond the scope of the current manuscript: Both
1777 Reviewer 1 and 3 (see below) have shared that the manuscript is too long and should be
1778 streamlined. Yet evaluating the full model space (e.g., comparing update rules for inferences
1779 about H and M , testing for an influence of beliefs about M on learning about H , validating
1780 oscillations in ω_{LLR} and omega_ψ using pupillometry, motor behavior, LFPs etc.) would make
1781 the manuscript even longer. We are therefore happy to follow Prof. Fristons suggestions to
1782 omit section 5.8. We have changed the manuscript in the following ways:

- 1783 • When introducing ω_{LLR} and omega_ψ , we identify these parameters as precision, refer-
1784 ring to the Bayesian framework: *TODO*
- 1785 • When identifying fluctuations in mode, we introduce this as a hyperprior, again referring
1786 to the Bayesian framework: *TODO*
- 1787 • We have deleted the section 5.8 and added a summary of our modeling approach to
1788 the discussion, including the text recommended by of Prof. Friston: (...) *Yet relying*
1789 *too strongly on serial dependencies may come at a cost: When accumulating over time,*
1790 *internal predictions may eventually override external information, leading to circular*
1791 *and false inferences about the state of the environment. In this work, we used model*
1792 *simulations to show that, akin to the wake-sleep-algorithm in machine learning⁶¹, bi-*
1793 *modal inference may help to determine whether errors result from external input or*
1794 *from internally-stored predictions (Figure 7): During internal mode, sensory process-*
1795 *ing is more strongly constrained by predictive processes that auto-encode the agent's*
1796 *environment. Conversely, during external mode, the network is driven predominantly*
1797 *by sensory inputs¹⁸. Between-mode fluctuations may thus generate an unambiguous*

1798 error signal that aligns internal predictions with the current state of the environment in
1799 iterative test-update-cycles⁶¹. On a broader scale, between-mode fluctuations may thus
1800 regulate the balance between feedforward versus feedback contributions to perception and
1801 thereby play a adaptive role in metacognition and reality monitoring⁶².

1802 From the perspective of the Bayesian brain hypothesis, we hypothesized that observers have
1803 certain hyperpriors that are apt for accommodating fluctuations in the predictability of their
1804 environment, i.e., people believe that their world is inherently volatile. To be Bayes optimal,
1805 it is therefore necessary to periodically re-evaluate posterior beliefs about the parameters that
1806 define an internal generative model of the external sensory environment. One way to do this
1807 is to periodically suspend the precision of prior beliefs and increase the precision afforded
1808 to sensory evidence that updates Bayesian beliefs about model parameters. The empirical
1809 evidence above suggests that the timescale of this periodic scheduling of evidence accumulation
1810 is scale invariant. This means there exists a timescale of periodic fluctuations in precision
1811 over every window or length of perceptual decision-making. Our bimodal inference approach
1812 models perceptual decisions under a generative model (based upon a hazard function to model
1813 serial dependencies between subsequent trials) with periodic fluctuations in the precision of
1814 sensory evidence relative to prior beliefs at a particular timescale. This ad-hoc-modification
1815 allowed us to quantify the dominant timescale of periodic fluctuations at approximately 0.11
1816 $1/N_{\text{trials}}$ in humans and mice that is appropriate for these kinds of paradigms.

1817 TODO: Model comparison

1818 10.1.10 Comment 11

1819 This begs the question as to whether you want to pursue the 1/f story. You
1820 refer to this as “noise”. However, there is no noise in this setup. I think what
1821 you meant was that the fluctuations are scale free, because they evinced a power
1822 law. I am sure that there are scale free aspects of these kinds of hyperpriors;

1823 however, in the context of your paradigm I wonder whether you should just
1824 ignore the scale free aspect and focus on your estimated temporal scale implicit
1825 in f. This means you don't have to hand wave about self-organized criticality in
1826 the discussion and focus upon your hypothesis.

1827 With respect to the result section, we would suggest reporting the 1/f/fluctuations and
1828 stating - as outlined above - that our model captures the dominant time-scale via the variable
1829 f , while reproducing the 1/f feature (for frequencies $< 1/N_{trials}$). We agree with the reviewer
1830 that the discussion of self-organized criticality is far from the data. We have omitted this
1831 section from the discussion.

1832 To Do: Discuss the value of f and report the result.

1833 10.1.11 Comment 12

1834 A final move—to make the paper more focused and digestible—would be to
1835 put a lot of your defensive analyses (e.g. about general arousal et cetera) in
1836 supplementary material. You have to be careful not to exhaust the reader by
1837 putting up a lot of auxiliary material before the important messages in your
1838 report.

1839 Minor points

1840 10.1.12 Comment 13

1841 I cannot resist suggesting that you change your title to “Bimodal Inference in
1842 Mice and Men”

1843 We thank you for this suggestion and have changed the title accordingly.

¹⁸⁴⁴ **10.1.13 Comment 14**

¹⁸⁴⁵ Please replace “infra-slow fluctuations” with “slow fluctuations”. slow has some
¹⁸⁴⁶ colloquial meaning in fMRI studies but not in any scale free context.

¹⁸⁴⁷ Done.

¹⁸⁴⁸ **10.1.14 Comment 15**

¹⁸⁴⁹ Please replace “simulated data” with “simulations” in the abstract. Finally,
¹⁸⁵⁰ please replace “robust learning and metacognition in volatile environments” with
¹⁸⁵¹ “enable optimal inference and learning in volatile environments.”

¹⁸⁵² Done. Since we have followed the Reviewer suggestion to delete section 5.8, we have
¹⁸⁵³ rephrased the last paragraph of the abstract into “We propose that between-mode fluctua-
¹⁸⁵⁴ tions may benefit perception by generating unambiguous error signals that enable optimal
¹⁸⁵⁵ inference and learning in volatile environments”.

¹⁸⁵⁶ **10.1.15 Comment 16**

¹⁸⁵⁷ Line 50, please replace “about the degree of noise inherent in encoding of sen-
¹⁸⁵⁸ sory information” with “the precision of sensory information relative to prior
¹⁸⁵⁹ (Bayesian) beliefs.”

¹⁸⁶⁰ Done.

¹⁸⁶¹ **10.1.16 Comment 17**

¹⁸⁶² Line 125: please replace “a source of error” with “a source of bias”

¹⁸⁶³ Done.

1864 10.1.17 Comment 18

1865 Line 141: please replace “one 1/f noise” with a scale invariant process with a
1866 1/f power law” (here and throughout) this is not “noise” it is a particular kind
1867 of fluctuation.

1868 Done.

1869 10.1.18 Comment 19

1870 Line 178, when you say that the fluctuations may arise due to “changes in level
1871 of tonic arousal or on-task attention”, I think you need to qualify this. In
1872 predictive processing, on-task attention is exactly the modulation of sensory
1873 precision, relative to prior precision that you are characterising here. Tonic
1874 arousal may be another thing may or may not confound your current results.

1875 TODO: work out the differences between on-task attention and the hyperprior.

1876 10.1.19 Comment 20

1877 When introducing Equation 2, please make it clear that the omega terms stand in
1878 for the precisions afforded to the likelihood (`omega_LLR`) and prior (`omega_`)
1879 that constitute the log posterior.

1880 We have modified the introduction of equation 2 as follows: Following Bayes’ theorem, we
1881 reasoned that binary perceptual decisions depend on the posterior log ratio L of the two alter-
1882 native states of the environment that participants learn about via noisy sensory information⁵⁴.
1883 We computed the posterior by combining the sensory evidence available at time-point t (i.e.,
1884 the log likelihood ratio LLR) with the prior probability ψ , weighted by the respective
1885 precision terms ω_{LLR} and ω_ψ :

$$L_t = LLR_t * \omega_{LLR} + \psi_t(L_{t-1}, H) * \omega_\psi \quad (41)$$

1886 You can then motivate Equation 6 and 7 as implementing the hyperprior in
1887 which the sensory and prior precisions fluctuate at a particular time scale.

1888 We would like to thank the reviewer for this suggestion, which we have added to the intro-
1889 duction of equations (6) and (7): To allow for *bimodal inference*, i.e., alternating periods
1890 of internally- and externally-biased modes of perceptual processing that occur irrespective
1891 of the sequence of preceding experiences, we assumed that the relative influences of likeli-
1892 hood and prior show coherent anti-phase fluctuations governed by ω_{LLR} and ω_ψ that are
1893 determined by amplitude a , frequency f and phase p . **This implements a hyperprior in**
1894 **which the sensory and prior precisions fluctuate at a particular time scale:**

$$\omega_{LLR} = a_{LLR} * \sin(f * t + p) + 1 \quad (42)$$

$$\omega_\psi = a_\psi * \sin(f * t + p + \pi) + 1 \quad (43)$$

1895 **10.1.20 Comment 21**

1896 You can also point out that the implicit anti-phase fluctuations are mandated
1897 by Bayes optimal formulations in which it is only the relative values of the prior
1898 and sensory precision that matter. Bayesian filters these precisions constitute
1899 the Kalman gain. You can find a derivation of why this in treatments of the
1900 hierarchical Gaussian filter is by Mathys et al.

1901 TODO: in the discussion?

1902 **10.1.21 Comment 22**

1903 In your first model simulations, I would make it clear in the main text which
1904 parameters you are optimizing's; namely (H, alpha, a_likelihood, a_prior f).
1905 Perhaps a little table with a brief description of the meaning of these hyper

¹⁹⁰⁶ parameters would be useful?

¹⁹⁰⁷ TODO

¹⁹⁰⁸ **10.1.22 Comment 23**

¹⁹⁰⁹ Please remove Section 5.8. If you do not, you need to explain why — on line
¹⁹¹⁰ 586 - setting $a = 0$ is appropriate when $a = 0$, the log posterior in Equation 2 is
¹⁹¹¹ zero because the precisions (omegas) are zero (by Equations 6 and 7).

¹⁹¹² We have removed the section 5.8. When setting the amplitude parameters to zero, ω_{LLR}
¹⁹¹³ and ω_ψ are constant at 1, creating a unimodal control model.

¹⁹¹⁴ Reviewer #2: Bimodal inference in humans and mice

¹⁹¹⁵ Veith Weilnhammer, Heiner Stuke, Kai Standvoss, Philipp Sterzer

¹⁹¹⁶ The authors elucidate whether periodicities in the sensitivity to external information repre-
¹⁹¹⁷ sent an epiphenomenon of limited processing capacity or, alternatively, result from a struc-
¹⁹¹⁸ tured and adaptive mechanism of perceptual inference. Analyzing large datasets of percep-
¹⁹¹⁹ tual decision-making in humans and mice, they investigated whether the accuracy of visual
¹⁹²⁰ perception is constant over time or whether it fluctuates. The authors found significant au-
¹⁹²¹ tocorrelations on the group level and on the level of individual participants, indicating that a
¹⁹²² stimulus-congruent response in a given trial increased the probability of stimulus-congruent
¹⁹²³ responses in the future. Furthermore, the authors addressed whether observers cycle through
¹⁹²⁴ periods of enhanced and reduced sensitivity to external information or whether observers rely
¹⁹²⁵ on internal information in certain phases. This was quantified by whether a response at a
¹⁹²⁶ given trial was correlated with responses in previous trials. The authors used computational
¹⁹²⁷ modeling to infer the origin of the different modes (internal vs. external).

¹⁹²⁸ Evaluation This is a very interesting and well-written manuscript, dealing with an important
¹⁹²⁹ question. The findings are novel and provide an innovative account of interpreting visual
¹⁹³⁰ perception. I am not an expert in modeling, so I will restrict my comments to the theoretical

₁₉₃₁ framework and the experimental approach. I have a few minor questions that I would like
₁₉₃₂ the authors to answer or clarify.

₁₉₃₃ Minor questions 1. History congruent perception was defined on the basis of response repe-
₁₉₃₄ titions. Are we really sure that responses are repeated due to some variant of a perceptual
₁₉₃₅ decision process (internal or external) or may arise on the motor-level - independent of a per-
₁₉₃₆ ceptual source? For instance, a response primed by residual activation in the motor system
₁₉₃₇ may represent a local effect independent from a general response bias. 2. If indeed, a re-
₁₉₃₈ sponse repetition is initiated by whatever reasons (non-perceptual), wouldn't this imply that
₁₉₃₉ the repeated response is per se more related to previous than to current visual information
₁₉₄₀ and would hence signal a reduced sensitivity to current external information? The authors
₁₉₄₁ are discussing the option of stereotypically repeated responses in the context of alertness.
₁₉₄₂ However, a tendency to repeat responses may arise due to other reasons. For instance, may
₁₉₄₃ the motor priming effects mentioned possibly explain faster RTs along with a stronger bias
₁₉₄₄ when in internal-mode.

₁₉₄₅ Reviewer #3: In this paper the authors propose that during perceptual decisions, humans
₁₉₄₆ and mice exhibit regular oscillatory fluctuations between an “external” (that places more
₁₉₄₇ weight on the perceptual evidence) and an “internal” (that places more weight on historical
₁₉₄₈ experiences) mode. In particular, the authors propose a computational scheme in which
₁₉₄₉ the influences of history and current stimulus on choice oscillate in anti phase, effectively
₁₉₅₀ implementing “bimodal inference”. The computational advantages of these scheme as well
₁₉₅₁ as its relation to the underlying neurophysiology are discussed.

₁₉₅₂ Overall, the authors make a very interesting proposal about what drives slow fluctuations
₁₉₅₃ in perceptual performance during randomised two-alternative choice tasks. This proposal
₁₉₅₄ relates changes in accuracy with changes in serial choice biases, which is a timely and syn-
₁₉₅₅ thesising contribution. Furthermore, this proposal is backed by analyses over several human
₁₉₅₆ datasets and a large dataset in mice.

1957 Despite its strong empirical contribution, the paper seems limited by the fact that alterna-
1958 tive computational hypotheses are not adequately considered (or at least considered in a
1959 systematic way). At the same time, and although the paper is well written, some parts are
1960 overly technical.

1961 Major comments:

1962 1) The authors collapse across various datasets in which different tasks were employed.
1963 However, some details on the nature of these different tasks and a discussion on the
1964 rationale of collapsing behavioural metrics across them is missing. The authors mention
1965 that all tasks involved binary perceptual decisions. In some parts of the manuscript
1966 the term “false alarms” is mentioned, indicating a detection protocol. Other terms
1967 in the methods section (e.g., “set size”) might need further clarification. Importantly,
1968 it is not clear how reaction times were calculated in the various tasks and whether
1969 some experiments involved free response paradigms while others interrogation/ cued
1970 paradigms (in which case RTs can be defined as the latency between the response cue
1971 and the response).

1972 2) The key premise that when participants do not rely on the external stimulus they rely
1973 more on the previous trial needs to be more clearly (and statistically) contrasted against
1974 a null hypothesis. For instance, an null hypothesis could be that when participants place
1975 a lower weight on the stimulus they simply choose randomly. It is important to specify
1976 a null hypothesis such that the key premise does not appear self-evident or circular.

1977 3) From a mechanistic (sequential sampling) perspective, several previous papers have
1978 examined whether choice history biases influence the starting point or the drift rate
1979 of the evidence accumulation process. Under the former formulation, reliance on the
1980 evidence vs. reliance on the previous choice will be naturally anti-correlated (the less
1981 weight you place on the evidence the more impactful the choice history will be, assuming
1982 that the last choice is represented as a starting point bias). This seems to be mapping

onto the computational model the authors describe, in which there is a weight on the prior, a weight on the likelihood and the assumption that these weights fluctuate in anti-phase. It is not obvious that this anti-phase relationship needs to be imposed ad-hoc. Or whether it would emerge naturally (using a mechanistic or Bayesian framework). More generally, the authors assert that without an external mechanism prior biases would be impossible to overcome, and this would misfit the data. However, it would be important to a) actually show that the results cannot be explained by a single mechanism in which the anti-phase relationship is emergent rather than ad-hoc, b) relate the current framework with previous mechanistic considerations of serial choice biases.

4) The authors need to unpack their definition of history biases since in previous work biases due to the response or the identity of the stimulus at the previous trial are treated differently. Here, the authors focus on response biases but it is not clear whether they could examine also stimulus-driven history biases (in paradigms where stimulus-response is remapped on each trial).

5) Previous work, which the authors acknowledges in their Discussion (6.5), distinguishes repetitive history biases from alternating biases. For instance, in Braun, Urai & Donner (2018, JoN) participants are split into repetitive or alternating. Shouldn't the authors define the history bias in a similar fashion? The authors point out that attracting and repelling biases operate simultaneously across different timescales. However, this is not warranted given Braun et. al and other similar papers. It is not clear how this more nuanced definition of history bias would alter the conclusions.

6) The arousal hypothesis seems to be ruled out too easily, merely in the presence of a non-monotonic “state” vs. RT pattern. Arousal can have an inverted U-shaped effect on behavioural performance and recent paper has demonstrated a non-monotonic effect of tonic arousal (baseline pupil) on RTs and accuracy (<https://www.biorxiv.org/abs/2018.08.01.218700.pdf>)

2009 ntent/10.1101/2023.07.28.550956.abstract). More generally, the RT and confidence
2010 analyses need to be complemented, perhaps by computational modelling using sequen-
2011 tial sampling models, as these behavioural metrics have multiple mechanistic mappings
2012 (e.g., a fast RT might correspond to high SNR or an impulsive decisions driven by a
2013 starting point bias).

2014 7) In several analysis the authors present an effect and then show that this effecs persists
2015 when key variables/ design aspects are also taken into account (see an example at around
2016 line 70). It makes more sense to present only one single analysis in which these key
2017 variables are controlled for. Results cannot be interpreted if they are spurious factors
2018 driving them so it is not clear why some of the results are presented in two versions
2019 (“uncontrolled” and “controlled” analyses).

2020 8) The central empirical finding is potentially important but is currently shadowed by
2021 more speculative sections/ discussions. For instance, the section on the adaptive merits
2022 of the computational model is relatively weaker compared to the empirical results. In
2023 particular, the model is simulated without feedback (whereas most experiments employ
2024 trial by trial feedback) and does not outperform the baseline model in accuracy but in
2025 other secondary metrics.

2026 Minor comments:

2027 – The amount of statistical analysis and results is often overwhelming. The authors could
2028 streamline the presentation better such that the main result is brought to the foreground.

2029 Currently the manuscript resembles a technical report.

2030 – Some typos or omissions may alter the meaning in various places. Indicatively, in lines 273,
2031 439, 649.

2032 **References**

- 2033 1. Schrödinger, E. *What is Life? The Physical Aspect of the Living Cell.* (Cambridge
2034 University Press, 1944).
- 2035 2. Ashby, W. R. Principles of the self-organizing dynamic system. *Journal of General
2036 Psychology* **37**, 125–128 (1947).
- 2037 3. Friston, K. Life as we know it. *Journal of The Royal Society Interface* **10**, 20130475
2038 (2013).
- 2039 4. Palva, J. M. *et al.* Roles of multiscale brain activity fluctuations in shaping the vari-
ability and dynamics of psychophysical performance. in *Progress in brain research* vol.
2040 193 335–350 (Elsevier B.V., 2011).
- 2041 5. VanRullen, R. Perceptual Cycles. *Trends in Cognitive Sciences* **20**, 723–735 (2016).
- 2042
- 2043 6. Verplanck, W. S. *et al.* Nonindependence of successive responses in measurements of
2044 the visual threshold. *Journal of Experimental Psychology* **44**, 273–282 (1952).
- 2045 7. Atkinson, R. C. A variable sensitivity theory of signal detection. *Psychological Review*
2046 **70**, 91–106 (1963).
- 2047 8. Dehaene, S. Temporal Oscillations in Human Perception. *Psychological Science* **4**,
2048 264–270 (1993).
- 2049 9. Gilden, D. L. *et al.* On the Nature of Streaks in Signal Detection. *Cognitive Psychology*
2050 **28**, 17–64 (1995).
- 2051 10. Gilden, D. L. *et al.* 1/f noise in human cognition. *Science* **67**, 1837–1839 (1995).
- 2052
- 2053 11. Monto, S. *et al.* Very slow EEG fluctuations predict the dynamics of stimulus detection
2054 and oscillation amplitudes in humans. *Journal of Neuroscience* **28**, 8268–8272 (2008).

- 2055 12. Ashwood, Z. C. *et al.* Mice alternate between discrete strategies during perceptual
2056 decision-making. *Nature Neuroscience* **25**, 201–212 (2022).
- 2057 13. Gilden, D. L. Cognitive emissions of 1/f noise. *Psychological Review* **108**, 33–56 (2001).
- 2058
- 2059 14. Duncan, K. *et al.* Memory’s Penumbra: Episodic memory decisions induce lingering
2060 mnemonic biases. *Science* **337**, 485–487 (2012).
- 2061 15. Clare Kelly, A. M. *et al.* Competition between functional brain networks mediates
2062 behavioral variability. *NeuroImage* **39**, 527–537 (2008).
- 2063 16. Hesselmann, G. *et al.* Spontaneous local variations in ongoing neural activity bias
2064 perceptual decisions. *Proceedings of the National Academy of Sciences of the United
States of America* **105**, 10984–10989 (2008).
- 2065 17. Schroeder, C. E. *et al.* Dynamics of Active Sensing and perceptual selection. *Current
2066 Opinion in Neurobiology* **20**, 172–176 (2010).
- 2067 18. Honey, C. J. *et al.* Switching between internal and external modes: A multiscale
2068 learning principle. *Network Neuroscience* **1**, 339–356 (2017).
- 2069 19. Weilnhammer, V. *et al.* Bistable perception alternates between internal and external
2070 modes of sensory processing. *iScience* **24**, (2021).
- 2071 20. Rahnev, D. *et al.* The Confidence Database. *Nature Human Behaviour* **4**, 317–325
2072 (2020).
- 2073 21. The International Brain Laboratory. Standardized and reproducible mea-
2074 surement of decision-making in mice. *bioRxiv* 2020.01.17.909838 (2020)
doi:10.1101/2020.01.17.909838.
- 2075 22. Fischer, J. *et al.* Serial dependence in visual perception. *Nat. Neurosci.* **17**, 738–743
2076 (2014).

- 2077 23. Liberman, A. *et al.* Serial dependence in the perception of faces. *Current Biology* **24**,
2078 2569–2574 (2014).
- 2079 24. Abrahamyan, A. *et al.* Adaptable history biases in human perceptual decisions. *Proceedings of the National Academy of Sciences of the United States of America* **113**,
2080 E3548–E3557 (2016).
- 2081 25. Cicchini, G. M. *et al.* Compressive mapping of number to space reflects dynamic
2082 encoding mechanisms, not static logarithmic transform. *Proceedings of the National
Academy of Sciences of the United States of America* **111**, 7867–7872 (2014).
- 2083 26. Cicchini, G. M. *et al.* Serial dependencies act directly on perception. *Journal of Vision*
2084 **17**, (2017).
- 2085 27. Fritzsche, M. *et al.* A bayesian and efficient observer model explains concurrent attrac-
2086 tive and repulsive history biases in visual perception. *eLife* **9**, 1–32 (2020).
- 2087 28. Urai, A. E. *et al.* Pupil-linked arousal is driven by decision uncertainty and alters
2088 serial choice bias. *Nature Communications* **8**, (2017).
- 2089 29. Akrami, A. *et al.* Posterior parietal cortex represents sensory history and mediates its
2090 effects on behaviour. *Nature* **554**, 368–372 (2018).
- 2091 30. Braun, A. *et al.* Adaptive history biases result from confidence-weighted accumulation
2092 of past choices. *Journal of Neuroscience* **38**, 2418–2429 (2018).
- 2093 31. Bergen, R. S. V. *et al.* Probabilistic representation in human visual cortex reflects
2094 uncertainty in serial decisions. *Journal of Neuroscience* **39**, 8164–8176 (2019).
- 2095 32. Urai, A. E. *et al.* Choice history biases subsequent evidence accumulation. *eLife* **8**,
2096 (2019).
- 2097 33. Hsu, S. M. *et al.* The roles of preceding stimuli and preceding responses on assimilative
2098 and contrastive sequential effects during facial expression perception. *Cognition and
Emotion* **34**, 890–905 (2020).

- 2099 34. Dong, D. W. *et al.* Statistics of natural time-varying images. *Network: Computation*
2100 *in Neural Systems* **6**, 345–358 (1995).
- 2101 35. Burr, D. *et al.* Vision: Efficient adaptive coding. *Current Biology* **24**, R1096–R1098
2102 (2014).
- 2103 36. Montroll, E. W. *et al.* On 1/f noise and other distributions with long tails. *Proceedings*
2104 *of the National Academy of Sciences* **79**, 3380–3383 (1982).
- 2105 37. Bak, P. *et al.* Self-organized criticality: An explanation of the 1/f noise. *Physical*
2106 *Review Letters* **59**, 381–384 (1987).
- 2107 38. Chialvo, D. R. Emergent complex neural dynamics. *Nature Physics* **6**, 744–750 (2010).
- 2108
- 2109 39. Wagenmakers, E. J. *et al.* Estimation and interpretation of 1/f α noise in human
2110 cognition. *Psychonomic Bulletin and Review* **11**, 579–615 (2004).
- 2111 40. Van Orden, G. C. *et al.* Human cognition and 1/f scaling. *Journal of Experimental*
2112 *Psychology: General* **134**, 117–123 (2005).
- 2113 41. Chopin, A. *et al.* Predictive properties of visual adaptation. *Current Biology* **22**,
2114 622–626 (2012).
- 2115 42. Cicchini, G. M. *et al.* The functional role of serial dependence. *Proceedings of the*
2116 *Royal Society B: Biological Sciences* **285**, (2018).
- 2117 43. Kiyonaga, A. *et al.* Serial Dependence across Perception, Attention, and Memory.
2118 *Trends in Cognitive Sciences* **21**, 493–497 (2017).
- 2119 44. McGinley, M. J. *et al.* Waking State: Rapid Variations Modulate Neural and Behav-
2120 ioral Responses. *Neuron* **87**, 1143–1161 (2015).
- 2121 45. Rosenberg, M. *et al.* Sustaining visual attention in the face of distraction: A novel
2122 gradual-onset continuous performance task. *Attention, Perception, and Psychophysics*
2122 **75**, 426–439 (2013).

- 2123 46. Zalta, A. *et al.* Natural rhythms of periodic temporal attention. *Nature Communications* **11**, 1–12 (2020).
- 2124
- 2125 47. Prado, J. *et al.* Variations of response time in a selective attention task are linked to variations of functional connectivity in the attentional network. *NeuroImage* **54**, 541–549 (2011).
- 2126
- 2127 48. St. John-Saaltink, E. *et al.* Serial Dependence in Perceptual Decisions Is Reflected in Activity Patterns in Primary Visual Cortex. *Journal of Neuroscience* **36**, 6186–6192 (2016).
- 2128
- 2129 49. Cicchini, G. M. *et al.* Perceptual history propagates down to early levels of sensory analysis. *Current Biology* **31**, 1245–1250.e2 (2021).
- 2130
- 2131 50. Kepcs, A. *et al.* Neural correlates, computation and behavioural impact of decision confidence. *Nature* **455**, 227–231 (2008).
- 2132
- 2133 51. Fleming, S. M. *et al.* How to measure metacognition. *Frontiers in Human Neuroscience* **8**, 443 (2014).
- 2134
- 2135 52. Leys, C. *et al.* Detecting outliers: Do not use standard deviation around the mean, use absolute deviation around the median. *Journal of Experimental Social Psychology* **49**, 764–766 (2013).
- 2136
- 2137 53. Maloney, L. T. *et al.* Past trials influence perception of ambiguous motion quartets through pattern completion. *Proceedings of the National Academy of Sciences of the United States of America* **102**, 3164–3169 (2005).
- 2138
- 2139 54. Glaze, C. M. *et al.* Normative evidence accumulation in unpredictable environments. *eLife* **4**, (2015).
- 2140
- 2141 55. Wexler, M. *et al.* Persistent states in vision break universality and time invariance. *Proceedings of the National Academy of Sciences of the United States of America* **112**, 14990–14995 (2015).
- 2142

- 2143 56. Rao, R. P. *et al.* Predictive coding in the visual cortex: a functional interpretation of
2144 some extra-classical receptive-field effects. *Nature neuroscience* **2**, 79–87 (1999).
- 2145 57. Jardri, R. *et al.* Experimental evidence for circular inference in schizophrenia. *Nature
2146 Communications* **8**, 14218 (2017).
- 2147 58. Guggenmos, M. *et al.* Mesolimbic confidence signals guide perceptual learning in the
2148 absence of external feedback. *eLife* **5**, (2016).
- 2149 59. Mathys, C. D. *et al.* Uncertainty in perception and the Hierarchical Gaussian Filter.
2150 *Frontiers in human neuroscience* **8**, 825 (2014).
- 2151 60. Sterzer, P. *et al.* The Predictive Coding Account of Psychosis. *Biological Psychiatry*
2152 **84**, 634–643 (2018).
- 2153 61. Bengio, Y. *et al.* Towards Biologically Plausible Deep Learning. *bioRxiv* (2015).
- 2154
- 2155 62. Dijkstra, N. *et al.* Perceptual reality monitoring: Neural mechanisms dissociating
2156 imagination from reality. *PsyArXiv* (2021) doi:10.31234/OSF.IO/ZNGEQ.
- 2157 63. Andrillon, T. *et al.* Predicting lapses of attention with sleep-like slow waves. *Nature
2158 Communications* **12**, 3657 (2021).
- 2159 64. Passingham, R. E. *Understanding the prefrontal cortex : selective advantage, connec-*
2160 *tivity, and neural operations.* (Oxford University Press).
- 2161 65. Ashwood, Z. C. *et al.* Mice alternate between discrete strategies during perceptual
2162 decision-making. *bioRxiv* 2020.10.19.346353 (2021) doi:10.1101/2020.10.19.346353.
- 2163 66. Denève, S. *et al.* Efficient codes and balanced networks. *Nature Neuroscience* **19**,
2164 375–382 (2016).
- 2165 67. Beggs, J. M. *et al.* Neuronal Avalanches in Neocortical Circuits. *Journal of Neuro-*
2166 *science* **23**, 11167–11177 (2003).

- 2167 68. Wang, X. J. Synaptic basis of cortical persistent activity: The importance of NMDA
2168 receptors to working memory. *Journal of Neuroscience* **19**, 9587–9603 (1999).
- 2169 69. Wang, X. J. Synaptic reverberation underlying mnemonic persistent activity. *Trends
2170 in Neurosciences* **24**, 455–463 (2001).
- 2171 70. Wang, M. *et al.* NMDA Receptors Subserve Persistent Neuronal Firing during Working
2172 Memory in Dorsolateral Prefrontal Cortex. *Neuron* **77**, 736–749 (2013).
- 2173 71. Bliss, D. P. *et al.* Synaptic augmentation in a cortical circuit model reproduces serial
2174 dependence in visual working memory. *PLOS ONE* **12**, e0188927 (2017).
- 2175 72. Stein, H. *et al.* Reduced serial dependence suggests deficits in synaptic potentiation
2176 in anti-NMDAR encephalitis and schizophrenia. *Nature Communications* **11**, 1–11
(2020).
- 2177 73. Durstewitz, D. *et al.* Neurocomputational Models of Working Memory. *Nature Neu-
2178 roscience* **3**, 1184–1191 (2000).
- 2179 74. Seamans, J. K. *et al.* Dopamine D1/D5 receptor modulation of excitatory synaptic
2180 inputs to layer V prefrontal cortex neurons. *Proceedings of the National Academy of
Sciences of the United States of America* **98**, 301–306 (2001).
- 2181 75. Kobayashi, T. *et al.* Reproducing Infra-Slow Oscillations with Dopaminergic Modula-
2182 tion. *Scientific Reports* **7**, 1–9 (2017).
- 2183 76. Chew, B. *et al.* Endogenous fluctuations in the dopaminergic midbrain drive behavioral
2184 choice variability. *Proceedings of the National Academy of Sciences of the United States
of America* **116**, 18732–18737 (2019).
- 2185 77. Fritzsche, M. *et al.* Opposite Effects of Recent History on Perception and Decision.
2186 *Current Biology* **27**, 590–595 (2017).
- 2187 78. Gekas, N. *et al.* Disambiguating serial effects of multiple timescales. *Journal of Vision
2188* **19**, 1–14 (2019).

- 2189 79. Weilnhammer, V. *et al.* Psychotic Experiences in Schizophrenia and Sensitivity to
2190 Sensory Evidence. *Schizophrenia bulletin* **46**, 927–936 (2020).
- 2191 80. Fletcher, P. C. *et al.* Perceiving is believing: a Bayesian approach to explaining the
2192 positive symptoms of schizophrenia. *Nature reviews. Neuroscience* **10**, 48–58 (2009).
- 2193 81. Corlett, P. R. *et al.* Hallucinations and Strong Priors. *Tics* **23**, 114–127 (2019).

2194